Carbon and oxygen fluxes in the Barents and Norwegian Seas:

Production, air-sea exchange and budget calculations

Caroline Kivimäe

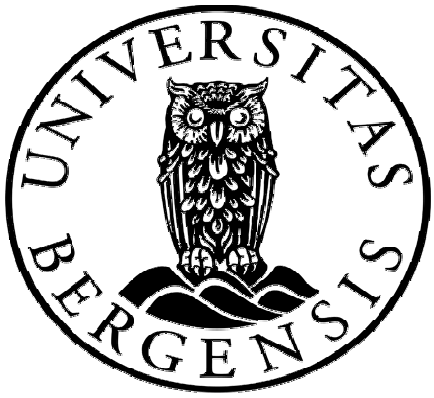

Dissertation for the degree philosophiae doctor (PhD)
at the University of Bergen

August 2007

ISBN 978-82-308-0414-8
Bergen, Norway 2007

Printed by Allkopi Ph: +47 55 54 49 40

Abstract

This thesis focus on the carbon and oxygen fluxes in the Barents and Norwegian Seas and presents four studies where the main topics are variability of biological production, air-sea exchange and budget calculations.

The world ocean is the largest short term reservoir of carbon on Earth, consequently it has the potential to control the atmospheric concentrations of carbon dioxide (CO_2) and has already taken up ~50 % of the antropogenically emitted CO_2. It is thus important to study carbon related processes in the ocean to understand their changes in the past, present, and future perspectives. The main function of the Arctic Mediterranean, within which the study area lies, in the global carbon cycle is to take up CO_2 from the atmosphere and, as part of the northern limb of the global thermohaline circulation, to convey surface water to the ocean interior.

A carbon budget is constructed for the Barents Sea to study the carbon fluxes into and out of the area. The budget includes advection, air-sea exchange, river runoff, land sources and sedimentation. The results reviel that ~5.6 Gt C annually is exchanged through the boundaries of the Barents Sea mainly due to advection, and that the carbon sources within the Barents Sea itself are larger than the sinks. The change in carbon content of the Atlantic Water as it passes through the Barents Sea is investigated, revieling that ~0.030 Gt C is taken up from the atmosphere and exported to the Arctic Ocean during one year. The main part of the increased carbon content is channelled through biological production.

Spatial and interannual variability of biological production and air-sea exchange is investigated in the north-western Barents Sea during the spring-summer season, interannual variability of oxygen and carbon fluxes due to biological production is also studied at Ocean Weather Station M in the Norwegian Sea. Both the spatial and interannual variability in the Barents Sea depend on the distribution of water masses and sea ice cover while the causes behind the variability at Ocean Weather Station M are more complex. Air-sea exchange was also studied in the Storfjorden polynya where it was discovered that formation of sea ice during winter is accompanied by a large air-sea CO_2 exchange.

Thálatta, thálatta!

Table of contents

List of papers

This thesis is based on the work presented in the following papers which will be referred to by their Roman numeral.

Paper I: Kivimäe, C., R. G. J. Bellerby, A. Fransson, M. Reigstad and T. Johannessen. A carbon budget for the Barents Sea. Submitted to Deep-Sea Research II.

Paper II: Kivimäe, C., R. G. J. Bellerby, A. Sundfjord, A. Omar and T. Johannessen. Variability of new production and CO_2 air-sea exchange in the north-western Barents Sea in relation to sea ice cover. In review, Journal of Marine Research.

Paper III: Omar, A., T. Johannessen, R. G. J. Bellerby, A. Olsen, L. G. Anderson and C. Kivimäe, 2005. Sea-ice and brine formation in Storfjorden: Implications for the Arctic wintertime air-sea CO_2 flux. *in* The Nordic Seas: an integrated perspective, H. Drange, T. Dokken, T. Furevik, R. Gerdes and W. Breger (eds), American Geophysical Union, Geophysical Monograph 158, 177-187.

Paper IV: Kivimäe, C. and E. Falck. Interannual variability of net community production at Ocean Weather Station M in the Norwegian Sea during 51 years. Submitted to Global Biogeochemical Cycles.

1. Backdrop: Climate, the global carbon cycle, and the world ocean

The study of the marine carbon cycle can be seen against the large scale backdrop of the global carbon cycle and the climatic system. Life in the ocean is both reliant on and an actor in the marine carbon cycle and can consequently affect the climate. The global carbon cycle and climate are intimately linked through the effect carbon dioxide (CO_2) has on the radiation (i.e. heat) balance of the atmosphere. Climate on the other hand is essential for most aspects of the global carbon cycle. Climate is a term that in a narrow sense refers to the long term weather and its variation, while in a wider sense it refers to the state of the climate system (IPCC, 2001). The global climate is thus determined by the state of, and interactions between, the parts of the climate system, see Figure 1.

The sun provides the major input to the radiation balance of the atmosphere, mainly as short wave radiation. The part of the solar radiation that is not absorbed or scattered as it passes through the atmosphere reaches and heats the surface of the Earth.

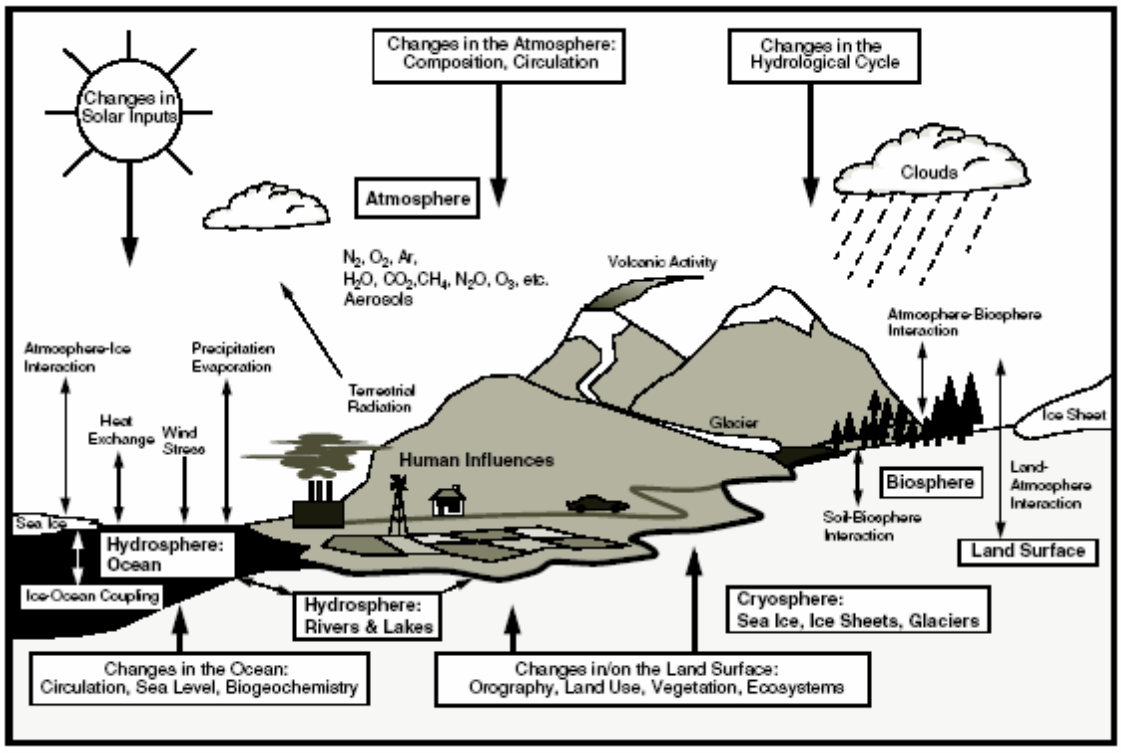

Figure 1: The components of the global climate system (bold), their processes and interactions (thin arrows) and some aspects that may change (bold arrows), figure from IPCC (2001).

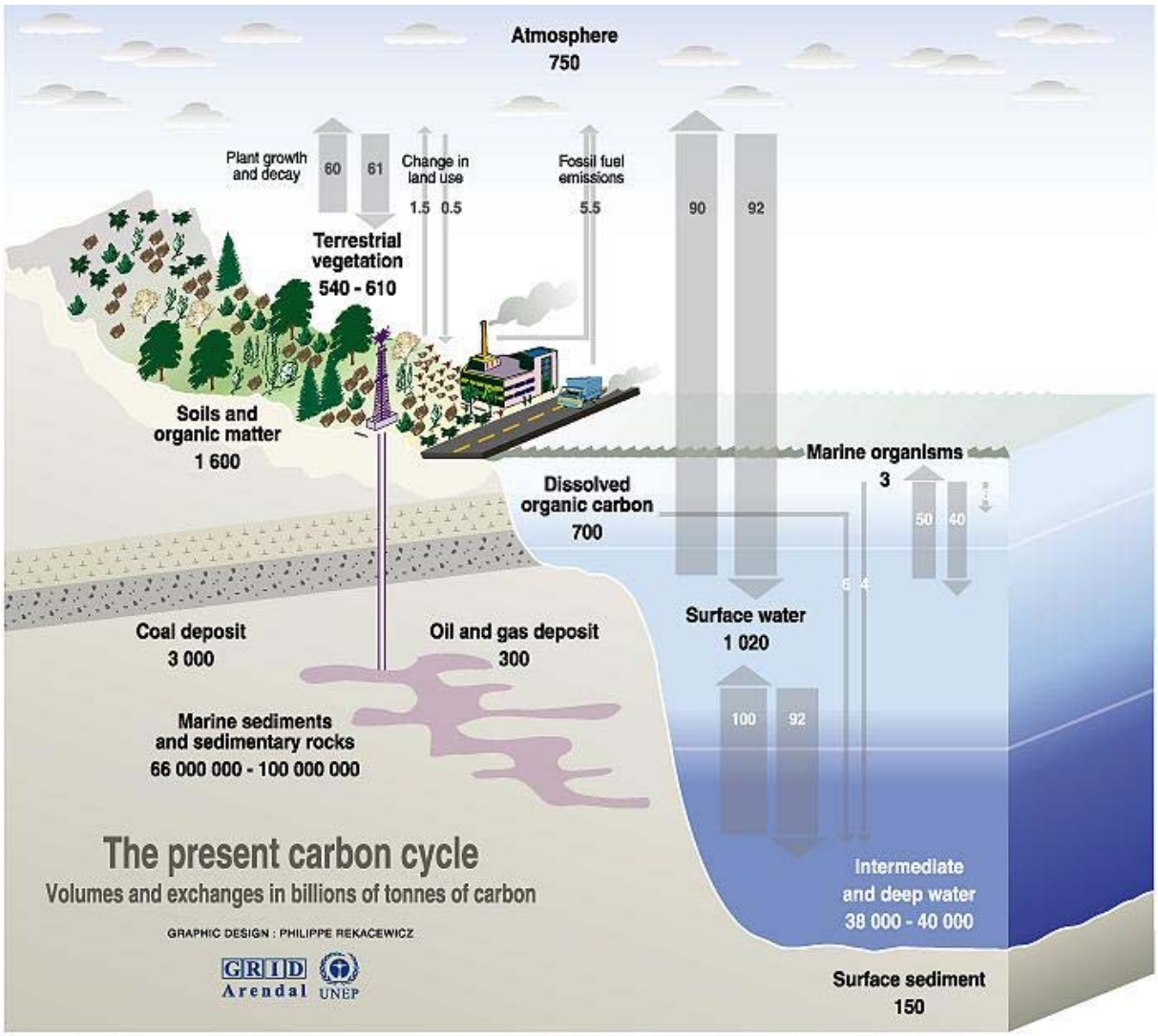

Sources: Center for climatic research, Institute for environmental studies, university of Wisconsin at Madison; Okanagan university college in Canada, Department of geography; World Watch, November-December 1998; Climate change 1995, The science of climate change, contribution of working group 1 to the second assessment report of the intergovernmental panel on climate change, UNEP and WMO, Cambridge press university, 1996.

Figure 2: The global carbon cycle with reservoirs in Gt C and fluxes in Gt C/yr. Picture taken from http://www.grida.no/climate/vital/13.htm.

The Earth on the other hand mainly emits long wave radiation back to the atmosphere. The CO_2 in the atmospheric is important for the global climate since it acts as a "greenhouse" gas, i.e. it absorbs and emits long waved radiation. The long wave radiation from the Earth's surface is thus absorbed and re-emitted by the CO_2, also back towards the surface of the Earth. Heat is thus kept trapped within the atmosphere and the net result is a temperature that is highest at the Earth's surface and decreases upwards in the atmosphere. Without the effect of the greenhouse gases (H_2O, CO_2, CH_4, N_2O, CFCs etc.) the surface of the Earth would be considerable colder (~33ºC) than it is at present (Graedel and Crutzen, 1993).

During the last 150 years human activities have increased the atmospheric CO_2 concentration through fossil fuel burning, land use changes, and cement production,

and the effect of this increased atmospheric CO_2 concentration is an alteration of the radiation balance of the atmosphere. The result is an increased altitude from which the long waved radiation effectively escapes into space (IPCC, 2001) and increasing temperatures at the surface of the Earth.

The global carbon cycle consists of the carbon fluxes between different reservoirs, i.e. the atmosphere, hydrosphere, lithosphere and biosphere as illustrated in Figure 2. The carbon fluxes into the ocean come from the atmosphere, river runoff, groundwater transport, and coastal abrasion. From the ocean there are fluxes of carbon back to the atmosphere and to the sediments. The effect of human activities on the global carbon fluxes consists of altering the size of the carbon fluxes between the reservoirs, both gross and net fluxes, and sometimes to alter the direction of the net flux.

The lithosphere is the largest reservoir of carbon on Earth followed by the deep ocean (Figure 2). The vegetation, organic matter, and soil on land contain about twice as much carbon as the surface ocean while the atmosphere is the smallest of the major reservoirs. The timescales for the accessibility of the carbon in these reservoirs are very different, with the carbon in the lithosphere only accessible on geological timescales (100 to millions years) while the processes associated with the atmospheric carbon by comparison are very fast (1-10 years). The deep ocean responds much slower to changes than the surface ocean, as the mean residence time of water in the deep ocean is 1000 years (Broecker and Peng, 1982). There are only a few areas of the surface ocean that communicate directly with the deep ocean and the slow transfer of surface water into the ocean interior is thus a bottleneck for the exchange of CO_2 between the atmosphere and the world ocean.

The role of the oceans in both the global carbon cycle and the climate system is very important since they contain large amounts of CO_2 and may in this sense control the atmospheric CO_2 concentration. The oceans also store and transport large amounts of heat. One of the important scientific questions is thus how much carbon that is sequestered in the oceans, dampening the effects of the anthropogenic emission of CO_2 in the atmosphere? There are still many unanswered questions in the field of climate and climate change, e. g. how does the climate system work and what are the roles of the different components? How to make reliable predictions for the future? How large an effect do the oceanic biogeochemical feedbacks have on atmospheric CO_2 concentrations and what is the net direction of all the feedbacks? The latter is still difficult to quantify due to lack of knowledge and has until recently not been taken into consideration in predictions for future climate and environmental change.

2. Motivation and aim for this thesis

In a global perspective the Arctic Mediterranean (the Arctic Ocean with its shelf seas and the Nordic Seas) is a small and remote area to a large degree covered by sea ice. Why should we, working with marine biogeochemistry, concern ourselves with this seemingly insignificant area? The answer to this question is that even if the area is small the processes that occur within it are significant on a larger scale.

The Arctic Mediterranean consists, together with the Labrador Sea, the northern limb of the large scale thermohaline circulation of the Atlantic Ocean and consequently has the ability to change this circulation. Large scale climate variations in the past has been associated with changes in the thermohaline circulation and it is speculated about whether the anthropogenic induced climate change we now are starting to observe may alter it. Being one of the few areas in the world where the surface ocean communicate directly with the deep ocean the result is that the biogeochemical processes in the Arctic Mediterranean is of importance for global biogeochemical cycling of many substances such as carbon, oxygen and nutrients.

Research based on the global carbon cycle has increased in later years as the importance of CO_2 as a greenhouse gas has become an important issue for society. In this context the most important process in the Arctic Mediterranean is the sequestration of atmospheric CO_2. This occurs through uptake of atmospheric CO_2 which is incorporated into produced intermediate and deep waters and through export of biological matter to depth. All the processes involved in the sequestration are important to study, physical, chemical and biological, especially since they may change following future climate and environmental changes. Due to its importance for climate and also its vulnerability to climate change it is important that the Arctic Mediterranean is thoroughly studied before major changes occur, such as total loss of summer sea ice.

The aim of this thesis is to explore the biogeochemistry of the Barents and Norwegian Seas to learn more about the carbon and oxygen fluxes in this area and the processes controlling them. The focus is the variability of biological production and air-sea exchange as well as budget calculations. Some of the results are also contemplated in a climate change perspective. The four papers included in the thesis present new knowledge which will add to the understanding of the marine carbon cycle in the study area.

3. Variables

3.1 The marine inorganic carbon system

The marine inorganic carbon system is described by the following four variables, fugacity of carbon dioxide (fCO_2), total dissolved inorganic carbon (C_T), total alkalinity (A_T), and pH. The system is described by these variables since the individual species (see Eq. 6) cannot be measured directly. If two of the variables and the equilibrium constants of the system are known the other two variables can be calculated. The measurement errors and the systematic errors introduced by the equilibrium constants limits the accuracy of the results of the calculations and direct measurements are to be preferred when possible, especially for fCO_2.

The concentration of CO_2 in water in equilibrium with the atmosphere can be described by Henry's law:

$$[CO_2\ (aq)] = fCO_2^{atm} \cdot K_H \qquad (1)$$

where CO_2 (aq) is the CO_2 dissolved in the water, fCO_2^{atm} is the fugacity of CO_2 in the atmosphere and K_H is Henry's law constant. This equation describes the interaction of the inorganic carbon system in the water with the atmosphere. The equation can also be used to determine the concentration of CO_2 (aq) by determining the fCO_2 in air that has been equilibrated with a water sample. fCO_2 in the equated air is determined by measuring the mole fraction, xCO_2, which is converted to the partial pressure of CO_2 (pCO_2) following

$$pCO_2 = xCO_2 \cdot P \qquad (2)$$

where P is the total pressure. fCO_2 is then calculated from the pCO_2 in order to account for the non-ideal behaviour of CO_2. The difference between pCO_2 and fCO_2 is small in the temperature range relevant for marine studies (the fCO_2 is 0.995-0.997 times the pCO_2 between -2º C and 25º C; DOE, 1994). The terms pCO_2 and fCO_2 are often used interchangeable, but in thermodynamic calculations fCO_2 should be used.

Some of the CO_2 that enters the sea water is hydrated and converted to carbonic acid (H_2CO_3):

$$[CO_2\ (aq)] + [H_2O] \leftrightarrow \frac{[H_2CO_3]}{K_0} \qquad (3)$$

where K_0 is the equilibrium constant. The carbonic acid can then be dissociated in two steps to bicarbonate ions (HCO_3^-) and carbonate ions (CO_3^{2-}):

$$[H_2CO_3] \leftrightarrow \frac{[H^+] + [HCO_3^-]}{K_1} \quad (4)$$

$$[HCO_3^-] \leftrightarrow \frac{[H^+] + [CO_3^{2-}]}{K_2} \quad (5)$$

Inorganic carbon is thus present as four species in the water and is summarized in the equation for C_T:

$$C_T = [CO_2\ (aq)] + [H_2CO_3] + [HCO_3^-] + [CO_3^{2-}] \quad (6)$$

Dickson (1981) defined A_T as "the number of moles of hydrogen ions equivalent to the excess of proton acceptors (bases formed from weak acids with a dissociation constant $K \leq 10^{-4.5}$ at 25º C and zero ionic strength) over proton donors (acids with $K > 10^{-4.5}$) in one kilogram of sea water". This corresponds to:

$$A_T = [HCO_3^-] + 2\,[CO_3^{2-}] + [B(OH)_4^-] + [HPO_4^{2-}] + 2\,[PO_4^{3-}] + [SiO(OH)_3^-] + [OH^-] + [NH_3] + [HS^-] + \text{other weak bases} - [H^+] - [HSO_4^-] - [HF] - [H_3PO_4] - \text{other weak acids} \quad (7)$$

Here $B(OH)_4^-$ represents the boric acid system, H_3PO_4, HPO_4^{2-}, and PO_4^{3-} represent the phosphoric acid system, and $SiO(OH)_3^-$ the silicic acid system. H^+ is the hydrogen ion and HF is hydrofluoric acid. The A_T expresses the buffering capacity of sea water, which is the ability of the sea water to resist the pH change an addition of an acid or base would cause. The buffering is mainly performed by the inorganic carbon system which in this context can be summarised as

$$[CO_2\ (aq)] + [CO_3^{2-}] + H_2O \leftrightarrow 2\,[HCO_3^-] \quad (8)$$

The consequence of the buffering is that uptake of CO_2 from the atmosphere "consumes" carbonate ions to produce bicarbonate ions. Following Eq. 6 and the A_T definition uptake of atmospheric CO_2 thus results in an increase in C_T but no change in A_T.

pH is calculated as the negative logarithm of the hydrogen ion activity, $\{H^+\}$:

$$pH = -\log\{H^+\} \quad (9)$$

The pH is central in the carbonate system. Figure 3 shows the dependence of the variables in Eq. 6 on pH and the pH found in oceanic waters today. At the pH in the present day ocean which is slightly above 8 the major part of the inorganic carbon is present as HCO_3^- (~90%).

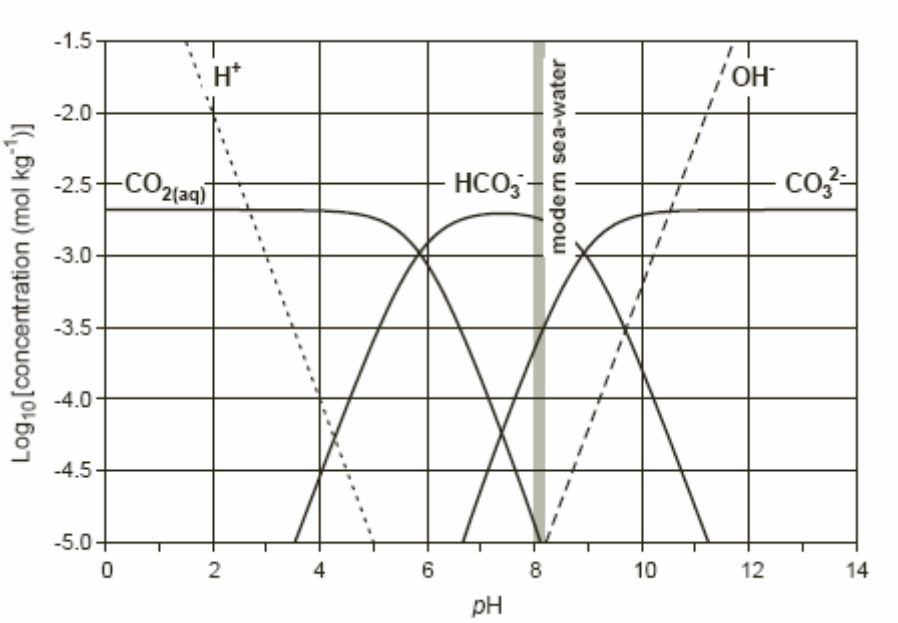

Figure 3: Bjerrum plot showing the concentrations of the different species in the inorganic carbon system in relation to pH. The thick grey vertical line indicates the pH span in the present day ocean. The diagram is taken from Ridgwell and Zeebe (2005).

Of the other three species CO_3^- occurs in the largest concentrations (~9%) followed by CO_2 (aq) (~1%) and very low concentrations of undissociated H_2CO_3.

There exist several pH definitions in sea water depending on which species are included in the definition and this lead to the existence of several pH scales. If only hydrogen ions (H^+) are included the resulting pH scale is called the free hydrogen ion concentration scale, when both H^+ and hydrogen sulphate ions (HSO_4^-) are included it results in the total hydrogen concentration scale, and if hydrogen fluoride (HF) is included as well the scale is called the seawater hydrogen ion concentration scale. The difference between pH values depending on the pH scale can be up to 0.12 units (Zeebe and Wolf-Gladrow, 2003) and failing to take the different pH scales into consideration can thus introduce large errors into calculations of other variables of the inorganic carbon system and acidity constants. The difference between pH values based on different scales is also much larger than the accuracy and precision of pH measurements.

3.1.1 Analytical methods

In this thesis many variables have been used to study the carbon fluxes; C_T, A_T, oxygen, nutrients, temperature, salinity, and volume fluxes. Of these variables C_T and A_T have been measured by the author and analytical methods will be presented only for these.

3.1.1.1 Total dissolved inorganic carbon (C_T)

C_T was measured by acidification of the sample followed by coulometric titration (Johnson et al., 1987; Johnson et al., 1993) on a SOMMA-type system. In practice this means that a known volume of sample is acidified by addition of phosphoric acid in order to transfer all dissolved inorganic carbon to CO_2. The resulting CO_2 is stripped out of the sample by bubbling the sample with an inert carrier gas (nitrogen) which subsequently is lead into a titration cell containing a solution including ethanolamine. The CO_2 reacts quantitatively with the ethanolamine to produce hydroxyethylcarbanic acid:

$$HO(CH_2)_2NH_2 + CO_2 \rightarrow HO(CH_2)_2NHCOO^- + H^+ \quad (10)$$

The hydrogen ions produced in this reaction is then titrated with hydroxide ions generated at the cathode due to an electrical current.

$$\text{Cathode reaction: } H_2O + e^- \rightarrow \tfrac{1}{2} H_2\,(g) + OH^- \quad (11)$$
$$\text{Anode reaction: } Ag\,(s) \rightarrow Ag^+ + e^- \quad (12)$$

The pH of the titration is monitored by measuring the transmittance of the indicator thymolphthalein which shows when the titration is finished. The amount of CO_2 in the sample is calculated based on the amount of used electrons. The ethanolamine is consumed during the analysis and is not regenerated between samples and after a certain amount of samples the solution has to be replaced.

The accuracy of the analysis is ensured by analysing Certified Reference Material (CRM) from A. Dickson, Scripps Institution of Oceanography (USA). The precision of the measurements was calculated as the standard deviation of duplicate samples.

3.1.1.2 Total alkalinity (A_T)

A_T was analysed by potentiometric titration with hydrochloric acid on a VINDTA 3S (Versatile Instrument for the Determination of Titration Alkalinity) system (Mintrop et al., 2000). During the titration the bases in the A_T definition are transferred to their acidic forms and the titration is monitored by a pH electrode. The result of the titration is evaluated with a Gran function (Gran, 1952). The accuracy was ensured by measuring CRMs and precision was calculated as for C_T.

3.2 Organic carbon in the ocean

Organic substances is chemically defined as compounds containing carbon, most of which are produced by biological processes. The sources of organic carbon (OC) in the ocean are either local (autochthonous sources), i.e. biological production, or land based (allochthonous sources, also called terrigenous). The OC from land is mainly transported into the oceans by river runoff, but additional transport ways are with

underground runoff , by direct erosion of the coast line (coastal abrasion) and by the atmosphere (eolian transport). Sinks for OC in the ocean are respiration, microbial degradation, burial in the sediments, and photooxidation. Concentrations of OC are highest in the surface water and close to the coasts (Eglinton and Repeta, 2004), suggesting a close coupling between production and degradation. The origin of the OC (marine vs. terrestrial) can be detected by determining its chemical composition (e. g. Dittmar and Kattner, 2003; Amon, 2004). Some of the OC present in the ocean cannot be degraded by the bacteria due to its chemical complexity and is referred to as refractory as compared to the easily degradable labile OC. The OC present in deep water, whatever its source, is considered to represent the refractory pool.

The measured quantities of OC in the ocean are operationally defined. The OC in sea water is divided into dissolved organic carbon (DOC) and particulate organic carbon (POC) by filtration and the fractions are thus determined by the pore size of the filter (usually 0.7μm). The major part of the OC in the ocean occurs as DOC, of which the world ocean contains approximately 680 Gt (Eglinton and Repeta, 2004). The large inventory is determined by the deep water concentration of DOC which is relatively constant world wide. The POC contribution to the OC in the ocean is 10-20 Gt while the marine biota only constitutes ~3 Gt (Eglinton and Repeta, 2004). In the Arctic Ocean the rivers carry large amounts of DOC into the shelf seas while most of the POC carried by the rivers is lost in the estuaries (the so called marginal filter (Lisitzin, 1995)). The sea water POC concentrations are thus much smaller than the DOC concentrations (e.g. Wheeler et al., 1997). There is still much to learn about DOC and POC concentrations, distributions, function in the ecosystem, and importance for climate change.

3.3 Oxygen

The study of oxygen in the ocean is less complicated than the study of the inorganic carbon system as it does not dissociate in water and thus only appears as dissolved oxygen (O_2). Oxygen is however affected by the same physical forces as inorganic carbon, advection, mixing etc. The marine oxygen and inorganic carbon cycles are intimately linked through the biological processes of production, respiration and remineralisation. In the atmosphere oxygen is consumed during burning of fossil fuel but due to its high concentration this is of little concern in the environmental change perspective. The concentration of dissolved oxygen in the ocean is determined by the atmosphere where it is a major component contrary to inorganic carbon for which the atmospheric concentration is determined by the oceans (Broecker and Peng, 1982).

4. Important processes for the marine carbon cycle

4.1 Biological production

Primary production has a profound impact on the marine carbon cycle. During photosynthesis CO_2 is taken up from the water and turned into organic matter:

$$CO_2 + NO_3^- + HPO_4^- + M^{2+} + H^+ + H_2O \rightarrow (CH_2O)_x(CH_2)_y(NHCH_2CO)_z(CHPO_4M) + O_2 \quad (13)$$

Note that the equation is unbalanced. Some marine organisms also form hard shells made of calcium carbonate:

$$[Ca^{2+}] + 2\,[HCO_3^-] \rightarrow CaCO_3 + CO_2 + H_2O \quad (14)$$

Note that it is the acid, CO_2, which is consumed during photosynthesis while the base, HCO_3^-, is consumed when shells are formed. The effect photosynthesis have on the inorganic carbon system is a decrease in C_T and fCO_2 and an increase in A_T and pH. Formation of shells, on the other hand, leads to a decrease of C_T, A_T and pH while the fCO_2 increases. It is important to remember that the building of $CaCO_3$ shells always occurs together with production of soft organic matter (photosynthesis). When shells are formed the net effect on the inorganic carbon system will thus be something intermediate between the effect of photosynthesis and formation of $CaCO_3$. The easiest way to trace shell building is through the change in A_T since this processes decrease A_T by two units per unit formed $CaCO_3$. The decrease in C_T and fCO_2 that follows biological production leads to increasing potential for CO_2 uptake from the atmosphere.

In the ocean biological production is detected through the change of the chemical composition of the water or through the accumulation of organic matter. Production in the water can be traced by a decrease in C_T, nitrate (NO_3), phosphate (PO_4^{3-}) or an increase in dissolved oxygen (O_2). Biologists often study primary production by the inclusion of different isotopes of carbon and nitrogen such as carbon-14 (^{14}C) and nitrogen-15 (^{15}N) into organic matter. When production is studied through the change of constituents the production in terms of carbon can be established by converting between the different elements included in organic matter according to Eq. 13. In order to do this conversion x, y and z in Eq. 13 has to be known. Redfield et al. (1963) studied the relation between C, N, and P and found the relation 106:16:1 on atom basis and this relation is known as the much used Redfield (Redfield-Ketchum-Richards, RKR) ratio. The oxygen consumed during remineralisation, and produced during photosynthesis, in relation to P, would be 212 atoms if only oxidation of carbon was

considered and 276 if oxidation of the nitrogen was included (Redfield et al., 1963). This gives a C:N:P:O_2 ratio of 106:16:1:-138 (note that -138 refers to the molecule O_2). Today there exist several studies of the 'Redfield ratio' made with different techniques and in different areas of the world ocean (Takahashi et al., 1985; Sambrotto et al., 1993; Anderson and Sarmiento, 1994; Broström, 1998; Daly et al., 1999; Körtzinger et al., 2001). There is still a debate on the correct ratio in organic matter but it is also recognised that the ratio is not constant but changes due to species, phytoplankton growth state, and environmental conditions such as nutrient availability.

Depending on the method used to estimate the biological production different types (amounts or rates) of production are achieved. This is mainly due to the fact that production and respiration goes on simultaneously and also that the major nutrients occur in more than one form. The common notions of production, how they are defined and how they can be measured are:

- Gross primary production: The total amount of carbon fixed during primary production (Platt et al., 1989). The only method for measuring gross primary production is the ^{14}C method (Steemann Nielsen, 1952), there have however been a lot of debate around this method and what it actually measures (e. g. Peterson, 1980).

- Net primary production: The gross primary production minus the respiration of the autotrophs (Platt et al., 1989). This is the part of primary production available for other trophic levels and can be calculated from remotely sensed information (Falkowski et al., 1998).

- Net community production: The gross primary production minus the respiration of both autotrophs and heterotrophs (Platt et al., 1989). Can be measured by increase in O_2 or depletion of C_T in the euphotic zone.

- New production: The part of primary production based on nitrate, NO_3^- (Dugdale and Goering, 1967). Can be measured by NO_3^- depletion in or flux into the euphotic zone and by ^{15}N assimilation experiments.

- Regenerated production: The part of primary production based on regenerated organic matter including nitrogen, ammonia (NH_4^+) and other dissolved organic nitrogen (Dugdale and Goering, 1967). Can be measured by ^{15}N assimilation experiments.

- Export production: The part of the primary production that is exported out of the euphotic zone. Under steady state conditions equal to net community and new production. Can be measured with sediment traps (N or C) and by consumption of O_2 below the euphotic zone

The difference in time and space scales of the different techniques calls for caution when the results are compared, production in the ocean can vary on almost all time and

space scales. The strength of the methods that consider the change in constituents in the water column is that the signal represents the integration of production over a longer time than the measurements made *in situ* in bottles and this decreases the uncertainty when extrapolations are done. The weakness with this approach is the uncertainty the horizontal advection of the water column introduces into the calculations since this often is difficult to quantify. The 'biological pump' refers to the fixation of carbon and nutrients into organic matter by phytoplankton in the euphotic zone and subsequent export to the deep ocean, which in practice makes it equal to the new and export production.

The size of the primary production is limited by several variables, e. g. light, nutrients, and grazing. At high latitudes light is limiting in winter due to the short days and low solar angle or indeed total absence of sunlight. Clouds, fog, ice, and snow can also decrease the amount of light that reaches the water, especially snow on top of ice. During the period of enough sunlight the depth of the mixed layer is important for the production since the amount of light decreases with increasing depth. Photosynthesis is proportional to light intensity and will thus decrease downwards in the water column while respiration (which is independent of light) is more or less constant with depth. When the mixed layer is deep the integrated respiration will be larger than the integrated production. According to Sverdrup (1953) the spring bloom in temperate and polar waters occurs when the depth of the mixed layer has decreased to the point where the integrated production exceeds the integrated respiration. The decrease and stabilisation of the mixed layer in spring has the opposite effect on nutrient limitation as compared to the light limitation. As the spring bloom proceeds in the shallow mixed layer the concentration of NO_3^- and PO_4^- decrease and sometimes even become depleted. New nutrients to fuel the new or export production can however be introduced from below during the productive season if the mixed layer deepens e.g. due to storms (Sakshaug and Slagstad, 1992). Grazing of the primary producers reduces their standing stock and thus the size of the primary production.

4.2 Air-sea exchange

The second process of great importance for the marine carbon cycle is air-sea gas exchange. The exchange of a gas across the air-sea interface is determined by the difference in concentration between the atmosphere and the ocean and how fast the transfer can occur;

$$F_A = k \cdot \Delta[A] \qquad (15)$$

where F_A is the flux of the gas A, $\Delta[A]$ is the difference between the present concentration in the water (A^{SW}) and the concentration in the water if it is in equilibrium with the atmosphere (A^{EQ}) and k is the transfer velocity (also called piston velocity). For oxygen $\Delta[A]$ is expressed as ($[O_2]^{SW}$ - $[O_2]^{EQ}$) while $\Delta[A]$ for CO_2 is expressed as $K_0 \cdot (fCO_2^{SW} - fCO_2^{ATM})$ which is equal to ($[CO_2\ (aq)]^{SW} - [CO_2\ (aq)]^{EQ}$). The water concentration (in this case of CO_2 and O_2) varies more than the atmospheric

concentration and the concentration in the water is thus the most important factor for the air-sea exchange since it determines the net direction of the flux. The saturation concentration or solubility of a gas in sea water is dependent on temperature, salinity, and pressure.

Since the air-sea exchange is very difficult to measure directly the value of the transfer velocity is estimated by indirect techniques, The widely used estimates of transfer velocity are based on measurements of natural and/or deliberately released tracers, but it can also be estimated with the eddy correlation method, the inertial dissipation method, and the profile method (Donelan and Wanninkhof, 2002 and references therein). The transfer velocity depends on the molecular diffusivity of the gas, the kinematic viscosity of water and the turbulence at the air-water interface, which in turn depends on several factors such as wind speed, surface film, waves, bubbles etc (e.g. Jähne et al., 1987). Many of the factors influencing the turbulence are difficult to measure and thus conceptual models are used to parameterize the transfer of gas. These models include the stagnant (thin) film model, the surface renewal model, and the boundary layer model (Ledwell, 1984 and references therein).

In order to be able to calculate air-sea exchange relatively easily the transfer velocity is usually parameterized in terms of wind speed since wind speed has a major effect on the turbulence. Wind speed is also easily measured and available for large areas over a long period of time. Several parameterizations of transfer velocity based on wind speed exist; in this thesis the parameterization by Wanninkhof (1992) has been used:

$$k = 0.39 \cdot u_{10}^{2} \cdot \left(\frac{Sc}{Sc_{20}} \right)^{-0.5} \qquad (16)$$

where u_{10} is the wind speed at 10 m above the surface, Sc_{20} is the Schmidt number of the gas in sea water at 20º C (660 for CO_2 and 600 for O_2, see e.g. Wanninkhof (1992)) and Sc is the Schmidt number at the present temperature. The Schmidt number is defined as the ratio between the kinematic viscosity of water and the molecular diffusivity of the gas in question. The number 0.39 is a proportionality factor between the transfer velocity and the wind speed, in this case for long term wind speeds. If short term or instantaneous wind speeds are used for the calculations a proportionality factor of 0.31 should be used instead (Wanninkhof, 1992). The averaging of the wind speeds may have a large impact on the air-sea fluxes and care should be taken when selecting the appropriate parameterization of k. Other parameterizations of the transfer velocity (Figure 4) can be found in Smethie et al. (1985), Liss and Merlivat (1986), Wanninkhof and McGillis (1999) and Nightingale et al. (2000). The different parameterizations agree within a factor of three on the size of the transfer velocity (Donelan and Wanninkhof, 2002), but this is a large uncertainty which indicates the complexity of the subject. In some types of calculations this uncertainty is too large, e.g. when the CO_2 uptake by the ocean is calculated in the context of climate change, in these cases an alternative approaches may be used.

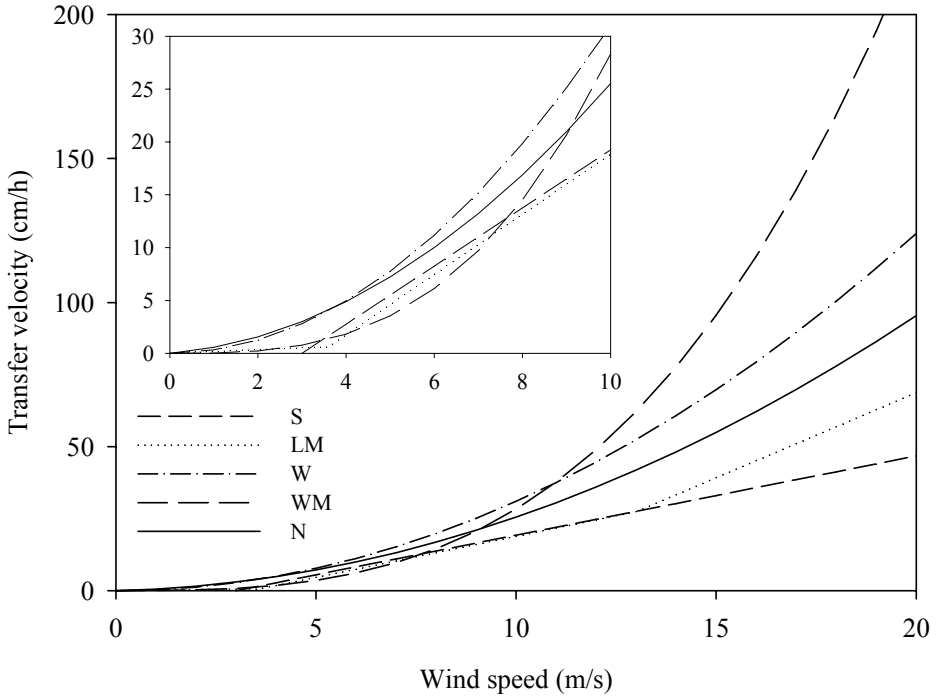

Figure 4: Different parameterisations of the transfer velocity. Abbreviations in the legend are S for Smethie et al. (1985), LM for Liss and Merlivat (1986), W for Wanninkhof (1992), WM for Wanninkhof and McGillis (1999), and N for Nightingale et al. (2000). Inlay is an enlargement of the wind speeds up to 10 m/s.

One such is the property change in the ocean; after relevant physical, chemical and biological processes have been taken into account this will represent the exchange with the atmosphere.

The transfer velocity estimation by Wanninkhof (1992) was based on CO_2 exchange but the air-sea exchange of CO_2 and O_2 are slightly differently affected by some processes, however, due to the difference in solubility and atmospheric concentration between the two. Due to its low solubility the transfer of O_2 is considerably more affected by bubble injection than the highly soluble CO_2. Thus corrections are sometimes made for injection of bubbles when air-sea O_2 fluxes are calculated. In an equilibrium situation the injection of bubbles can support super saturation of a gas. This super saturation will be greatest for the less soluble gases such as oxygen where bubble injection can maintain a super saturation of over 1 % (Woolf and Thorpe, 1991). The super saturation is much smaller for CO_2 and this correction is thus not necessary when calculating CO_2 fluxes but necessary for O_2 fluxes. The result of the correction proposed by Woolf and Thorpe (1991) is an increasing super saturation with increasing wind speeds with a 1 % super saturation occurring at a wind speed of 9 m/s.

The air-sea flux of a gas is also affected by changes in sea level pressure and this has to be considered when fluxes are calculated in areas with changing sea level pressure

(SLP), e.g. in the Nordic Seas. The correction is done since the variation in SLP induces a variation in the atmospheric concentration (and thus saturation concentration) of the gas that is so large that it can not be neglected (Najjar and Keeling, 2000). When calculating CO_2 flux this correction is unnecessary since fCO_2 in itself is dependent on the total pressure. The effect on O_2 at high latitudes is to increase the $\Delta[O_2]$ (the difference between atmosphere and ocean) on annual scale and to decrease the seasonal amplitude of $\Delta[O_2]$ (Najjar and Keeling, 1997). When calculating both CO_2 and O_2 air-sea fluxes corrections can also be made for the skin temperature (the temperature in the very thin uppermost layer of the water) since this is slightly lower compared to the temperature of the bulk of the water (Saunders, 1967; Fairall et al., 1996). Such a correction will give a slightly different saturation concentration; this has however not been included in this thesis.

The cooling of water that occurs along the route of the Atlantic Water as it flows north creates a potential for annual net uptake of both CO_2 and O_2. The uptake of CO_2 is also increased by the biological production that lowers the fCO_2 in the water during the productive season. The uptake of CO_2 due to the cooling of the surface water (and consequent increase in solubility) is often referred to as the 'physical pump' (compare 'biological pump').

Extra uptake of CO_2 from the atmosphere has been reported in brine water in Storfjorden (Anderson et al., 2004). This extra uptake was believed to be promoted by formation of ice in the surface water. They believed that this faster uptake was caused by the salt rejection during ice formation and the following sinking of the very surface water in which the addition of salt increased the density. Rysgaard et al. (2007) observed elevated pCO_2 and C_T in the surface water underlying sea ice and attributed this to rejection of C_T from the ice. The rejected C_T may then be carried to deeper layers in the surface water that has achieved increased density due to the rejection of salt from the ice.

4.3 Environmental change

Environmental change is a concept that refers to change in chemical and biological parameters. Some of these changes are, similar to some parts of climate change, due to human activities. Among these activities is emission of chemicals, intentional or accidental, including CO_2, nutrients, heavy metals, pesticides, nuclear material etc. Humans also affect the environment by interfering in ecosystems, via hunting and fishing, and by changing biotopes e.g. by deforestation, agriculture, and aquacultures.

The result of the rising atmospheric CO_2 concentrations in the ocean is an increase in the surface water fCO_2 and C_T concentrations while the pH decreases. During the last 25 years the oceans have taken up ~30% or ~2 Gt C/yr of the anthropogenically emitted CO_2 (Solomon et al., 2007). Since the start of the industrial revolution the oceans have in total taken up ~ 50% of the anthropogenically emitted CO_2 (Sabine et al., 2004), this uptake has resulted in a total anthropogenic carbon inventory of ~120

Gt C in the oceans today (Sabine et al., 2004). The increase in C_T concentrations has lead to an average pH decrease of 0.1 units in surface water (Solomon et al. 2007). Changes in C_T and pH change the buffer capacity of the surface water. The Revelle factor is often used to quantify the buffer capacity:

$$\text{Revelle factor} = \left(\frac{\delta\,[CO_2(aq)]}{[CO_2(aq)]}\right) \Big/ \left(\frac{\delta\,C_T}{C_T}\right) = \left(\frac{\delta\; fCO_2}{fCO_2}\right) \Big/ \left(\frac{\delta\,C_T}{C_T}\right)$$

In oceanic waters today typical values of the Revelle factor lie between 8 and 15 (Zeebe and Wolf-Gladrow, 2003). The lower the Revelle factor is the lower the fractional change in CO_2 (aq) or fCO_2 is compared to the fractional change in C_T, which means that the water has a high capacity to buffer. The two main effects of increasing anthropogenic CO_2 concentrations in the atmosphere on the surface ocean are increasing fCO_2 and temperature. If all other variables are constant increasing fCO_2 increases the Revelle factor while increasing temperatures results in a decrease of the Revelle factor (Zeebe and Wolf-Gladrow, 2003). For a more thorough discussion of the Revelle faction the reader is refered to Zeebe and Wolf-Gladrow (2003) and Butler (1982) A decrease in the capacity of the surface water to buffer leads to decreasing potential for uptake of atmospheric CO_2 and the effect is a positive feedback on the increasing atmospheric CO_2 concentrations.

The buffer capacity feedback is only one of the potential feedbacks from the marine inorganic carbon cycle on atmospheric CO_2 concentrations; others include the solubility, carbon overconsumption, and calcification feedbacks. The decreasing solubility due to increasing temperatures and changing salinity is a positive feedback on the atmospheric CO_2 concentrations while the two other feedbacks are negative. Overconsumption of carbon (Toggweiler, 1993) in relation to nitrate and phosphate increases the potential of export production to remove carbon from the surface waters to depth. Decreasing pH leads to a decreasing potential for calcification and since calcification increases the fCO_2 decreasing calcification acts as a negative feedback. The sizes of the different feedbacks are not well known.

5. The study area

5.1 Hydrography

5.1.1 General circulation in the Arctic Mediterranean

The Arctic Mediterranean (Figure 4) consists of the deep basins of the Arctic Ocean (AO), the surrounding shelf seas and the Nordic Seas. The area is restricted by the shallow Bering Strait, the Canadian Archipelago and the Greenland-Scotland Ridge. The main exchange with the surrounding area takes place across the Greenland-Scotland Ridge where the relatively warm and salty Atlantic Water enters the area and cold and fresh surface water exits along with the dense overflow waters (Hansen and Østerhus, 2000). The surface circulation of the Nordic Sea is dominated by the northward flow of Atlantic Water in the Norwegian Atlantic Current (NwAC) in the east and the southward flow of polar waters in the East Greenland Current (EGC) in the west (Blindheim and Østerhus, 2005). In the northern Norwegian Sea the Atlantic Water divides into two branches, one branch passes through the Barents Sea and the other enters the deep AO through Fram Strait and flows eastwards along the northern Barents Sea slope (Rudels et al., 1999). The two branches unite again north of the Kara Sea (Schauer et al., 2002b), by the time the two branches meet they have submerged below fresher and colder water and been modified by cooling and mixing with low salinity waters. They travel around the deep AO counter-clockwise as a subsurface boundary current (Rudels et al., 1999). The surface circulation in the AO is dominated by the transpolar drift from the eastern Arctic shelf seas toward Fram Strait and the Beaufort gyre in the Canadian basin. As the EGC exits the AO it carries surface, intermediate, and deep waters from the central AO into the Nordic Seas and toward the North Atlantic (Rudels et al., 2004). Some of the modified, intermediate layer of the Atlantic Water finally exits the Arctic Mediterranean as part of the dense overflow waters which together with dense water formed in the Labrador Sea forms the North Atlantic Deep Water, the densest water formed in the North Atlantic (Dickson and Brown, 1994).

5.1.2 Atlantic and Coastal Water in the Norwegian Sea

The current structure of the Atlantic Water close to the Iceland-Scotland ridge is complex (Hansen and Østerhus, 2000) but further north it forms two current cores, the Faroe Current in the west and the Norwegian Atlantic Slope Current in the east (Orvik and Niiler, 2002). The two current cores constitute the eastern and western cores of the NwAC which are fairly distinct in the southern Norwegian Sea.

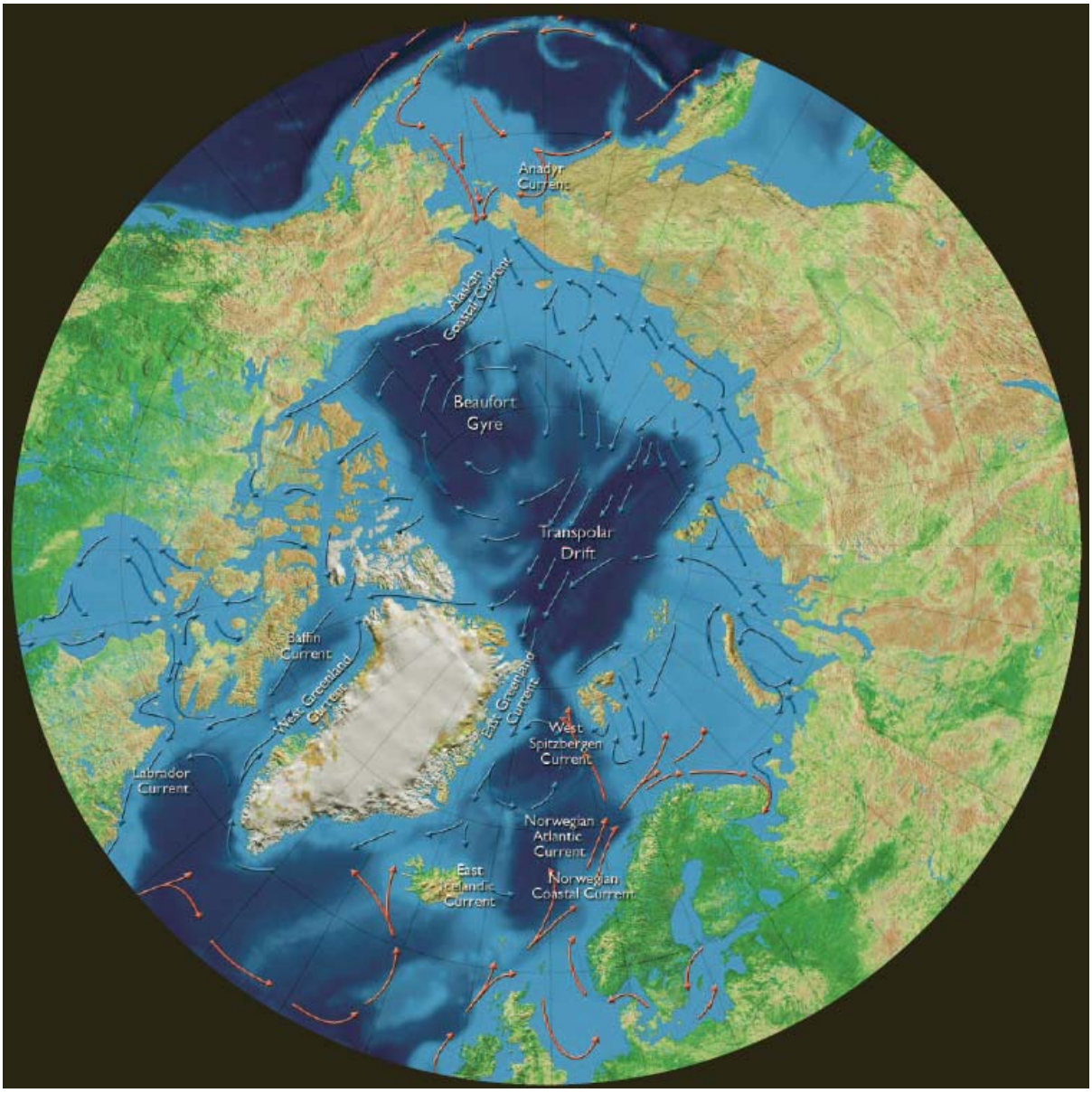

Figure 5: The surface circulation in the Arctic Mediterranean. Red arrows represent warm water while blue arrows represent cold water (modified from ACIA, 2005).

As the NwAC reaches about 70º N it splits into two branches, one branch continues northwards along the west coast of Svalbard as the West Spitsbergen Current (WSC) and the other branch turns east into the Barents Sea Opening (BSO; the passage between Norway and Svalbard) as the North Cape Current (NCC). The water in the NwAC is to the west bordered by the Arctic Front separating the Atlantic Water from the colder and less saline Arctic Surface Water. On the eastern side, and inshore of the NwAC, the Norwegian Coastal Current (NwCC) flows along the Norwegian coast. The NwCC has its origin in the Baltic Current in Skagerrak and it carries water from the Baltic and North Seas mixed with Atlantic Water. As the NwCC flows northwards along the Norwegian coast the exchange with the NwAC is large and the current gradually loses its characteristics (Gascard et al., 2004).

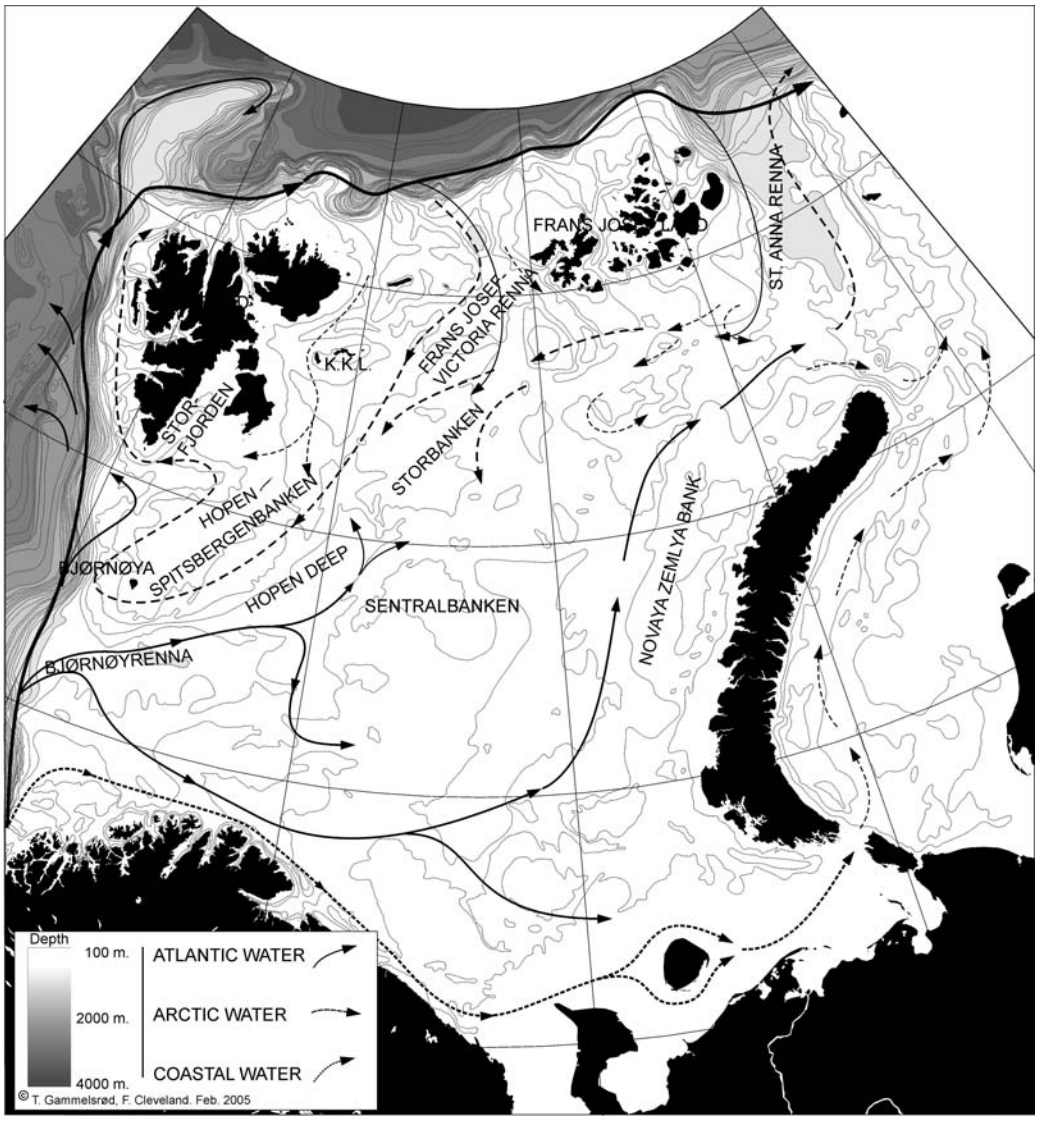

Figure 6: Map of the Barents Sea with surface currents and some topographical features. Solid arrows represent Atlantic Water, dashed arrows Arctic Water and dotted arrows coastal water. K.K.L. is Kong Karls Land. Figure by courtesy of T. Gammelsrød and F. Cleveland, Geophysical institute, University of Bergen.

5.1.3 Barents Sea circulation

The NCC enters the Barents Sea along Bear Island Trough (Bjørnøyrenna; Figure 6) at the eastern extend of which the current divides in two, one part continues east while the other part turns north into Hopen Deep and divides into smaller branches. As the Atlantic Water moves north and north-eastwards it encounters the Arctic Water at the Polar Front. The Polar Front is controlled by topography in the western part of the Barents Sea while it is more diffuse in the eastern Barents Sea. The Arctic Water enters the Barents Sea in the northern (between Svalbard and Franz Josef Land) and eastern (between Franz Josef Land and Novaya Zemlya) passages and flows south and south-westwards. When the Atlantic Water and Arctic Water meet, the Atlantic Water

is submerged below the fresher and lighter Arctic Water and continues east and north-eastwards as a subsurface current.

The southern and northern parts of the Barents Sea are often referred to as the Atlantic and Arctic domains due to the dominance of the Atlantic and Arctic water masses in the south and north respectively. The Arctic domain is seasonally ice covered while the Atlantic domain remains ice free also in winter due to the high sea surface temperatures of the Atlantic Water. The extent of the ice cover is however variable and ice can drift into the Atlantic domain due to wind but as soon at it encounters Atlantic Water it will start to melt. The sea ice in the Barents Sea is formed locally but some is imported, mainly from the Kara Sea but also directly from the AO in the north (e.g. Korsnes et al., 2002; Martin and Augstein, 2000). At the Polar Front but also throughout the Barents Sea mixing occurs between the Atlantic and Arctic water masses and/or freshwater (sea ice melt water and river runoff), resulting in the formation of local water masses (e.g. Loeng, 1991; Pfirman et al., 1994). The Atlantic Water that exits the Barents Sea is colder, fresher, and denser as compared to the entering water mass due to the heat loss and admixture of low salinity water it experiences as it flows across the Barents Sea. Another important water mass transformation in the Barents Sea is the formation of brine water. The major part of the brine water forms in the polynyas, areas within the sea ice that are opened by wind or currents. When the sea water in the polynyas is exposed to the atmosphere the intense heat loss results in rapid sea ice growth. During the ice formation salt is expelled from the ice, increasing the salinity of the underlying cold surface water. The elevated salinity increases the density of the water resulting in convection. In the Barents Sea brine water is formed from some type of Arctic Water or Coastal Water (Schauer et al., 2002a; Skogseth et al., 2005).

The brine water formed in Storfjorden enters the Norwegian Sea and flows north into Fram Strait, where it has been observed as deep as 2000 m (Quadfasel et al., 1988), but the major part of the dense modified Atlantic Water and brine water formed in the Barents Sea enters the deep AO through the northern and eastern passages (Schauer et al., 1997). These waters contribute to the intermediate layer in the AO and can be found between 200 and 1300 m in the eastern Nansen Basin (Schauer et al., 1997; Rudels et al., 2000). How deep down into the Nansen Basin brine water from the Barents Sea can penetrate is still uncertain. Plumes of brine water such as the ones found by Schauer et al. (1997) northwest of Franz Josef Land may, if they are dense enough, at least penetrate into the Atlantic Layer. The draining of brine water from the shelf in such plumes is intermittent in time and space and thus difficult to quantify. The modified Atlantic Water on the other hand is a steady flow that mainly enters the Nansen Basin through St. Anna Trough (St. Anna Renna Figure 6). As the Atlantic Water exits St. Anna Trough it turns eastwards along the continental slope and displaces the Atlantic Water from the Fram Strait branch away from the continental slope (Schauer et al., 2002b). The volume flow of the Barents Sea branch of Atlantic Water seems to be at least as large as that of the Fram Strait branch (e.g. Maslowski et al., 2004 and references therein). The difference between the two branches when they enter the deep AO is the larger heat content of the Fram Strait branch; the Barents Sea

branch has lost more heat after the branching of the NwAC during its passage of the Barents Sea than the Fram Strait branch on its passage west of Svalbard. If the Barents Sea branch has a larger volume transport it provides larger amounts of salt to the AO (Maslowski et al., 2004).

5.2 Climate change in the Arctic

The Arctic average air temperature has increased almost twice as fast as the global average temperature during the last 100 years, with significant decadal variability (IPCC, 2007). This implies that the increase in the Arctic does not simply follow the global increase but is affected by regional processes. The temperature increase has been 2-3º C since the 1950s, largest over land areas and during winter (ACIA, 2005). The results of the increasing temperature in the Arctic has been melting of glaciers, thawing of permafrost and decreasing sea ice extent (ACIA, 2005). The sea ice extent has decreased at least during the last 25 years, e. g. Johannessen et al. (2004) found a decrease of 7.4 % from 1978 to 2003. The effect of these changes can already be seen in the Arctic environment (Weller, 1998) and includes effects on ecosystem, economy and cultures. According to the ACIA report (ACIA, 2005) projections for future changes indicate further air temperature increases of 2-3º C by 2050 with following increasing sea surface temperatures in ice free areas. The sea ice extent will decrease with 15-20 % in winter and 30-50 % in summer compared to the present, there is even one model that predicts an ice free AO in summer by 2050 (ACIA, 2005). The result of the difference between summer and winter will be a larger seasonal ice zone which undergoes seasonal freezing and melting of sea ice compared to the present.

Even if the decrease in sea ice extent is projected to be smaller in winter than in summer it is possible that the Barents Sea will be totally ice free by the middle of this century, it is also possible that the western AO where the Atlantic Water inflow in the Fram Strait branch takes place will remain ice free during winter. The disappearance of the ice cover will have effects on surface circulation, water mass properties and mixed layer depth. Ice cover also comprises a hindrance for air-sea exchange and absorbs much light, reducing primary production. Since the production of dense waters in the Arctic Mediterranean is important for the thermohaline circulation through the formation of North Atlantic Deep Water changes in water mass properties in the Arctic Mediterranean may have large consequences.

The amount and properties of inflowing Atlantic Water to the Arctic Mediterranean is of large importance both for its heat and salt balance and for the carbon cycle. Changes in the Atlantic Water inflow has e.g. been observed in changing core temperatures along the Atlantic Water route northwards (Holliday et al., 2007) and changing front position between Atlantic and Pacific Water in the central AO (McLaughlin et al., 1996; Morison et al., 1998). The inflow of Atlantic Water to the Nordic Seas is projected to increase slightly by 2020 and by ~12 % to the Barents Sea by 2070 (ACIA, 2005). The decreasing sea ice cover and increasing inflow of Atlantic Water

will lead to an 'Atlantification' (sensu Wassmann et al., 2004) of the Barents Sea, meaning an expansion of the Atlantic domain northwards.

5.3 Air-sea CO_2 exchange and biological production in the study area

The Norwegian, Iceland and southern Barents Seas are permanently ice free while the rest of the Arctic Mediterranean to a smaller or larger degree is covered by seasonal and/or multiyear sea ice. The presence of the ice is of large importance for the carbon cycling in the area. An ice cover is generally considered as an effective barrier to air-sea CO_2 exchange even though recent observations have shown transport of CO_2 through ice (Semiletov et al., 2004; 2007). Exchange of CO_2 with the atmosphere in the permanently ice covered regions thus mainly occurs through leads and polynyas.

The ice free parts of the Arctic Mediterranean and the seasonally open waters generally act a sink for atmospheric CO_2 (Table 1) although smaller areas can act as sources. The chemical potential for uptake of atmospheric CO_2 is created by cooling of the water as it is transported north and/or primary production. The amount of primary production and its export or remineralisation in the mixed layer is thus of large importance for the amount of CO_2 taken up from the atmosphere. On an area basis the strongest sinks in the Arctic Mediterranean are located in the Chukchi and Greenland Seas but the Iceland, Barents and Norwegian Seas are also clearly acting as sinks (see Table 1). The Russian shelf seas (the Kara, Laptev, and East Siberian Seas) act as weaker sinks, or indeed sources, compared to the other areas due to their heavy ice cover and the large discharge of freshwater they receive from rivers. The river plumes tend to be sources of CO_2 to the atmosphere since river water contain high concentrations of terrigenous organic carbon that can be remineralised making the water net heterotrophic (Nitishinsky et al., 2007; Semiletov et al., 2007). Areas removed from the river plumes on the other hand tend to be sinks for atmospheric CO_2. This is illustrated in Semiletov et al. (2007) where they found that the western part of the East Siberian Sea, which is heavily influenced by river runoff, acted as a source of CO_2 while the eastern Pacific Water influenced part of the sea acted as a sink. Little is known about the CO_2 exchange in the Kara Sea; the *Eastwind* expedition in 1967 found pCO_2 values well below the atmospheric (down to -160 ppm) in the larger part of the Kara Sea (Kelley, 1970) and this indicate that the area acted as a sink at that time.

Lundberg and Haugan (1996) found a net CO_2 uptake in the entire Arctic Mediterranean of 110 Tg C/yr while Anderson et al. (1998) calculated a flux of 24 Tg C/yr into the Arctic Ocean. The difference of these two estimates, 86 Tg C/yr, should then be ascribed to the Nordic Seas. Given the large sinks in the Barents and Chukchi Seas (Table 1) a total uptake of 24 Tg C/yr in the Arctic Ocean may seem low and would require substantial loss of CO_2 within the ice covered regions. Bates, (2006) has added their estimate for the Chukchi Sea to earlier mass balance estimates of other areas within the Arctic Ocean and found an total uptake of ~66 Tg C/yr. The uptake of CO_2 in the Arctic Ocean has earlier been neglected on a larger scale since the air-sea

exchange has been assumed to be small in the area due to the hindrance of the ice cover. If considerable amounts of CO_2 are transported through sea ice it will change the estimate of net uptake of CO_2 in the Arctic Ocean. Summer data of pCO_2 under the ice in the deep Arctic Ocean show undersaturation (Jutterström, pers. com.), this gives the potential for uptake of CO_2, but if exchange of CO_2 through sea ice will result in a net uptake or outgassing is uncertain due to lack of winter data. The global uptake of CO_2 from the atmosphere is today 2.2 ±0.5 Gt C/yr (Denman et al. 2007), if the uptake in the Arctic Ocean is assumed to be 66 Tg C (Bates, 2006) the uptake in the Arctic Ocean constitutes 3 % of the global while the 110 Tg C/yr estimated by Lundberg and Haugan (1996) corresponds to 5%.

The sea ice cover in the Arctic Mediterranean is as important for the primary production as for CO_2 exchange. In the ice free areas of the Nordic Seas and the Barents Sea, production starts when the mixed layer has been decreased sufficiently due to thermal heating. The spring bloom continues as long as there are enough nutrients. After the spring bloom production decreases but can increase again if the mixed layer deepens and new nutrients are injected from deeper layers e.g. due to storms (Sakshaug and Slagstad, 1992). In the marginal ice zone the water column is stratified by ice melt water, production can start as soon as the ice starts to melt and the peak of production follows the retreating ice. The rate of production can be very high in the marginal ice zone bloom but the bloom is short so the annual production can be much smaller than in the open water further south. The stratification is strong in the marginal ice zone and difficult to erode and the spring bloom thus contributes the main part of the annual production (Wassmann, 2006b).

In the Arctic Mediterranean, the highest production on the annual scale occurs in the Chukchi Sea (Table 2 and Sakshaug, 2004) where the nutrient rich water from the Pacific Ocean enters the Arctic Ocean. The other highly productive area within the Arctic Ocean is the Atlantic domain of the Barents Sea while the Arctic domain of the Barents Sea and the rest of the ice covered central Arctic Ocean is much less productive. The figures presented in Table 2 are production estimates based on water column changes and in the Russian shelf seas no information of this kind is available. Sakshaug (2004) presented data on ^{14}C-production indicating that the production in these areas is low. In the ice covered areas production by ice algae also takes place within the ice, in seasonally ice covered areas this production generally only accounts for a few percent of the total water column plus ice production while it in multiyear ice can account for the major part of the production (Sakshaug, 2004; Carmack et al., 2006 and references therein; Wassmann et al., 2006a). The productivity of the central Arctic Ocean, although small, has been adjusted upwards in later years since earlier estimates did not include the ice algae production (Sakshaug, 2004).

The fate of the organic matter resulting from primary production depends on the physical and biological conditions where it is produced; it can be utilized by other organisms, transported away from the production area, or buried in the sediments.

Table 1: Uptake of atmospheric CO_2 estimated from measurements in the major seas of the Arctic Mediterranean and total amount of CO_2 uptake if the uptake is extrapolated to the entire area of the respective sea. Areas of the central Arctic Ocean and its shelf seas are taken from Jakobsson (2002) while the areas for the Nordic Seas Simonsen and Haugan (1996).

	CO_2 uptake g C/m^2	Period	Reference	Area 10^3 km^2	Total uptake 10^{12} g C/m^2
Norwegian Sea	36	annual	Skjelvan et al. (2005)	1390	49
	20	winter[1]	Olsen et al. (2003)		28
	32	annual	Falck & Anderson (2005)		26
Greenland Sea	54	annual	Hood et al. (1999)	810	31[2]
	53	annual	Anderson et al. (2000)		30[2]
	40-50	winter[1]	Olsen et al. (2003)		23-28[2]
	67-85	annual	Skjelvan et al. (2005)		38-48[2]
	52	annual	Nakaoka et al. (2006)		29[2]
Iceland Sea	69	annual	Skjelvan (1999)	510	25
	40-50	winter[1]	Olsen et al. (2003)		20-26
Barents Sea	44[3]	during passage	Fransson et al. (2001)	1512	9.2[4]
	29[3]	seasonal[5]	Kaltin et al. (2002)		29[6]
	13[7]	seasonal[5]	Kaltin et al. (2002)		6.2[6]
	46	annual	Nakaoka et al. (2006)		47[13]
	51[3]	annual	Omar et al. (2007)		51[6]
Chukchi Sea	86[8]	during passage	Kaltin & Anderson (2005)	620	22[4]
	49	ice free period	Bates et al. (2005)		29[9]
	64	annual	Bates et al. (2005)		38[9]
Kara Sea	?			926	?
Laptev Sea	3[10]	ice free period	Nitishinsky et al. (2007)	498	1.5
East Siberian Sea	-0.4[10]	ice free period	Nitishinsky et al. (2007)	987	-0.43
Arctic Mediterranean	10[11]	annual	Lundberg & Haugan (1996)	10720[12]	110
Arctic Ocean	2.5[11]	annual	Anderson et al. (1998)	9541	24
Nordic Seas	19[11]	annual	Anderson et al. (1998)	4489	86

1. October to March. 2. Assuming 30% ice cover. 3. In Atlantic Water only. 4. Combined with volume transport in original publication. 5. Late winter to late June/early July. 6. Assuming that the Atlantic Water covers 2/3 and Arctic Water 1/3 of the total area. 7. Recalculated from published values in Arctic Water. 8. Estimate for passage from the water enters the Bering Sea shelf until it reaches the northern Chukchi Sea shelf slope. 9. Calculated based on an area of 595 km^2 in the original publication. 10. Recalculated from the original publication assuming an ice free season of 120 days. 11. Calculated from the total flux and area. 12. Area taken from Bates et al. (2006). 13. Assuming this flux is representative for the Atlantic Water.

Table 2: Primary production estimated based on water column measurements in the major seas of the Arctic Mediterranean and total amount production if the production is extrapolated to the entire area of the respective sea. Areas of the central Arctic Ocean and its shelf seas are taken from Jakobsson (2002) while the areas for the Nordic Seas Simonsen and Haugan (1996). E=Export production, N=New production, NCP=Net Community Production, T=Total production.

	Production g C/m^2	Period	Reference	Area 10^3 km^2	Total production 10^{12} g C/m^2
Norwegian Sea	24-32^{NCP}	annual	Skjelvan et al. (2001)	1390	33-45
	62^{NCP}	annual	Falck & Anderson (2005)		86
	14-18^{E}	annual	Falck & Anderson (2005)		20-25
	79^{NCP,1}	annual	Falck & Gade (1999)		110
Greenland Sea	34^{N}	annual	Anderson et al. (2000)	810	19[2]
	62^{N}	seasonal[3]	Rey et al. (2000)		35[2]
Nordic Seas	36^{NCP}	annual	Falck and Gade (1999)	ice free area	
Barents Sea	62.5^{E}	during passage	Fransson et al. (2001)	1512	9.6[4]
	71^{N,5}	seasonal[6]	Kaltin et al. (2002)		72[7]
	32^{N,8}	seasonal[6]	Kaltin et al. (2002)		16[7]
	21-30^{NCP}	annual	Olsen et al. (2003)		21-30[7]
Chukchi Sea	68^{E}	during passage	Kaltin & Anderson (2005)	620	17[4]
	~120-240	ice free period	Bates et al. (2005)		8.9-17.8[9]
Canadian Basin	2.2-6.5	seasonal [10]	Bates et al. (2005)		
Nansen Basin	19$^{N, 11}$	annual	Zheng et al. (1997)		
	3$^{N, 12}$				
Arctic Ocean	0.6-1.3^{E}	annual	Anderson et al. (2003)	4489	2.7-5.8

1. Estimate for Ocean Weather Station M. 2. Assuming 30% ice cover. 3. From May to August. 4. Combined with volume transport in original publication. 5. In Atlantic Water only. 6. Late winter to late June/early July. 7. The total production is calculated assuming that the Atlantic Water covers 2/3 and Arctic Water 1/3 of the total area. 8. Recalculated from published values in Arctic Water. 9. Estimate is for eastern Chukchi Sea shelf and slope region. 10. A growing season of 120 days is assumed in the original publication. 11. Southern part. 12. Northern part.

The amount of organic matter that reaches the sediments is affected by the zooplankton grazing; the larger the grazing is the smaller the fraction of organic matter is that reaches the sediments. The abundance and temporal distribution of the zooplankton stock can thus have large implications for the carbon fluxes, especially in areas with a short and intensive bloom (the concept of match and mismatch; Sakshaug, (2004)). The large primary production in the Chukchi Sea and southern Barents Sea can sustain large production of zooplankton, fish and animals higher up in the food chain. In the Arctic Ocean, burial of organic matter of marine origin (in contrast to organic matter from land sources) is highest in the Chukchi and Barents Seas (Stein and Macdonald, 2004).

Some of the organic matter produced on the shelves is transported out into the deep Arctic Ocean. Both the Barents and Chukchi Seas, being inflow shelves, export considerable amounts of water to the central Arctic Ocean. Shelf pumping is a concept that refers to the carbon enrichment of water on a shelf by air-sea uptake and biological production followed by export of this water to depth in the nearby open ocean so it loses contact with the atmosphere. Cooling and uptake of CO_2 along with large primary production occurs both in the Chukchi and southern Barents Sea and gives the potential for transport of both organic and inorganic carbon of shelf origin into the central Arctic Ocean. Olli et al. (2007) presented the notion that the central Arctic Ocean is net heterotrophic due to transport of organic matter of both terrigenous and primary production origin from the shelves.

6. Results and discussion

This thesis is based on four papers, three of these papers study processes occurring in the Barents Sea and one in the Norwegian Sea. This section will first focus on the main findings in the Barents Sea and then move to the Norwegian Sea.

To learn more about the carbon fluxes into, out of and within the Barents Sea a carbon budget was constructed for the area in paper I. The budget includes advection of C_T, DOC and POC, air-sea exchange, river runoff and sedimentation. Information about these variables in and around the Barents Sea is limited and this is the first attempt to combine the available information in the form of a budget. The results show that $\sim 5600 \cdot 10^6$ t C is exchanged through the boundaries of the Barents Sea during one year. There is a net import of water and carbon to the Barents Sea through the BSO and a net export through the other three passages (see Figure 6). Considering all passages into the AO the Barents Sea net C_T export is $\sim 2500 \cdot 10^6$ t C/yr of which $\sim 1800 \cdot 10^6$ t C/yr (72%) is in subsurface water masses and thus sequestered from the atmosphere. The Barents Sea is also a source of organic carbon to the AO; it exports $\sim 80 \cdot 10^6$ t C/yr to the AO of which $\sim 20 \cdot 10^6$ t C/yr is labile. It have been proposed that the central, deep AO is net heterotrophic (Olli et al., 2007) and the net export of labile organic matter from the Barents Sea could support such a net heterotrophy.

Advection of C_T is the single largest component of the carbon budget and the Atlantic Water and the modified Atlantic Waters are the most important water masses for the advection of carbon. These water masses contribute the major part of the volume flow through the two main passages into (Norway-Svalbard) and out of (Franz Josef Land-Novaya Zemlya) the Barents Sea, they also have the highest C_T concentrations due to their high salinity. In addition the strength of the inflow of Atlantic Water controls the areal extent of the Atlantic and Arctic domains within the Barents Sea which in turn determine the amounts of primary production and uptake of atmospheric CO_2. The advection of organic carbon was the second largest contributor to the budget followed by the sources and sinks within the Barents Sea itself, uptake of atmospheric CO_2, river runoff, land sources, and finally burial in the sediments. Considering the difference in volume flows the net advective influx of carbon through the BSO is similar to the flux estimated by Anderson et al. (1998) through the same passage. The net advective of carbon influx through the BSO is also about half of the carbon influx in the North Atlantic Water and Coastal Water Lundberg and Haugen (1996) estimated across the Iceland-Scotland ridge.

As the Atlantic Water flows across the Barents Sea its carbon content increase due to uptake of CO_2 from the atmosphere and remineralisation of export production. The increase in the carbon content of the modified Atlantic Water is important since it is

this water that contributes to the intermediate Atlantic Layer in the AO and the carbon it contains is sequestered from the atmosphere for decades to hundreds of years. In modified Atlantic Water the Barents Sea exports ~$1800 \cdot 10^6$ t C/yr to the AO, where $30 \cdot 10^6$ t C/yr of this is CO_2 taken up from the atmosphere within the Barents Sea. The major part of this carbon, $23 \cdot 10^6$ t C/yr, enters the modified Atlantic Water as export production which is converted to C_T.

In paper II seasonal CO_2 air-sea exchange and new production was studied in the north-western Barents Sea (seasonal here refers to the end of winter until July). This study was based on data obtained in 2003 from ice covered Atlantic Water and Arctic Water. The Atlantic domain of the Barents Sea is a sink for CO_2 throughout the year (Omar et al., 2007) due to cooling of the surface water in winter and primary production in summer. Less is known about the air-sea CO_2 exchange in the Arctic domain since the area is ice covered. Even though some CO_2 may penetrate through the sea ice (Semiletov et al., 2004), it is generally assumed that a sea ice cover is an effective barrier for gas exchange. The phytoplankton bloom that occurs as the ice melts reduces the fCO_2 and thus induces an uptake of atmospheric CO_2.

The seasonal uptake of CO_2 was at least twice as high in the Atlantic Water as in the Arctic Water, 29 g C/m^2 compared to 6-14 g C/m^2. Kaltin et al. (2002) presented similar values in the Atlantic Water based on data from 1999, but in the Arctic Water there were clear differences between the years. The estimated seasonal uptake of CO_2 in the Atlantic Water in paper II and Kaltin et al. (2002) are larger than the 16 g C/m^2 obtained by Omar et al. (2007) for March-July. This is probably due to the differences in methodology; the seasonal estimates in paper II and Kaltin et al. (2002) are based on water column changes while Omar et al. (2007) calculated the air-sea exchange directly from fCO_2. The amounts of air-sea exchange presented above were calculated with the Takahashi et al. (1985) C:N ration, 8.75. A higher C:N ration than the classical 6.6 (Redfield et al., 1963) is required to prevent surface water outgassing of CO_2 at some of the stations. There are no records of outgassing of CO_2 in the Barents Sea and the surface fCO_2 were below atmospheric levels at the time of the investigation. Calculations were also made with the Redfield et al. (1963) ratio and when the Redfield et al. (1963) ratio was used the resulting uptake of CO_2 in the Atlantic Water was 16 g C/m^2 similar to what Omar et al. (2007) obtained.

The total uptake of atmospheric CO_2 in the Barents Sea is augmented by the increased CO_2 uptake in polynyas within otherwise ice covered areas as found for the Storfjorden polynya in paper III. Investigations in Storfjorden in 2001 and 2002 showed that the brine enriched shelf water produced during ice formation was enriched in C_T (17 ± 4 µmol/kg) due to uptake of CO_2 from the atmosphere. The total winter time uptake of CO_2 in Storfjorden due to this intense air-sea exchange was 65 ± 40 g C/m^2, which may be compared to the yearly uptake of CO_2 in the Atlantic Water of 51 g C/m^2 found by Omar et al. (2007). If the same behaviour can be expected from all the coastal polynyas in the AO, an total uptake of $2.3 \pm 1.4 \cdot 10^{12}$ g C/yr would take place within them. On the other hand, the uptake of CO_2 due to ice formation in the non-polynya part of Storfjorden was much lower than in the polynya, 5.2 g C/m^2, but

extrapolated to the seasonally ice covered area of the Arctic it resulted in a total uptake of $36 \pm 22 \cdot 10^{12}$ g C/yr.

The same south-north difference that was found for the seasonal air-sea exchange of CO_2 in paper II was also found in the seasonal new production. The results revealed a seasonal new production of 52 g C/m^2 in the Atlantic Water and 20-27 g C/m^2 in the Arctic Water. Comparisons with the study by Kaltin et al. (2002) show that the interannual variability in the area can be large. Kaltin et al. (2002) found a seasonal new production of about 70 g C/m^2 in the non-ice affected Atlantic Water. The difference is not surprising since the climatic state of the Barents Sea was cold in 2003 while 1999 was a warm year. The larger production in the Atlantic Water compared to the Arctic Water has also been shown in models, Wassmann et al. (2006b) modelled annual total primary production for the Atlantic and Arctic domains of 130 and 68 g C/m^2 respectively. From the variability of the seasonal air-sea exchange of CO_2 and new production it was concluded that the concentration and melting of the sea ice cover is of importance for the resulting carbon fluxes in addition to the water mass.

The only annual estimate of production based on measurements in the Barents Sea to my knowledge is the estimate by Olsen et al. (2002). They estimated production in the Atlantic domain along the Kola section (33.5º E) during both warm and cold years based on deficits of phosphate. The result was a production of 30 g C/yr during cold and 21 g C/yr during warm years. These results are not only smaller than the seasonal estimates in Atlantic Water in paper II and Kaltin et al. (2002), but they also indicate more production during cold than warm years. The latter is surprising since other available information point at the opposite; both the comparison between paper II and Kaltin et al. (2002) and several modelling studies (e.g. Slagstad and Wassmann, 1996; Wassmann et al. 2006b) show larger production during warm years. It is possible that the parameterisation of the vertical mixing in Olsen et al. (2002) to some degree is responsible for the unexpected results (Olsen pers. comm.).

In paper IV the annual net community production (NCP) and its variability is studied during the years 1955-2005 at Ocean Weather Station M (OWS M, 66º N, 2ºE) in the Norwegian Sea. The annual NCPs were calculated with a box model for the mixed layer based on the unique time series of oxygen collected at OWS M. The mean annual NCPs for the period 1955-2005 was 103 g C/m^2 yr (11.1 mol O_2 /m^2 yr), while the minimum and maximum annual NCPs were 43 and 169 g C/m^2 yr (4.7 and 18.3 mol O_2 /m^2 yr) respectively. Falck and Gade (1999) made similar NCP calculations at OWS M based on data for 1955-1988, but the data was only used to calculate a mean NCP for that period. Their result was similar to the mean NCP from paper IV calculated for the same time period when their mean NCP was calculated with the same air-sea exchange formulation. Since the NCP in both studies was represented by the difference between the change in oxygen content, air-sea exchange, and vertical eddy diffusion the choice of formulation of the air-sea oxygen exchange becomes essential for the calculated amount of NCP. If a formulation that resulted in smaller amounts of air-sea exchange was used consequently the NCP also decreased.

OWS M lies in the path of the Atlantic Water on its way north into the AO. The width and strength of the NwAC in the Norwegian Sea makes it the most "stable" area in hydrographic sense within the Nordic Seas. The production and its variability found at OWS M may thus be representative for the surrounding Atlantic Water. Falck and Gade (1999) found similar NCP at OWS M and in the entire ice free part of the Nordic Seas (these results were calculated with another air-sea exchange formulation and are thus not directly comparable to the results from paper IV). Skjelvan et al. (2001) on the other hand found smaller NCPs in the northern Norwegian Sea, 32 and 24 g C/m^2 in the Bjørnøya-W and Gimsøy-NW sections respectively. It was not possible to attribute the variability of the annual NCPs in paper IV to a single environmental parameter even though the NCPs clearly were influenced by the temperature and depth of the mixed layer in the beginning of the productive season (May). The cause for the variability is probably due to several interacting factors. In addition to temperature and mixed layer depth both wind speed and presence of Coastal Water were identified as important for the amount of NCP during single years. Other potentially important factors are for example insolation and species composition. A shift to generally higher NCPs occurred in the early 1990s which could not be explained with the data at hand.

Even though it is complicated to compare different types of production the results from paper II together with results from Kaltin et al. (2002) and several modelling studies (e.g. Sakshaug and Slagstad, 1992; Wassmann et al., 2006b) indicate higher production in the Atlantic Water in the Barents Sea than in the same water in the Norwegian Sea (paper IV). When making this comparison it has to be remembered that NCP on shorter time scales always is larger than new production since the NCP represents the sum of the new and regenerated production. In order to make a proper comparison between new production and NCP the ratio between new and regenerated production has to be known. A larger production in the Barents Sea may be due to the high grazing pressure in the Norwegian Sea (Rey, 2004).

In a global perspective the carbon fluxes in the Norwegian and Barents Seas may seem insignificant due to the small area and volume flows into and out of these seas, but their importance is not due to their size but to the processes that occur within them. It is the modification of the Atlantic Water as it passes through that makes the Norwegian and Barents Seas so urgent to study. In a future of changing climate the Barents Sea is also one of the areas that will be severely affected. The south-north gradient of new production and air-sea exchange found in paper II indicate that an Atlantification of the northern Barents Sea will increase both these processes in that area. Since model studies (e.g. Sakshaug and Slagstad, 1992; Wassmann et al., 2006b) have shown higher production in the Atlantic domain during warm than cold years it is also possible that the predicted increasing temperatures in the Atlantic Water advected into the BSO (ACIA, 2005) will result in increasing production in the Atlantic domain. Another result of climate change in the Barents Sea may, as mentioned in paper I be a decrease or total stop in the production of the densest part of the modified Atlantic Water. This part of the modified Atlantic Water includes brine water and in a future Barents Sea with little or no sea ice the production of brine water will decrease or stop altogether. This would change the depth to which water from the Barents Sea can

penetrate the AO and thus the storage of the carbon sequestered in the Barents Sea. It is however possible that the extra uptake of CO_2 in brine water during formation of sea ice may increase in the central AO in the future if the area of polynyas and the extent of the seasonal ice covered area increase (paper III).

Acknowledgements

There are many persons without whom this thesis would never have come into existence and I am grateful to them all. After all this time measuring, calculating, writing, thinking, and discussing it is interesting to note how much more than pure science I have learnt!

I wish to start with thanking my supervisors Truls Johannessen and Richard Bellerby for giving me the opportunity to do the research and write this thesis. I am grateful for the opportunities to go on cruises and meetings to expand my horizons. Truls, your help in the final stage of the writing was invaluable.

There are three persons that has been crucial for my work and whom I cannot thank enough:

- Abdir – you have patiently answered all my more or less answerable questions about the Barents Sea, inorganic carbon, and the philosophy of research.
- Eva – you have helped me to work patiently with "our" time series throughout these years and I am grateful for all our discussions about oxygen, production - and almost everything else.
- Ingunn – thank you for always being there to support me, to answer questions or discuss obstacles on the way to this thesis.

My office mates during these years are all thanked for their friendliness and willingness to help with everyday questions and computer trouble. The people I shared office with the larger part of the time I have worked on this thesis, Abdir and Anders, I remember all our discussions on every possible subject, some of which made us laugh so much that the people down the corridor wondered what we were doing… I had a great time!

Furthermore I wish to thank the other members of the observational chemical oceanography group, Are, Craig, Kelly and Solveig for answering questions, reading manuscripts, packing instruments and support during nice as well as frustrating times at sea and in the lab.

I also wish to send a 'thank you' to Sara; if you survived that first Greenland Sea cruise thanks to me I survived the Oden cruise in 2002 thanks to you!

A large part of the fun working with science is all the people you meet and work with; I wish to thank all the people at the Bjerknes Centre for Climate Research (Allégaten 55), at the Geophysical Institute and in the CABANERA project for fun times around

the lunch table, at coffee, and at sea. A special ‘thank you’ to my fellow PhD students, past or present, who understand the ups and downs of being a PhD student.

Finally, family and friends thank you for all your support which I could not have lived without! This tome is why I moved to Norway…

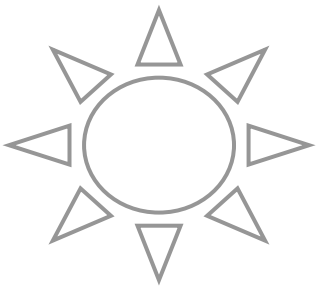

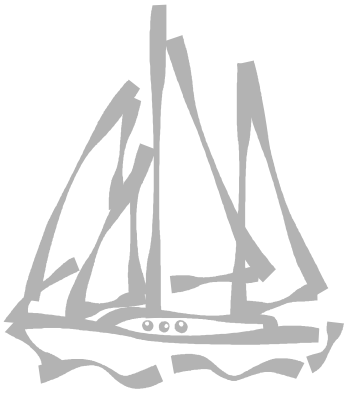

References

ACIA, 2005. Arctic Climate Impact Assessment, ACIA Scientific report, Cambridge University Press.

Amon, R.M., 2004. The role of dissolved organic matter for the organic carbon cycle in the Arctic Ocean. In: R. Stein and R.W. Macdonald (Editors), The organic carbon cycle in the Arctic Ocean. Springer-Verlag, Berlin Heidelberg New York, pp. 83-99.

Anderson, L.A. and J. L. Sarmiento, 1994. Redfield Ratios of Remineralization Determined by Nutrient Data-Analysis. Global Biogeochemical Cycles, 8(1): 65-80.

Anderson, L.G., K. Olsson, and M. Chierici, 1998. A carbon budget for the Arctic Ocean. Global Biogeochemical Cycles, 12(3): 455-465.

Anderson, L.G., H. Drange, M. Chierici, A. Fransson, T. Johannessen, I. Skjelvan and F. Rey, 2000. Annual carbon fluxes in the upper Greenland Sea based on measurements and a box-model approach. Tellus, 52B: 1013-1024.

Anderson, L.G., Jones, E.P. and Swift, J.H., 2003. Export production in the central Arctic Ocean evaluated from phosphate deficits. Journal of geophysical research, 108(C6): 3199.

Anderson, L.G., E. Falck, E. P. Jones, S. Jutterström, and J. H. Swift, 2004. Enhanced uptake of atmospheric CO_2 during freezing of seawater: A field study in Storfjorden, Svalbard. Journal of geophysical research, 109: C06004.

Bates, N.R., M. H. P. Best and D. A. Hansell, 2005. Spatio-temporal distribution of dissolved inorganic carbon and net community production in the Chukchi and Beaufort Seas. Deep Sea Research II, 52: 3303-3323.

Bates, N.R., 2006. Air-sea CO_2 fluxes and the continental shelf pump of carbon in the Chukchi Sea adjacent to the Arctic Ocean. Journal of geophysical research, 111: C10013.

Blindheim, J. and S. Østerhus, 2005. The Nordic Seas, main oceanographic features. In: H. Drange, T. Dokken, T. Furevik, R. Gerdes and W. Berger (Editors), The Nordic Seas: An integrated perspective. Geophysical Monograph 158. American Geophysical Union, Washington DC, pp. 11-37.

Broecker, W.S. and T.-H. Peng, 1982. Tracers in the sea. Lamont-Doherty Geological Observatory, Columbia University, New York, 690 pp.

Broström, G., 1998. A note on the C/N and C/P ratio of the biological production in the Nordic Seas. Tellus, 50B: 93-109.

Butler, J.N., 1982. Carbon dioxide equilibria and their application. Addison-Wesley Publishing Company, 259 pp.

Carmack, E.C., D. Barber, J. Christensen, R. W. Macdonald, B. Rudels and E. Sakshaug, 2006. Climate variability and physical forcing of the food webs and the carbon budget on panarctic shelves. Progress in oceanography, 71: 145-181.

Daly, K.L., D. W. R. Wallace, W. O. Jr. Smith, A. Skoog, R. Lara, M. Gosselin, E. Falck and P. L. Yager, 1999. Non-Redfield carbon and nitrogen cycling in the Arctic: Effects of ecosystem structure and dynamics. Journal of geophysical research, 104(C2): 3185-3199.

Denman, K.L., G. Brasseur, A. Chidthaisong, P. Ciais, P.M. Cox, R.E. Dickinson, D. Hauglustaine, C. Heinze, E. Holland, D. Jacob, U. Lohmann, S Ramachandran, P.L. da Silva Dias, S.C. Wofsy and X. Zhang, 2007. Couplings Between Changes in the Climate System and Biogeochemistry. In: Climate Change 2007 The Physical Science Basis. Contribution of Working Group I to the Fourth Assessment Report of the Intergovernmental Panel on Climate Change. Solomon, S., D. Qin, M. Manning, Z. Chen, M. Marquis, K.B. Averyt, M.Tignor and H.L. Miller (Editors.). Cambridge University Press, Cambridge, United Kingdom and New York, NY, USA.

Dickson, A.G., 1981. An exact definition of total alkalinity and a procedure for the estimation of alkalinity and total inorganic carbon from titration data. Deep Sea Research, 28A(6): 609-623.

Dickson, R.R. and J. Brown, 1994. The production of North Atlantic Deep Water: Sources, rates and pathwaiys. Journal of geophysical research, 99(C6): 12319-12341.

Dittmar, T. and G. Kattner, 2003. The biogeochemistry of the river and shelf ecosystem of the Arctic Ocean: a review. Marine chemistry, 83(3-4).

DOE, 1994. Handbook of methods for the analysis of the various parameters of the carbon dioxide system in sea water; version 2. ORNL/CDIAC-74.

Donelan, M.A. and R. Wanninkhof, 2002. Gas transfer at water surfaces—concepts and issues. In: M.A. Donelan, W.M. Drennan, E.S. Saltzman and R. Wanninkhof (Editors), Gas transfer at water surfaces. Geophysical Monograph. American Geophysical Union, Washington, DC, pp. 1-10.

Dugdale, R.C. and J. J. Goering, 1967. Uptake of new and regenerated forms of nitrogen in primary production. Limnology and Oceanography, 12: 196-206.

Eglinton, T.I. and D. J. Repeta, 2004. Organic matter in the contemporary ocean. In: H. Elderfield (Editor), The oceans and marine geochemistry. Treatise on Geochemistry. Elsevier-Pergamon, Oxford, pp. 145-180.

Fairall, C.W., E. F. Bradley, J. S. Godfrey, G. A. Wick, J. B. Edson and G. S. Young, 1996. Cool-skin and warm-layer effects on sea surface temperature. Journal of geophysical research, 101(C1): 1295-1308.

Falck, E. and H. G. Gade, 1999. Net community production and oxygen fluxes in the Nordic Seas based on O_2 budget calculations. Global biogeochemical cycles, 13(4): 1117-1126.

Falck, E. and L. G. Anderson, 2005. The dynamics of the cabon cycle in the surface water of the Norwegian Sea. Marine chemistry, 94(1-4): 43-53.

Falkowski, P.G., R. T. Barber.and V. Smetacek, 1998. Biogeochemical controls and feedbacks on ocean primary production. Science, 281: 200-206.

Fransson, A., M. Chierici, L. G. Anderson, I. Bussmann, G. Kattner, E. P. Jones and J. H. Swift, 2001. The importance of shelf processes for the modification of chemical consistuents in the waters of the Eurasian Arctic Ocean: impliactions for carbon fluxes. Continental shelf research, 21: 225-242.

Gascard, J.-C., G. Raisbeck, S. Sequeira, F. Yiou, and K. A. Mork, 2004. The Norwegian Atlantic Current in the Lofoten basin inferred from hydrological and tracer data (^{129}I) and its interaction with the Norwegian Coastal Current. Geophysical Research Letters, 31: L01308.

Graedel, T. E. and P. J. Crutzen, 1993 Atmosheric change: A earth system perspective. W. H. Freeman and Company, New York, 446 pp.

Gran, G., 1952. Determination of the equivalence point in potentiometric titrations. Part II. Analyst, 77: 661-671.

Hansen, B. and S. Østerhus, 2000. North Atlantic-Nordic Seas exchange. Progress in oceanography, 45: 109-208.

Holliday, N.P., S. L. Hughes, A. Lavin, K. A. Mork, G. Nolan, W. Walczowski, and A. Beszczynska-Möller, 2007. The end of a trend? The progression of unusually warm and saline water from the eastern North Atlantic into the Arctic Ocean. Newsletter of the Climate Variability and Predictability Programme, 12(1): 19-20.

Hood, E.M., L. Merlivat and T. Johannessen, 1999. Variation of fCO_2 and air-sea flux of CO_2 in the Greenland Sea gyre using high-frequency time series data from CARIOCA drift buoys. Journal of geophysical research, 104(C9): 20571-20583.

IPCC, 2001. The climate system: an overview. Baede, A. P. M., E. Athlonsou, Y. Ding, D. Schimel, B. Bolin, S. Pollonais, Climate change 2001: The scientific basis. Cambridge University Press, pp. 85-98.

IPCC, 2007. Summary for policymakers, Climate change 2007: The physical science basis. Cambridge University Press.

Jakobsson, M., 2002. Hypsometry and volume of the Arctic Ocean and its constituent seas. Geochemistry, Geophysics, Geosystems, 3(5).

Jähne, B., K. O. Münnich, R. Bösinger, A. Dutzi, W. Huber and P. Libner, 1987. On the parameters influencing air-water gas exchange. Journal of geophysical research, 92(C2): 1937-1949.

Johannessen, O.M., L. Bengtsson, M. W. Miles, S. I. Kuzima, V. A. Semenov, G. V. Alekseev, A. P. Nagurnyi, V. F. Zakharov, L. P. Bobylev, L. H. Pettersson, K. Hasselmann and H. P. Cattle, 2004. Arctic climate change: observed and modelled temperature and sea-ice variability. Tellus, 56A: 328-341.

Johnson, K.M., J. M. Sieburth, P. J. leB. Williams and L. Brändström, 1987. Coulometric total carbon dioxide analysis for marine studies: Automation and calibration. Marine chemistry, 21: 117-133.

Johnson, K.M., K. D. Wills, D. B. Butler, W. K. Johnson, and C. S. Wong, 1993. Coulometric total carbon dioxide analysis for marine studies: maximizing the performance of an automated gas extraction system and coulometric detector. Marine chemistry, 44: 167-187.

Kaltin, S., L. G. Anderson, K. Olsson, A. Fransson, and M. Chierici, 2002. Uptake of atmospheric cabon dioxide in the Barents Sea. Journal of marine systems, 38: 31-45.

Kaltin, S. and L. G. Anderson, 2005. Uptake of atmospheric carbon dioxide in Arctic shelf seas: evaluation of the relative importance of processes that influence

pCO(2) in water transported over the Bering-Chukchi Sea shelf. Marine Chemistry, 94(1-4): 67-79.
Kelley, J.J., Jr., 1970. Carbon dioxide in the surface waters of the North Atlantic Ocean and the Barents and Kara Seas. Limnology and Oceanography, 15: 80-87.
Korsnes, R., O. Pavlova, and F. Godtliebsen, 2002. Assessment of potential transport of pollutants into the Barents Sea via sea ice - an observational approach. Marine pollution bulletin, 44: 861-869.
Körtzinger, A., J. I. Hedges, and P. D. Quay, 2001. Redfield ratios revised: removing the biasing effect of anthropogenic CO_2. Limnology and Oceanography, 46(4): 964–970.
Ledwell, J.R., 1984. The variation of the gas transfer coefficient with molecular diffusivity. In: W. Brutsaet and G.H. Jirka (Editors), Gas transfer at water surfaces. D. Reidel Publishing Company, pp. 293-302.
Lisitzin, A. P., 1995. The mariginal filter of the ocean. Oceanology, 34, 583-590.
Liss, P.S. and L. Merlivat, 1986. Air-sea gas echange rates: Introduction and synthesis. In: P. Buat-Ménard (Editor), The role of air-sea echange in geochemical cycling. D. Reidel Publishing Company, Hingham, Mass, pp. 113-129.
Loeng, H., 1991. Features of the physical oceanographic conditions of the Barents Sea. In: E. Sakshaug, C.C.E. Hopkins and N.A. Øritsland (Editors), Proceedings of the Pro Mare symposium on polar marine ecology, Trondheim, pp. 5-18.
Lundberg, L. and P. M. Haugan, 1996. A Nordic Seas- Arctic Ocean carbon budget from volume flows and inorganic carbon data. Global Biogeochemical Cycles, 10(3): 493-510
Martin, T. And E. Augstein, 2000. Large-scale drift of Arctic Sea ice retrieved from passive microwave satellite data. Journal of geophysical research, 105(C4): 8775-8788.
Maslowski, W., D. Marble, W. Walczowski, U. Schauer, J. L. Clement and A. J. Semtner, 2004. On climatological mass, heat, and salt transports through the Barents Sea and Fram Strait from a pan-Arctic coupled ice-ocean medel simulation. Journal of geophysical research, 109: C03032.
McLaughlin, F., E. C. Carmack, R. W. Macdonald, and J. K. B. Bishop, 1996. Physical and geochemical properties across the Atlantic/Pacific water mass front in the southern Canadian Basin. Journal of geophysical research, 101(C1): 1183-1197.
Mintrop, L., F. F. Pérez, M. Gonzalez-Dávila, J. M. Santana-Casiano and A. Körtzinger, 2000. Alkalinity determination by potentiometry: intercalibration using three different methods. Ciencias Marinas, 26(1): 23-37.
Morison, J., M. Steele and R. Andersen, 1998. Hydrography of the upper Arctic Ocean measured from the nuclear submarine U.S.S. *Pargo*. Deep Sea Research I, 45: 15-35.
Najjar, R.G. and R. F. Keeling, 1997. Analysis of the mean annual cycle of the dissolved oxygen anomaly in the World Ocean. Journal of marine research, 55(117-151).
Najjar, R.G. and R. F. Keeling, 2000. Mean annual cycle of the air-sea oxygen flux: A global view. Global Biogeochemical Cycles, 14(2): 573-584.

Nakaoka, S.-I., S. Aoki, T. Nakazawa, G. Hashida, S. Morimoto, T. Yamanouchi, H. Yoshikawa-Inoue, 2006. Temporal and spatial variations of oceanic pCO_2 and air-sea CO_2 flux in the Greenland Sea and the Barents Sea. Tellus, 58B(2): 148-161.

Nightingale, P.D., G. Malin, C. S. Law, A. J. Watson, P. S. Liss, M. I. Liddicoat, J. Boutin, and R. C. Upstill-Goddard, 2000. In situ evaluation of air-sea gas exchange parameterizations using novel conservative and volatile tracers. Global Biogeochemical Cycles, 14(1): 373-387.

Nitishinsky, M., L. A. Anderson and J. A. Hölemann, 2007. Inorganic carbon and nutrient fluxes on the Arctic Shelf. Continental shelf research, 27: 1584-1599.

Olli, K., P. Wassmann, M. Reigstad, T. N. Ratkova, E. Arashkevich, A. Pasternak, P. A. Matrai, J. Knulst, L. Tranvik, R. Klais and A. Jacobsen, 2007. The fate of production in the central Arctic Ocean - top-down regulation by zooplankton expatriates? Progress In Oceanography, 72(1): 84-113.

Olsen, A., L. G. Anderson and T. Johannessen, 2002. The impact of climate variations on fluxes of oxygen in the Barents Sea. Continental shelf research, 22: 1117-1128.

Olsen, A., R. G. J. Bellerby, T. Johannessen, A. M. Omar and I. Skjelvan, 2003. Interannual variability in the wintertime air-sea flux of carbon dioxide in the northern North Atlantic, 1981-2001. Deep-sea research I, 50: 1323-1338.

Omar, A.M., T. Johannessen, A. Olsen, S. Kaltin and F. Rey, 2007. Seasonal and interannual variability of the air-sea CO_2 flux in the Atlantic sector of the Barents Sea. Marine chemistry, 104: 203-213.

Orvik, K.A. and P. Niiler, 2002. Major pathways of Atlantic water in the northern North Atlantic and Nordic Seas toward Arctic. Geophysical Research Letters, 29(19): 1896.

Peterson, B.J., 1980. Aquatioc primary productivity and the ^{14}C-CO_2 method: A history of the productivity problem.

Pfirman, S.L., D. Bauch and T. Gammelsrød, 1994. The Northern Barents Sea: Water mass distribution and modification, The polar oceans and their role in shaping the global environment. American Geophysical Union, pp. 77-94.

Platt, T., W. G. Harrison, M. R. Lewis, W. K. W. Li, S. Sathyendranath, R. E. Smith and A. F. Vezina, 1989. Biological production of the oceans: the case for a consensus. Marine ecology progress series, 52: 77-88.

Quadfasel, D., B. Rudels and K. Kurz, 1988. Outflow of dense water from a Svalbard fjord into the Fram Strait. Deep Sea Research, 35(7): 1143-1150.

Ridgewell, A. and R. E. Zeebe, 2005. The role of the global carbonate cycle in the regulation and evolution of the Earth system. Earth and Planetary Science Letters, 234: 299-315.

Redfield, A.C., B. H. Ketchum and F. A. Richards, 1963. The influence of organisms on the composition of sea-water. In: M.N. Hill (Editor), The Sea. Interscience, New York, pp. 26-77.

Rey, F., T. T. Noji and L. A. Miller, 2000. Seasonal phytoplankton development and new production in the central Greenland Sea. Sarsia, 85(329-344).

Rey, F., 2004. Phytoplankton: The grass of the sea. In: H.R. Skjoldal (Editor), The Norwegian Sea ecosystem. Tapir Academic Press, Trondheim, pp. 97-136.

Rudels, B., H. J. Friedrich and D. Quadfasel, 1999. The Arctic Circumpolar Boundary Current. Deep-Sea Research II, 46: 1023-1062.

Rudels, B., R. D. Muench, J. Gunn, U. Schauer and H. J. Friedrich, 2000. Evolution of the Arctic Ocean boundary current north of the Siberian shelves. Journal of marine systems, 25: 77-99.

Rudels, B., G. Björk, J. Nilsson, P. Winsor, I. Lake and C. Nohr, 2004. The interaction between waters from the Arctic Ocean and the Nordic Seas north of Fram Strait and along the East Greenland Current: results from the Arctic Ocean-02 Oden expedition. Journal of marine systems, 55(1-2): 1-30.

Rysgaard, S., R. N. Glud, M. K. Sejr, J. Bendtsen and P. B. Christensen, 2007. Inorganic carbon transport during sea ice growth and decay: A carbon pump in the polar seas. Journal of geophysical research, 112: C03016.

Sabine, C. L., R. A. Feely, N. Gruber, R. M. Key, K. Lee, J. L. Bullister, R. Wanninkhof, C. S. Wong, D. W. R. Wallace, B. Tilbrook, F. J. Millero, T.-H. Peng, A. Kozyr, T. Ono and A. Rios, 2004. The oceanic sink for anthropogenic CO_2. Science, 305: 367-371.

Sakshaug, E. and D. Slagstad, 1992. Sea ice and wind: Effects on primary productivity in the Barents Sea. Atmosphere-Ocean, 30(4): 579-591

Sakshaug, E., 2004. Primary and secondary production in the Arctic Seas. In: R. Stein and R.W. Macdonald (Editors), The organic carbon cycle in the Arctic Ocean. Springer-Verlag, Berlin Heidelberg New York, pp. 57-81.

Sambrotto, R.N., G. Savidge, C. Robinson, P. Boyd, T. Takahashi, D. M. Karl, C. Langdon, D. Chipman, J. Marra and L. Codispoti, 1993. Elevated consumption of carbon relative to nitrogen in the surface ocean. Nature, 363: 248-250.

Saunders, P.M., 1967. The temperature at the ocean-air interface. Journal of the atmospheric sciences, 24: 269-273.

Schauer, U., R. D. Muench, B. Rudels and L. Timokhov, 1997. Impact of eastern Arctic shelf waters on the Nansen Basin intermediate layers. Journal of geophysical research, 102(C2): 3371-3382.

Schauer, U., H. Loeng, B. Rudels, V. K. Ozhigin and W. Dieck, 2002a. Atlantic Water flow through the Barents and Kara Seas. Deep-Sea Research I, 49(12): 2281-2298.

Schauer, U., B. Rudels, E. P. Jones, L. G. Anderson, R. D. Muench, G. Björk, J. H. Swift, V. V. Ivanov and A.-M. Larsson, 2002b. Confluence and redistribution of Atlantic Water in the Nansen, Amundsen and Makarow basins. Annales Geophysicae, 20: 257-273.

Semiletov, I., A. Makshtas, S.-I. Akasofu and E. L. Andreas, 2004. Atmospheric CO_2 balance: The role of Arctic sea ice. Geophysical Research Letters, 31: L05121.

Semiletov, I.P., I. I. Pipko, I. Repina and N. E. Shakhova, 2007. Carbon chemistry dynamics and carbon dioxide fluxes across the atmosphere-ice-water interfaces in the Arctic Ocean: Pacific sector of the Arctic. Journal of marine systems, 66: 204-226.

Simonsen, K. and P. M. Haugan, 1996. Heat budgets of the Arctic Mediterranean and sea surface heat flux parameterizations for the Nordic Seas. Journal of geophysical research, 101(C3): 6553-6576.

Skjelvan, I., 1999. Horizontal distribution of NC_T, NA_T and fCO_2 in the Nordic Seas. In: Carbon and oxygen fluxes in the Nordic Seas. PhD thesis, University of Bergen, Norway.

Skjelvan, I., E. Falck, L. G. Anderson and F. Rey, 2001. Oxygen fluxes in the Norwegian Atlantic Current. Marine chemistry, 73: 291-303.

Skjelvan, I., A. Olsen, L. G. Anderson, R. G. J. Bellerby, E. Falck, Y. Kasajima, C. Kivimäe, A. M. Omar, F. Rey, K. A. Olsson and T. Johannessen, 2005. A review of the inorganic carbon cycle of the Nordic Seas and the Barents Sea. In: H. Drange, T. Dokken, T. Furevik, R. Gerdes and W. Berger (Editors), The Nordic Seas: An integrated perspective. Geophysical Monograph. American Geophysical Union, Washington DC, pp. 157-175.

Skogseth, R., P. M. Haugan and M. Jakobsson, 2005. Watermass transformations in Storfjorden. Continental shelf research, 25: 667-695.

Slagstad, D. and P. Wassmann, 1996. Climate change and carbon flux in the Barents Sea: 3-D simulations of ice-distribution, primary production and vertical export of particulate organic matter. Proceedings of the International Symposium on Environmental Research in teh Arctic. Memoirs of National Institute of Polar Research, Tokyo, Japan, pp. 119-141.

Smethie, J., M. William, T. Takahashi and J. R. Ledwell, 1985. Gas exchange and CO_2 flux in the tropical Atlantic Ocean determined from ^{222}Rn and pCO_2 measurements. Journal of geophysical research, 90(C4): 7005-7022.

Solomon, S., D. Qin, M. Manning, R.B. Alley, T. Berntsen, N.L. Bindoff, Z. Chen, A. Chidthaisong, J.M. Gregory, G.C. Hegerl, M. Heimann, B. Hewitson, B.J. Hoskins, F. Joos, J. Jouzel, V. Kattsov, U. Lohmann, T. Matsuno, M. Molina, N. Nicholls, J. Overpeck, G. Raga, V. Ramaswamy, J. Ren, M. Rusticucci, R. Somerville, T.F. Stocker, P. Whetton, R.A. Wood and D. Wratt, 2007. Technical Summary. In: Solomon, S., D. Qin, M. Manning, Z. Chen, M. Marquis, K.B. Averyt, M. Tignor and H.L. Miller (Editors), Climate Change 2007: The Physical Science Basis. Contribution of Working Group I to the Fourth Assessment Report of the Intergovernmental Panel on Climate Change. Cambridge University Press, Cambridge, United Kingdom and New York, NY, USA.

Steemann Nielsen, E., 1952. The use of radio-active carbon (C^{14}) for measuring organic production in the sea. Journal du Conseil International pour l'Exploration de la Mer, 18: 117-140.

Stein, R. and R. W. Macdonald, 2004. Organic carbon budget: Arctic Ocean vs. Global Ocean. In: R. Stein and R.W. Macdonald (Editors), The organic carbon cycle in the Arctic Ocean. Springer-Verlag, Berlin Heidelberg New York, pp. 315-322.

Sverdrup, H.U., 1953. On conditions for the vernal blooming of phytoplankton. Journal du Conseil International pour l'Exploration de la Mer, 18: 287-295.

Takahashi, T., W. S. Broecker and S. Langer, 1985. Redfield ratio based on chemical data from isopycnal surfces. Journal of geophysical research, 90: 6907-6924.

Toggweiler, J.R., 1993. Carbon overconsumption. Nature, 363: 210-211.

Wanninkhof, R., 1992. Relationship between wind speed and gas exchange over the ocean. Journal of geophysical research, 97(C5): 7373-7382.

Wanninkhof, R. and W. R. McGillis, 1999. A cubic relationship between air-sea CO_2 exchange and wind speed. Geophysical Research Letters, 26(13): 1889-1892.
Wassmann, P., E. Bauerfeind, M. Fortier, M. Fukuchi, B. Hargrave, B. Moran, T. Noji, E.-M. Nöthig, K. Olli, B. Peinert, H. Sasaki and V. Shevchenko, 2004. Particulate organic carbon flux to the Arctic Ocean sea floor. In: R. Stein and R.W. Macdonald (Editors), The organic carbon cycle in the Arctic Ocean. Springer-Verlag, Berlin Heidelberg New York, pp. 101-138.
Wassmann, P., M. Reigstad, T. Haug, B. Rudels, M. L. Carrol, H. Hop, G. W. Gabrielsen, S. Falk-Petersen, S. G. Denisenko, E. Arashkevich, D. Slagstad and O. Pavlova, 2006a. Food webs and carbon flux in the Barents Sea. Progress in oceanography, 71: 232-287.
Wassmann, P., D. Slagstad, C. Wexels Riser and M. Reigstad, 2006b. Modelling the ecosystem dynamics of the Barents Sea including the marginal ice zone II. Carbon flux and interannual variability. Journal of marine systems, 59: 1-24.
Weller, G., 1998. Regional impacts of climate change in the Arctic and Antarctic. Annals of glaciology, 27: 543-552.
Wheeler, P.A., J. M. Watkins and R. L. Hansing, 1997. Nutrients, organic carbon and organic nitrogen in the upper water column of the Arctic Ocean: implications for the sources of dissolved organic carbon. Deep Sea Research II, 44(8): 1571-1592.
Woolf, D.K. and S. A. Thorpe, 1991. Bubbles and the air-sea exchange of gases in near-saturation conditions. Journal of marine research, 49: 435-466.
Zeebe, R.E. and D. Wolf-Gladrow, 2003. CO_2 in seawater: Equilibrium, kinetics, isotopes. Elsevier Oceanography Series, 65. Elsevier, 346 pp
Zheng, Y., P. Schlosser, J. H. Swift and E. P. Jones, 1997. Oxygen utilization rates in the Nansen Basin, Arctic Ocean: inplications for new production. Deep-Sea Research I, 44(12): 1923-1943.

Paper I

A carbon budget for the Barents Sea

Kivimäe, C., R. G. J. Bellerby, A. Fransson, M. Reigstad and T. Johannessen

Submitted to Deep-Sea Research II.

A carbon budget for the Barents Sea

Caroline Kivimäe[a], Richard G. J. Bellerby[b,a] Agneta Fransson[c], Marit Reigstad[d] and Truls Johannessen[a,b]

[a] Geophysical Institute, University of Bergen, Norway
[b] Bjerknes Centre for Climate Research, University of Bergen, Norway
[c] Department of Earth Sciences, Göteborg University, Box 460, 405 30 Göteborg, Sweden
[d] Norwegian College of Fishery Science, University of Tromsø, 9037 Tromsø, Norway

Corresponding author:
Caroline Kivimäe
Phone number: +47 5558 2704
Fax number: +47 5558 4330
E-mail: caroline.kivimae@gfi.uib.no

Abstract

The first carbon budget constructed for the Barents Sea to study the fluxes of carbon into, out of, and within the region is presented. The budget is based on volume flows and dissolved inorganic carbon (DIC), dissolved organic carbon (DOC), and particulate organic carbon (POC) concentrations. The location of the Barents Sea between the Nordic Seas and the Arctic Ocean makes it a site for large variations in both physical, chemical, and biological parameters and also sensitive to future climate change. Since the Barents Sea is a site for formation of intermediate and deep waters penetrating into several layers of the Arctic Ocean, the processes determining the Barents Sea carbon budget has significance also for the Arctic Ocean carbon budget. The results of the budget show that ~$5600 \cdot 10^6$ t C is exchanged through the boundaries of the Barents Sea during one year. The Barents Sea is a net exporter of carbon to the Arctic Ocean; the net DIC export is ~$2500 \cdot 10^6$ t C yr^{-1} of which ~$1800 \cdot 10^6$ t C yr^{-1} (72%) is in subsurface water masses and thus sequestered from the atmosphere. The net total organic carbon export to the Arctic Ocean is $80 \cdot 10^6$ t C yr^{-1} of which $20 \cdot 10^6$ t C yr^{-1} is labile. Shelf pumping in the Barents Sea results in an uptake of $30 \cdot 10^6$ t C yr^{-1} from the atmosphere which is exported out of the area in the dense modified Atlantic Waters. The main part of this carbon was channelled through export production ($23 \cdot 10^6$ t C yr^{-1}).

1. Introduction

The Barents Sea is an important transformation area within the Arctic Mediterranean where properties such as temperature, salinity, and carbon concentration of the water masses can change considerably. Both intermediate and deep waters are produced within the Barents Sea and the carbon contained in these waters is sequestered for decades to hundreds of years when the waters exit into the neighbouring deep basins of the Nordic Seas and Arctic Ocean (Bönisch and Schlosser, 1995; Anderson et al., 1998). In an era of climate change it is important to quantify the carbon fluxes both

into, out of, and within the ocean since the fluxes of total dissolved inorganic carbon (DIC), dissolved organic carbon (DOC) and particulate organic carbon (POC) control many aspects of the marine carbon cycle, such as the potential for uptake of atmospheric CO_2, availability of labile organic matter and sequestration of CO_2. A carbon budget for the Barents Sea will reveal how large these carbon fluxes are.

The Barents Sea is the largest of the Arctic Ocean shelf seas ($1.512 \cdot 10^6$ km^2) with a mean depth of 200 m (Jakobsson, 2002). It acts as a conduit for the Atlantic Water (AW) on its way north into the Arctic Ocean (AO) and due to the presence of the AW it is one of the most productive areas in the AO (Sakshaug, 2004). The AW that enters the south-western Barents Sea through the Barents Sea Opening (BSO) is warm and relatively saline; it also has high concentrations of DIC and nutrients. From the BSO the AW flows east and north-eastwards (Figure 1) to the Polar Front where it encounters and is subducted below the cold and fresh Arctic Water (ArW) (Loeng, 1991; Schauer et al., 2002a). The ArW is advected into the Barents Sea from the north and northeast (Novitsky, 1961; Loeng, 1991; Pfirman et al., 1994). The warm AW keeps the southern Barents Sea ice free during the entire year while the ArW is seasonally ice covered, the majority of the ice is produced within the Barents Sea but some is also imported from the Kara Sea and Arctic Ocean (Martin and Augstein, 2000). The distribution of water masses and sea ice cover is important for the processes in the carbon cycle since it determines the amount of CO_2 uptake from the atmosphere and primary production. Ice cover reduces the CO_2 uptake from the atmosphere and seasonal studies has shown that the uptake north of the Polar Front is significantly lower than in the AW (Kaltin et al., 2002; Kivimäe et al., submitted). The primary production in ArW below the ice is lower than in the AW due to light limitation and less favourable nutrient conditions (Sakshaug and Slagstad, 1992; Wassmann et al., 2006). North of the Polar Front the larger part of the annual production occurs during the spring bloom due to the limited access to new nutrients in the strongly stratified waters while the periodic passage of low pressure systems introduces new nutrients to the euphotic zone in the less stratified AW (Sakshaug and Slagstad, 1992).

The strength and properties of the AW inflow determines the climatic state of the Barents Sea with respect to the distribution of hydrographic conditions and sea ice. Hence, the Barents Sea climate has a cold and a warm state (Loeng, 1991; Ådlandsvik and Loeng, 1991). The AW looses heat and mixes with lower salinity water as it passes through the Barents Sea (Schauer et al., 2002a). The heat loss during winter which increases the solubility of CO_2 and the primary production during summer results in a fCO_2 in the seawater that is lower than the atmospheric throughout the year (Omar et al. 2007) and thus potential for CO_2 uptake from the atmosphere. When the AW reaches the passages between Svalbard-Franz Josef Land and Franz Josef Land-Novaya Zemlya the AW has been extensively transformed so that it no longer is recognised as AW according to the classical definitions (Hopkins, 1991; Loeng, 1991). In this work it will be referred to as Barents Sea modified Atlantic Water.

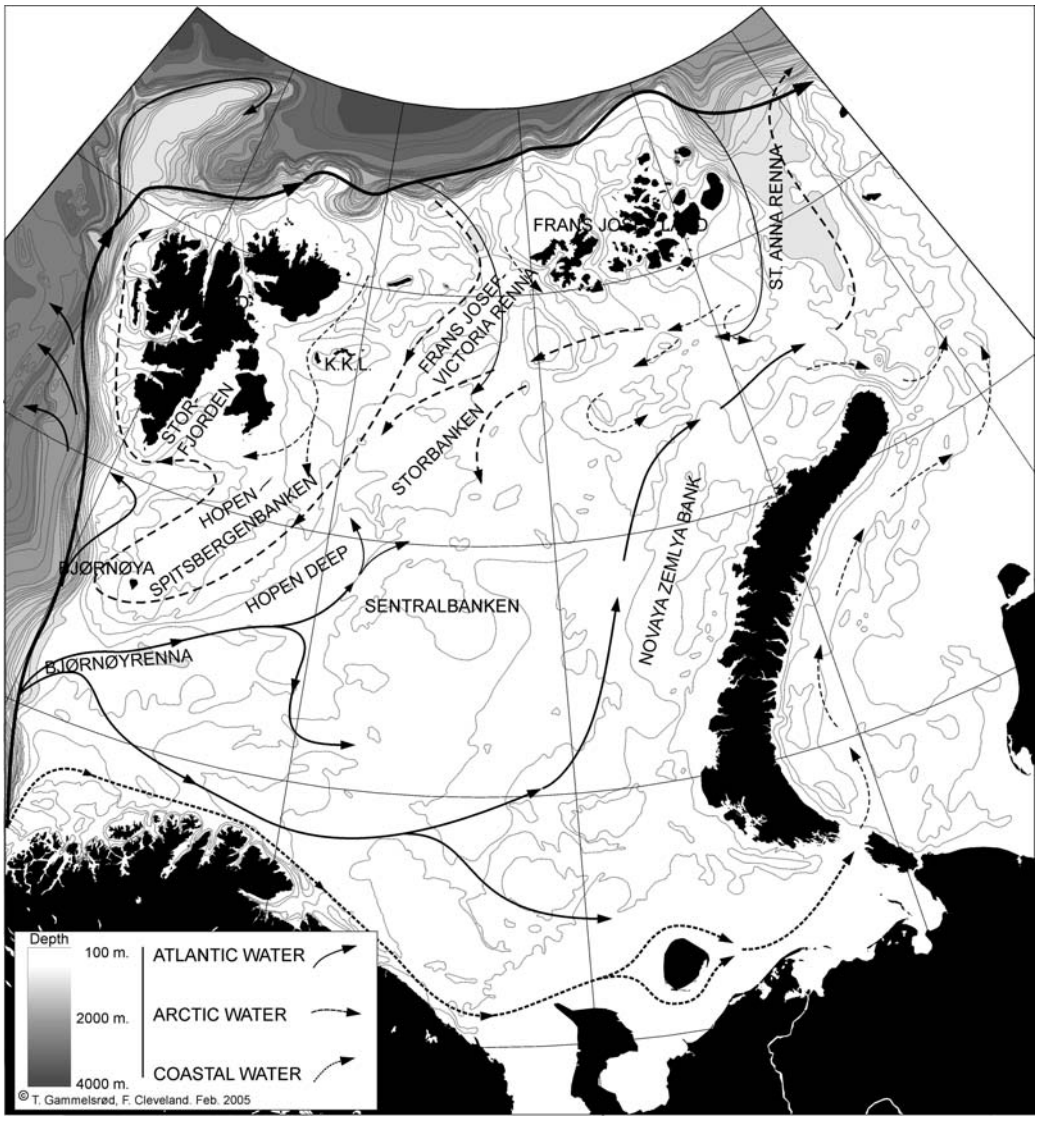

Figure 1: Map of the Barents Sea with main surface currents and some topographical features. Solid arrows represent Atlantic Water, dashed arrows Arctic Water and dotted arrows Coastal Water. K.K.L is Kong Karls Land. Figure by courtesy of T. Gammelsrød and F. Cleveland, Geophysical institute, University of Bergen.

The Barents Sea is also a production area for brine water (Midttun, 1985) which forms when sea ice freezes and the salts are rejected into the surface water. The result is cold, relatively salty, and dense water that can sinks to considerable depth depending on its density. Brine water can thus be an effective conduit for carbon from the atmosphere to the deeper layers of the ocean (Omar et al., 2005; Anderson et al., 2004; Rysgaard et al., 2007). Brine water is known to form in the polynyas of Storfjorden (Skogseth et al., 2004), west and northwest of Novaya Zemlya and around Franz Josef Land (Martin and Cavalieri, 1989). The densest part of the outflow from the Barents Sea, through the passage between Franz Josef Land and Novaya Zemlya, consists of a mixture of brine water and modified AW (Schauer et al., 2002b) and will be referred to as Barents Sea Bottom Water in this work.

In the BSO the inflowing AW is accompanied by the Coastal Water which flows along the coast of Norway and Russia until it reaches the south-eastern Barents Sea. Here some parts of the water exits through the Kara Gate (the straits of Karskie Vorota and Yugorsky Shar), the straits between Novaya Zemlya and the Russian mainland, while some turns north along the western coast of Novaya Zemlya. The Coastal Water constitutes a freshwater source for the Barents Sea due to its low salinity, along its way eastwards it is supplied with even more river runoff.

A carbon budget for the Barents Sea has not hitherto been attempted but a carbon budget for the Arctic Ocean has been constructed by Anderson et al. (1998). They found that the AW transported $1291 \cdot 10^6$ tons C yr^{-1} into the AO through the BSO while the central AO was supplied with $863 \cdot 10^6$ tons C yr^{-1} from the lower halocline and Atlantic layer inflow through Fram Strait. This implies that the Barents Sea branch of AW is at least as important as the Fram Strait branch for the carbon budget of the AO. The carbon budget made by Lundberg and Haugan (1996) covered the entire Arctic Mediterranean and they concluded that the role of this area in the global carbon cycle was as a transit area for carbon from the Pacific Ocean and river runoff. In addition, the area was a sink for atmospheric CO_2 as well as an area of substantial transformation from surface water to deep water. The objective of the present study is to focus exclusively on the Barents Sea and construct a carbon budget based on volume flows and concentrations of DIC, DOC, and POC. The part of the budget associated with the local change in carbon properties in and export of the transformed AW, the shelf pumping (Tsunogai et al., 1999), is also studied in detail.

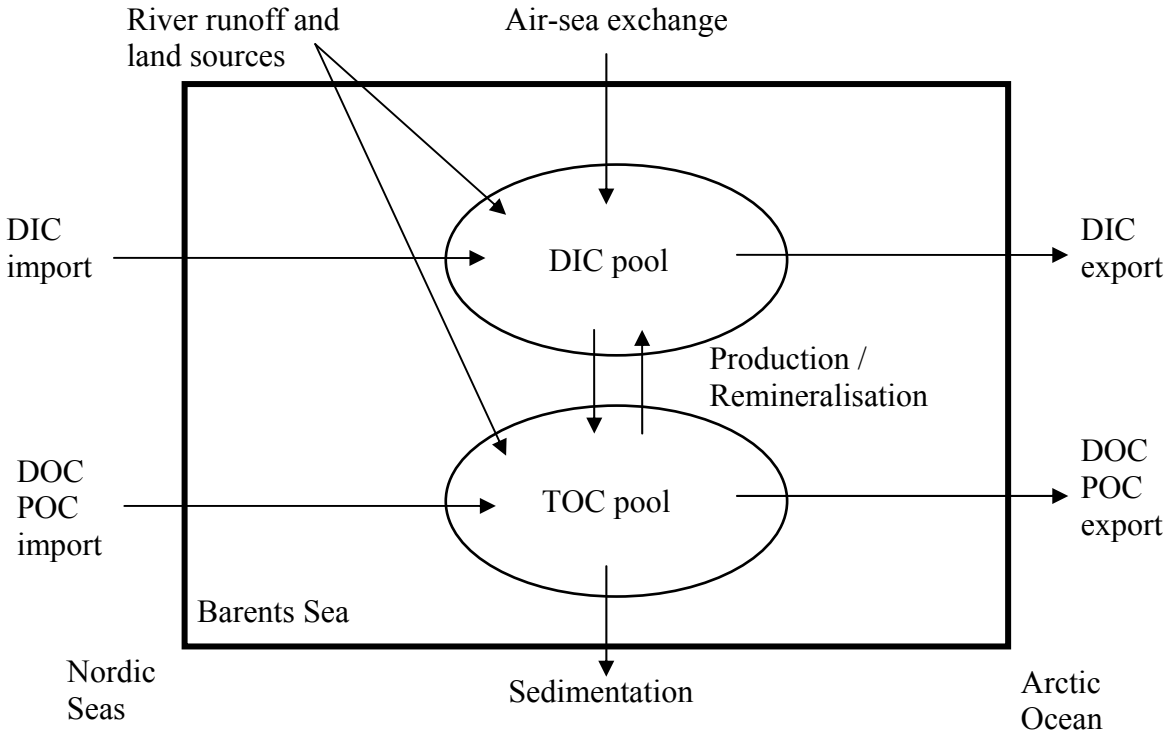

Figure 2: Conceptual model showing the DIC and TOC pools with their sources and sinks and the processes that act upon them.

2. Method

The carbon in the Barents Sea was divided into two pools, one for total dissolved inorganic carbon (DIC) and one for total organic carbon (TOC) which contains dissolved organic carbon (DOC) and particulate organic carbon (POC). Figure 2 shows the conceptual model of the carbon flows into, out of, and within the Barents Sea. The sources and sinks for carbon in the area can be written as

$$\text{Carbon in} = DIC^{adv} + DOC^{adv} + POC^{adv} + DIC^{rl} + DOC^{rl} + POC^{rl} + DIC^{air\text{-}sea} + DIC^{eif}$$

$$\text{Carbon out} = DIC^{adv} + DOC^{adv} + POC^{adv} + POC^{sed}$$

The superscripts in the equations above stand for advection (adv), river and land sources (rl), air-sea exchange (air-sea), extra uptake from the atmosphere during ice formation (eif), and burial in the sediments (sed). Transformation between DIC, DOC, and POC inside the Barents Sea is assumed to be through biological production and remineralisation (Figure 2). Section 2.1 will outline the construction of the carbon budget and section 2.2 will show how the shelf pumping is evaluated.

2.1 Barents Sea carbon budget

2.1.1 Volume flows and water masses

Volume flows were taken from the model by Maslowski et al. (2004), see Table 1, who computed climatological (1979-2001) volume and salt transports. 0.04 Sv was added to the outflow between Franz Josef Land and Novaya Zemlya from Maslowski et al. (2004) to balance the volume flows. Five water masses were defined within the in- and outflows: Atlantic Water (AW), Coastal Water (CW), Arctic Water (ArW), Barents Sea modified Atlantic Water (BSAW) and Barents Sea Bottom Water (BSBW). The fraction of each water mass in each in/outflow (Table 2) was calculated based on the mean salinity of each in/outflow, mean salinities of the water masses and mass conservation. The mean salinity for an inflow or outflow was calculated from the salt and volume flows according to Maslowski et al. (2004). It was assumed that the added 0.04 Sv had the same mean salinity as the other outflow in the same passage.

Table 1: Volume flows (Sv) from Maslowski et al. (2004) with direction in/out of the Barents Sea in parenthesis.

Passage	Net	Positive	Negative
Svalbard - Norway	3.27 (in)	5.07 (in)	-1.8 (out)
Svalbard - Franz Josef Land	0.36 (out)	1.17 (out)	-0.81 (in)
Franz Josef Land - Novaya Zemlya	2.56 (out)	3.16 (out)	-0.61 (in)
Kara Gate	0.32 (out)	0.33 (out)	-0.01 (in)

Table 2: Contribution from each water mass to the total in- or outflow through the four passages into the Barents Sea. Abbreviations are f=fraction, CW=Coastal Water, AW=Atlantic Water, ArW=Arctic Water, BSAW=Barents Sea modified Atlantic Water, BSBW=Barents Sea Bottom Water, No=Norway, Sv=Svalbard, FJL=Franz Josef Land, NZ=Novaya Zemlya and KG=Kara Gate.

Passage	f CW	f AW	f ArW	f BSAW	f BSBW
IN					
No - Sv	0.220	0.780			
Sv - FJL		0.837	0.163		
FJL - NZ		0.049	0.951		
KG	1				
OUT					
No - Sv		0.896	0.104		
Sv - FJL			0.073	0.927	
FJL - NZ			0.458	0.125	0.417
KG	1				

The salinity range and mean salinity (Table 3) of the five water masses were chosen based on comparison of cruise data with existing water mass definitions (Loeng, 1991; Pfirman et al., 1994; Steele et al., 1995; Harris et al., 1998; Schauer et al., 2002b; Leikvin, 2003; Smolyar and Adrov, 2003; Panteleev et al., 2004). The flows through Kara Gate were assumed to be 100 % CW due to their low mean salinities. The outflow between Franz Josef Land and Novaya Zemlya consists of three water masses and the fractions could thus not be calculated (since only salinity was known along with mass conservation).

Table 3: Mean salinities used for fraction calculations (Table 2). Abbreviations as in Table 2.

Passage	CW	AW	ArW	BSAW	BSBW
IN					
No - Sv	34.5	35.07			
Sv - FJL		34.94	34.4		
FJL - NZ		34.94	34.4		
KG	27				
OUT					
No - Sv		35.07	34.4		
Sv - FJL			34.4	34.909	
FJL - NZ			34.4	34.909	34.904
KG	33.06				

The fractions for this outflow were therefore based on the percentages of the different water masses present in this outflow as found by Leikvin (2003) and the assumption that the low-salinity surface water encountered in that study was melt water and not present in winter. The mean salinity was also kept close to the mean salinity from the model by Maslowski et al. (2004).

It was assumed that BSAW is formed by mixing of cooled AW with ArW (Loeng, 1991) and that BSBW is formed by mixing of cooled AW with brine water, the latter being formed from ArW. The fractions of cooled AW and ArW that contribute to BSAW were calculated based on salinities while the fractions in BSBW were calculated based on temperature since salinity of brine water varies widely in the Barents Sea (Midttun, 1985; Pfirman et al., 1994; Maus, 2003; Skogseth et al., 2004; Skogseth et al., 2005) and the water mass is formed subsurface. The temperature for brine water was assumed to be at the freezing point (-1.8º C) and the AW was assumed to have a temperature of 1º C.

2.1.2 Water mass carbon concentrations

The DIC concentrations in the five water masses were taken from field observations (Table 4) while the DOC and POC concentrations were obtained from the literature (Table 5 and 6). DIC concentrations were normalised to the mean salinity when there was a clear relationship between DIC concentration and salinity (Friis et al., 2003) in absence of a relationship a mean value was used. CW was treated as AW diluted with freshwater (i.e. salinity normalised to the assumed salinity for the CW with zero intercept). The exchange between the Norwegian Coastal Current and the Norwegian Atlantic Current is large as they flow north (Gascard et al., 2004) and when the CW arrives in the BSO the traces of the Baltic Sea water is small. The DIC concentrations in the surface water change during a year, mainly due to biological production. The production is not easily corrected for when data from several cruises are used together and to decrease the uncertainties added by biological production the budget was set up to represent the winter situation. Since winter data was not available DIC concentrations were only used from the lower part of the winter mixed layer, not from the surface where production had taken place. In the case of AW data below ~100 m was used while data below ~50 m was used in ArW since the production does not occur as deep here as in AW (Kaltin et al., 2002; Kivimäe et al., submitted).

Olsen et al. (2006) found an increase of seawater DIC due to anthropogenic sources of CO_2 in the Nordic Seas of 0.6-0.9 μmol kg^{-1} yr^{-1} during the period 1981 to 2002/2003. Due to the long time span of the cruises from which data has been used in this study, 1996-2005, a correction for this increase was done. The DIC concentration in the waters of the West Spitsbergen Current was found to increase by 12-14 μmol kg^{-1} during 21 years giving a mean increase of 0.62 μmol kg^{-1} yr^{-1} (Olsen et al., 2006). It was assumed that the increase in the DIC concentration in the North Cape Current kept track with the West Spitsbergen Current and thus an increase of 0.62 μmol kg^{-1} yr^{-1} was used for all AW associated waters in the budget. All DIC concentrations were normalised to 2003.

Table 4: Concentrations of DIC (µmol kg^{-1}) for the five water masses of the budget with cruise(s) from which the data was taken. The concentrations have been corrected for the increase of CO_2 due to increasing atmospheric concentration. Abbreviations as in Table 2.

Passage	Water mass IN	Data source	DIC (µmol /kg)	Water mass OUT	Data source	DIC (µmol /kg)
No - Sv	CW	Diluted AW	2112	AW	Knorr 2002[a], G. O. Sars 2003[b]	2145
	AW	Knorr 2002[a], G. O. Sars 2003[b]	2145	ArW	Jan Mayen 1999[c], Håkon Mosby 2000[d], CABANERA 2003-5[e]	2128
Sv - FJL	ArW	Jan Mayen 1999[c], Håkon Mosby 2000[d], CABANERA 2003-5[e]	2128	ArW	Jan Mayen 1999[c], Håkon Mosby 2000[d], CABANERA 2003-5[e]	2128
	AW	Polarstern ARK XII 1996[f]	2149	BSAW	Polarstern ARK XII 1996[f]	2155
FJL - NZ	ArW	Polarstern ARK XII 1996[f]	2147	ArW	Polarstern ARK XII 1996[f]	2147
	AW	Polarstern ARK XII 1996[f]	2149	BSAW	Polarstern ARK XII 1996[f]	2155
				BSBW	Polarstern ARK XII 1996[f]	2188
KG	CW	Diluted AW	1653	CW	Diluted AW	2024

Originator of dataset:
[a] R. Bellerby/T. Johannessen, University of Bergen
[b] A. Olsen/T. Johannessen, University of Bergen
[c] M. Chierici/A. Fransson/L. G. Anderson, Göteborg University
[d] A. Olsen/A. Omar/T. Johannessen, University of Bergen
[e] R. Bellerby/C. Kivimäe/T. Johannessen, University of Bergen
[f] M. Chierici/A. Fransson/L. G. Anderson, Göteborg University

The changes in DIC concentration in ArW due to uptake of anthropogenic CO_2 are not well known, the increase has been lower in the Polar Water of the East Greenland Current than in the AW of the West Spitsbergen Current (Olsen et al., 2006) but the concentration of anthropogenic carbon is fairly similar in the two currents, 34 and 38.9 µmol kg^{-1} respectively (Jutterström, 2006). Since the ArW has a stronger relation to AW than to Polar Water the same increase rate as in AW was assumed. The DIC concentrations presented in Table 4 are corrected for the increase due to uptake of anthropogenic carbon.

Table 5: Concentrations of DOC (µmol/l) for the five water masses of the budget with literature source(s).

Passage	Water mass IN	Data source	DOC (µmol/l)	Water mass OUT	Data source	DOC (µmol/l)
No - Sv	CW	Assumption	70	AW	Amon and Budéus (2003)	58.2
	AW	Amon and Budéus (2003)	58.2	ArW	Modified from Gasparovic et al. (2007)	62.5
Sv - FJL	ArW	Modified from Gasparovic et al. (2007)	62.5	ArW	Modified from Gasparovic et al. (2007)	62.5
	AW	Amon and Budéus (2003)	58.2	BSAW	AW + ArW	60.7
FJL - NZ	ArW	Bussmann and Kattner (2000)	77	ArW	Bussmann and Kattner (2000)	77
	AW	Amon and Budéus (2003)	58.2	BSAW	AW + ArW	60.7
				BSBW	AW + brine	63.6
KG	CW	Amon (2004)	196	CW	Amon (2004)	85

The DOC and POC concentrations in and around the Barents Sea presented in Table 5 and 6 represent either wintertime values or values from the base of the mixed layer during the productive season where it is assumed that the influence of the active biological production is small. DOC and POC concentrations in BSAW and BSBW are based on the fractions and concentrations in their source waters.

2.1.3 River runoff and land sources

Values for water discharge and concentration of hydrogen carbonate (HCO_3^-) were taken from Gordeev et al. (1996), see Table 7, giving a total HCO_3^- inflow of $31.9 \cdot 10^6$ t yr^{-1} to the Barents Sea corresponding to $6.27 \cdot 10^6$ t C yr^{-1}. Vetrov and Romankevich (2004) found a total DOC flow from land of $6.05 \cdot 10^6$ t C yr^{-1} including river runoff and ground water transport (underground runoff) while the total POC flow, including river runoff, wave abrasion, and eolian transport amounted to $1.7 \cdot 10^6$ t C yr^{-1}. The POC flux also included contributions from the White Sea.

2.1.4 Air-sea exchange of CO_2

The net CO_2 flux in the Barents Sea is from the atmosphere to the surface water due to cooling of the water in winter and biological (export) production in summer and hence, atmospheric uptake of CO_2 is a local source of DIC in this area.

Table 6: Concentrations of POC (µg C l^{-1}) for the five water masses of the budget with literature source(s).

Passage	Water mass IN	Data source	POC (µg C/l)	Water mass OUT	Data source	POC (µg C/l)
No - Sv	CW	Wassmann et al. (1999)	100	AW	Olli (pers. comm.)	50
	AW	Olli (pers. comm.)	50	ArW	Andreassen et al. (1996), Olli et al. (2007)	60
Sv - FJL	ArW	Andreassen et al. (1996), Olli et al. (2007)	60	ArW	Andreassen et al. (1996), Olli et al. (2007)	60
	AW	Olli (pers. comm.)	50	BSAW	AW + ArW	52
FJL - NZ	ArW	Andreassen et al. (1996), Olli et al. (2007)	60	ArW	Andreassen et al. (1996), Olli et al. (2007)	60
	AW	Olli (pers. comm.)	50	BSAW	AW + ArW	52
				BSBW	AW + brine	55
KG	CW	Wassmann et al. (1999)	100	CW	Wassmann et al. (1999)	100

The amount of CO_2 uptake from the atmosphere in the AW of the Barents Sea was taken from Omar et al. (2007) who found a mean annual uptake of 4.27 ±0.68 mol C m^{-2} (51.3 ±8.2 g C m^{-2}). The uptake of CO_2 in ArW was assumed to be half of that in AW (Kaltin et al., 2002; Kivimäe et al., submitted). To find the total CO_2 uptake it was assumed that 2/3 of the Barents Sea area is covered by AW and 1/3 by ArW.

Table 7: Water and HCO_3^- discharges of the rivers entering the Barents Sea from Gordeev et al. (1996).

River	Discharge	$[HCO_3^-]$	HCO_3^-
	$km^3\ yr^{-1}$	$mg\ l^{-1}$	$10^6\ t\ yr^{-1}$
Onega	15.9	102	1.5
N. Dvina	110	106	11.5
Mezen	27.2	87.3	2.19
Pechora	131	39.5	5.68
Other area	179		10.9
Total	463		31.9

2.1.4.1 Air-sea uptake of CO_2 during ice formation

Brine water is formed during ice formation when salts are rejected from the ice and accumulates in the surface water. Polynyas at several locations in the Barents Sea produce large amounts of brine water, especially the Storfjorden polynya, the polynyas west and northwest of Novaya Zemlya, and around Franz Josef Land (Martin and Cavalieri, 1989; Skogseth et al., 2004). Omar et al. (2005) found that there was an increase in the uptake of atmospheric CO_2 in relation with brine water formation in the Storfjorden polynya, resulting in an extra uptake of 59.8 g C m^{-2} during the winter in the polynya compared to the adjacent ice covered area. If it is assumed that this extra CO_2 uptake takes place in a similar way in all the polynyas in the Barents Sea the total amount of extra CO_2 taken up during brine water formation can be calculated from the total polynya area. Areas for the Storfjorden polynya and the polynyas west of Novaya Zemlya and south of Franz Josef Land were obtained from Skogseth et al. (2004) and Martin and Cavalieri (1989). The respective areas were then multiplied with the extra CO_2 uptake.

2.1.5 Burial of organic carbon in the sediments

Burial of organic carbon in the sediment is a sink for organic carbon in the ocean. Rates of organic carbon burial in the sediments of the Barents Sea have been estimated by Carrol et al. (this issue) based on measurements from sediment cores. They found rates of burial for the last ~150 years ranging between 3.7 and 8.5 g C m^{-2} yr^{-1} with a mean of 6.1 ±1.8 g C m^{-2} yr^{-1}. The mean burial rate was multiplied with the area of the Barents Sea to find the total burial of organic carbon.

2.2 Shelf pumping in the Barents Sea

Extensive cooling of water in winter and large biological production in summer on continental shelves lead to the production of dense, carbon enriched waters that flow into the subsurface layers of the adjacent deep basins. This process is sometimes referred to as “shelf pumping” (Tsunogai et al., 1999; Yool and Fasham, 2001; Thomas et al., 2004; Borges et al., 2005; Bates, 2006). Cooling of the water serves both to increase its density and to increase the solubility of CO_2.

DIC concentrations in BSAW and BSBW are larger than in their respective source waters (see section 2.1.1). This extra DIC content comes from uptake of atmospheric CO_2. In the Barents Sea this CO_2 uptake is driven by cooling of the surface water and export production. BSAW and BSBW are here seen as water masses that are formed by mixing of AW and ArW / brine water after the AW has been cooled and taken up CO_2 from the atmosphere. The change in DIC (ΔDIC) attributed to shelf pumping in BSAW and BSBW was calculated as the difference between the measured DIC concentration and the concentrations in the original mixed water mass. The concentration in the original mixed water mass for BSAW was calculated as the fractions of cooled AW and ArW times the DIC concentrations these waters had as they entered the Barents Sea. The concentration in the BSBW original mixed water

mass was calculated in the same way with cooled AW and brine water. To discern between the two drivers for increased DIC concentration the amount of CO_2 uptake due to cooling in the AW was calculated first and the residual ΔDIC was then attributed to remineralised export production.

2.2.1 DIC increase due to cooling

The net CO_2 flux mentioned in section 2.1.4 constrains the total CO_2 exchange forced by cooling and biological drawdown of CO_2 in the surface ocean in the entire Barents Sea. Here the uptake of CO_2 in the AW due to cooling of the water mass in winter will be calculated. In 2003 the AW in the BSO had a mean temperature of ~4ºC while it in the proximity of the Polar Front (where AW is subducted) in Hopen deep had been cooled to ~2ºC. The air-sea CO_2 flux into the AW was calculated based on atmospheric mole fraction of CO_2 (xCO_2), fCO_2 from stations in the BSO and in the proximity of the Polar Front, monthly mean wind speeds, and the formulation of k (exchange velocity) from Wanninkhof (1992). Atmospheric xCO_2 is measured at Zeppelin Mountain, Svalbard (79º N), and are available from the NOAA ESRL Global Monitoring Division. Monthly xCO_2 values for 2003 were obtained from ftp://140.172.192.211/ccg/co2/flask/month/sep_01D0_mm.co2. fCO_2 in the seawater was calculated from DIC concentration and total alkalinity with the program developed by Lewis and Wallace (1998) using the constants of Mehrbach et al. (1973) refitted by Dickson and Millero (1987). Monthly wind speeds were calculated from 6-hourly wind speeds from the Hindcast database from the Norwegian Meteorological Institute (Eide et al., 1985). The resulting air-sea flux estimate is the best possible with the available data but the scarceness of measured DIC concentration data has to be kept in mind when it is interpretated. It should also be noted that this estimate is not directly comparable with the results from Omar et al. (2007) mentioned in section *2.1.4.1* due to the differences in time span, data coverage, and calculation method.

The change in DIC concentration was then calculated as the result of six months (October to March) air-sea CO_2 flux into a mixed layer of 250 m (this is about the maximum mixed layer depth in AW during winter). The reason for using six months is that a residence time of two years is used for the AW in the Barents Sea in this work (for a discussion of the residence time see section 4.3) and further it was assumed that the AW is in contact with the atmosphere only during the first of these two years. During the first year cooling takes place during winter which is assumed to last for six months. Finally the concentration change in BSAW and BSBW was calculated according to the fractions of their source waters.

2.2.2 DIC increase due to export production

The size of the annual net CO_2 uptake driven by primary production is equal to the export production, which represents the amount of carbon, in form of organic carbon that is exported from the mixed layer to depth. Since the water below the mixed layer is isolated from the atmosphere, the CO_2 evolved during remineralisation can not be exchanged with the atmosphere and is accumulated in the water. Seasonal pycnoclines

exist in both AW and ArW but the significant permanent pycnocline in the Barents Sea is the separation between ArW and AW where AW is subducted below ArW. Thus BSAW and BSBW accumulate the export production from the ArW as it passes below it.

To find the ΔDIC caused by remineralisation of export production in BSBW both the CO_2 uptake in the AW and the extra CO_2 uptake as brine water forms, as described in section 2.1.4.1, must be subtracted. The extra CO_2 uptake in the Storfjorden polynya on volume basis was 0.15 ±0.044 g C m^{-3} (Omar et al., 2005).

3. Results

3.1 Barents Sea carbon budget

Volume flows for the separate water masses, calculated from the total volume flows from Maslowski et al. (2004) and the fractions in Table 2 are presented in Table 8. In the passage between Norway and Svalbard 3.96 Sv AW enters the Barents Sea of which about 40 % is recirculated back to the Norwegian Sea. The remaining AW entering the Barents Sea both in the BSO and in the north and northeast is transformed to BSAW, BSBW, or ArW. More CW enters the Barents Sea than exits, which indicates that the coastal current is a freshwater source for the water mass transformations that occur in the Barents Sea.

The results in Table 8 indicate that the main exchange in the passage between Svalbard and Franz Josef Land is made up of AW from the Fram Strait branch and BSAW from the Barents Sea while ArW has only a small contribution.

Table 8: Volume flows (Sv) through the different passages to the Barents Sea for the five water masses in the budget based on the volume flows in Table 1 and the fractions in Table 2. Abbreviations as in Table 2.

Passage	CW	AW	ArW	BSAW	BSBW
IN					
No - Sv	1.11	3.96			
Sv - FJL		0.68	0.13		
FJL - NZ		0.03	0.58		
KG	0.01				
OUT					
No - Sv		1.61	0.19		
Sv - FJL			0.09	1.08	
FJL - NZ			1.47	0.40	1.33
KG	0.33				

Table 9: The Barents Sea carbon budget, all entries are in 10^6 t C yr^{-1}.

Source / sink	DIC in	DOC in	POC in	DIC out	DOC out	POC out
Svalbard - Norway	4204.8	116.3	9.72	1497.0	39.8	2.89
Svalbard - Franz Josef Land	674.2	18.0	1.32	977.2	26.9	1.93
Franz Josef Land - Novaya Zemlya	508.0	17.5	1.14	2687.4	83.8	5.73
Kara Gate	6.37	0.74	0.03	258.7	10.6	1.04
River runoff and land sources	6.27	6.05	1.70			
Sedimentation						9.21
Air-sea uptake	64.6					
Extra CO_2 uptake in brine water	0.68					
Subtotal	5464.9	158.6	13.9	5420.3	161.1	20.8
Total		**5637**			**5602**	

The second major flow-through passage after Norway-Svalbard is the one between Franz Josef Land and Novaya Zemlya, here the inflow is mainly made up of ArW but there is also a small contribution from the Fram Strait branch of AW. The outflow is based on assumed fractions which were chosen so that the mean salinity corresponded closely to the mean value from the model by Maslowski et al. (2004). ArW and BSBW contribute with comparable amounts while the BSAW contributes about 15% of the flow. Flow through the Kara Gate is almost entirely to the east (out of the Barents Sea) and the assumption was that all this water is CW.

The Barents Sea carbon budget detailing advection, river runoff and land sources, total CO_2 air-sea exchange, extra uptake of CO_2 in the polynyas, and burial in the sediments is presented in Table 9. The budget show a total input of $5638 \cdot 10^6$ t C yr^{-1} to the Barents Sea and a total output of $5602 \cdot 10^6$ t C yr^{-1}. The DIC import to the Barents Sea is $5465 \cdot 10^6$ t C yr^{-1} while the export is $5420 \cdot 10^6$ t C yr^{-1}. The TOC pool is supplied with $173 \cdot 10^6$ t C yr^{-1} while $182 \cdot 10^6$ t C yr^{-1} is exported or buried in the sediments.

Divided by passage, the budget shows that the Barents Sea is a net importer of water and carbon between Norway and Svalbard while it is a net exporter of both water and carbon through the other three passages. The Barents Sea is a source of carbon to the Arctic Ocean; the net DIC export between Svalbard-Franz Josef Land and Franz Josef Land-Novaya Zemlya is $2474 \cdot 10^6$ t C yr^{-1} of which $1776 \cdot 10^6$ t C yr^{-1} is in subsurface water masses (BSAW and BSBW) and is therefore sequestered from the atmosphere. The net TOC export to the AO is $80 \cdot 10^6$ t C yr^{-1}. If the concentrations of refractory

DOC and POC are 50 µM and 50 µg C/l respectively the amount of labile organic carbon exported to the AO is $20 \cdot 10^6$ t C yr^{-1} of which $16 \cdot 10^6$ t C yr^{-1} is in the ArW. This result is consistent with the notion that the AO is net heterotrophic (Olli et al., 2007) in the sense that the Barents Sea is a net exporter of labile organic carbon to the AO.

3.2 Shelf pumping in the Barents Sea

Estimated from the salinities the BSAW was composed of 78 % AW and 22 % ArW. Based on these fractions the ΔDIC between measured DIC and DIC in the original contributing waters was 12.1 µmol kg^{-1}. Following the calculations outlined in section 2.2 the result was that 4.2 µmol kg^{-1} of these 12.1 µmol kg^{-1} originated from direct uptake of atmospheric CO_2 in the AW while 7.9 µmol kg^{-1} was channelled through export production. Multiplied by the volume flow of BSAW this corresponds to a total of $2.4 \cdot 10^6$ t C yr^{-1} and $4.1 \cdot 10^6$ t C yr^{-1} respectively. The BSBW, estimated from temperature, consisted of 54 % AW and 46 % brine water with a total ΔDIC of 46.9 µmol kg^{-1}, 2.8 µmol kg^{-1} from direct atmospheric uptake and 38.4 µmol kg^{-1} from export production. $4.4 \cdot 10^6$ t C yr^{-1} was thus taken up from the atmosphere in the AW before mixing with brine water while remineralisation contributed with $19.3 \cdot 10^6$ t C yr^{-1}.

4. Discussion

4.1 Barents Sea carbon budget

The carbon budget for the Barents Sea shows that ~$5600 \cdot 10^6$ t C is exchanged across the boundaries of the Barents Sea in one year, mainly in the form of advected DIC. The strength of the AW inflow through the BSO is important for the Barents Sea, both for the distribution and variability of temperature, salinity and ice cover (Loeng, 1991; Ådlandsvik and Loeng, 1991). The importance of the AW inflow is obvious also in the carbon budget, mainly through the relation between DIC concentration and salinity. The amount of AW in the Barents Sea also affects the carbon budget through its influence on the sea ice extent which, together with the residence time of the AW, determines the amounts of uptake of atmospheric CO_2 and primary production with subsequent export production. The advection of AW through the BSO has increased in later years (Ingvaldsen pers. comm.) and is projected to increase even more in the future (ACIA, 2005). Due to its importance for the carbon budget changing AW advection will have clear effects on the carbon budget and the result of an increased advection is an increased amount of carbon exchanged through the boundaries of the Barents Sea.

The second largest contribution to the budget is the advection of organic carbon followed by the total uptake of atmospheric CO_2 and river runoff and land sources. The burial of organic carbon in the sediments is the smallest entry in the budget. The difference between the advective in- and outflux of carbon to the area consists of the balance between the sources and sinks within the Barents Sea (Figure 2); the influx

through air-sea uptake of CO_2, river runoff, land sources, and loss through sedimentation. Since the sources are larger than the sink the advective influx of carbon to the Barents Sea in theory should be smaller than the advective outflux. Due to the uncertainties in the estimates of the advective fluxes in the presented budget we cannot say with confidence that this is the case (for discussion of the uncertainties see section 4.3).

The net advective influx through the BSO is ~$2800 \cdot 10^6$ t C yr^{-1} which is larger than the influx Anderson et al. (1998) calculated for this passage of 1.291 Gt C yr^{-1} (~$1300 \cdot 10^6$ t C yr^{-1}). The difference of the two estimates is mainly due to the larger net volume flow in this budget compared to the budget by Anderson et al. (1998), 3.3 Sv compared to 1.5 Sv, since Anderson et al.'s (1998) budget only included AW in the BSO. The net advective DIC influx from this work, ~$2700 \cdot 10^6$ t C yr^{-1}, is however only half of the DIC influx over the Iceland-Shetland ridge in the North Atlantic Water (NAW) and Norwegian Coastal Current (NwCC) calculated by Lundberg and Haugan (1996), $14.85 \cdot 10^6$ mol C s^{-1} (~$5600 \cdot 10^6$ t C yr^{-1}). Lundberg and Haugan's (1996) estimate was based on a volume flow of 6.85 Sv (6.2 Sv NAW and 0.65 Sv in the NwCC). The other half of the DIC transport to the Norwegian Sea estimated by Lundberg and Haugan (1996) can then be assumed to be transported northwards into Fram Strait or recirculated within the Nordic Seas. This rough comparison indicate that the DIC transport in Barents Sea branch of AW is equal to or larger (if some recirculation takes place in the Nordic Seas) than the transport in the Fram Strait branch, similar to what Anderson et al. (1998) found (1.291 Gt C yr^{-1} transported through the BSO in the Barents Sea branch and 0.863 Gt C yr^{-1} transported through Fram Strait in the lower halocline and Atlantic layer).

4.2 Shelf pumping in the Barents Sea

The transformation of water masses that occurs in the Barents Sea, the formation of the colder, fresher, and denser modified Atlantic Waters and brine water, is important for the carbon budget of the Arctic Mediterranean. The BSAW and BSBW that leaves the Barents Sea are enriched with CO_2 from atmospheric uptake and remineralisation of export production. The total amount of remineralised export production retrieved in BSAW and BSBW is in this work estimated to be $23.4 \cdot 10^6$ t C yr^{-1}. Reigstad et al. (this issue) estimated, based on sediment traps, an export production at 90 m in ArW in the Barents Sea of 31.8 g C m^{-2} yr^{-1}. This corresponds to a total export production of $15.8 \cdot 10^6$ t C yr^{-1} in ArW if it is assumed that ArW covers 1/3 of the Barents Sea. The 31.8 g C m^{-2} yr^{-1} found by Reigstad et al. (this issue) is equivalent to 47 % of the modelled annual primary production in ArW of 68 g C m^{-2} yr^{-1} reported by Wassmann et al. (2006). The amount of carbon attributed to export production in BSAW and BSBW is higher (~150%) than the export production found by Reigstad et al. (this issue) but lower (~70%) than the modelled primary production from Wassmann et al. (2006). This amount is unreasonable high; Reigstad et al. (this issue) found that 47% of the total production was exported past 90 m. An export in the ArW 50% larger than they found only accentuates this, and it can be assumed that some of the export production originates in the AW. If the export production in ArW is consistent with the findings

of Reigstad et al. (this issue), then the BSAW and BSBW together must contain 7.6 $\cdot 10^6$ t C yr^{-1} or 7.5 g C m^{-2} yr^{-1} from export production in the AW. This means that 17 % of the export production in the AW is retrieved in the BSAW and BSBW if again Reigstad et al.'s (this issue) estimations of the export production in the AW of 44.4 g C m^{-2} yr^{-1} (giving $44.9 \cdot 10^6$ t C yr^{-1} if 2/3 of the Barents Sea is covered by AW) is used. This is not unlikely considering 78 % and 54 % of the BSAW and BSBW respectively originates from AW.

The total amount of retrieved export production ($23.4 \cdot 10^6$ t C yr^{-1}) is also larger than the export production calculated by Fransson et al. (2001) for the water that had crossed the Barents Sea from the BSO to St. Anna Trough. Franzson et al. (2001) found a total export production from the upper 150 m of this water of $9.6 \cdot 10^{12}$ g C yr^{-1} ($9.6 \cdot 10^6$ t C yr^{-1}) by multiplying the deficit of phosphate with the volume flow. The different method along with a much smaller volume flow, 1.21 Sv compared to 2.8 Sv in this work, explains most of this difference.

If an Atlantification (*sensu* Wassmann et al., 2004) occurs in the Barents Sea along with the modelled decrease of the Northern Hemisphere sea ice cover (ACIA, 2005), the entire Barents Sea will become ice free also in winter. This will result in absence of ice formation and thus brine water formation, which will affect the formation of BSBW. BSBW is the water mass with the strongest shelf pumping signal and this water mass is also the densest with the deepest penetration depth in the Eurasian Basin of the AO. BSAW carries a smaller shelf pumping signal and is slightly less dense, but still dense enough to penetrate the AO below the halocline. According to Schauer et al. (1997) modified AW from the Barents Sea can be found between 200 and 1300 m in the Nansen Basin. The Barents Sea is also together with the Kara Sea the only source areas for shelf water able to ventilate the Eurasian Basin below the halocline (Schauer et al., 1997). The CO_2 content of these dense modified AWs is thus effectively sequestered within the deep AO. In a future with less cooling of the AW in the Barents Sea and less sea ice melt water in the surface the result may be that the AW still will be in contact with the atmosphere as it exits the Barents Sea to the north into the AO. The total uptake of atmospheric CO_2 in the Barents Sea under such a scenario will probably decrease since the shelf pump would be less effective.

4.3 Uncertainties

The advective fluxes of DIC, DOC, and POC are based on volume flows and carbon concentrations at the borders of the Barents Sea (Figure 1). Volume flows have been measured in three places, between Nordaustlandet and Kvitøya (Svalbard archipelago) 1980-81 (Aagard et al., 1983), between Franz Josef Land and Novaya Zemlya 1991-92 (Leikvin, 2003) and for five years in the BSO (Ingvaldsen et al., 2004). These studies together do not cover all the inflows to and outflows from the Barents Sea so in order to establish a balanced budget of volume flows data from a model had to be used. The volume flows from the model of Maslowski et al. (2004) are larger than those reported from measurements. Ingvaldsen et al. (2004) measured volume flows across the Fugløya (Norway)-Bjørnøya section during five years and found a mean annual net

inflow of 1.5 Sv AW. Maslowski et al. (2004) found a net inflow for the whole passage between Norway and Svalbard of 3.27 Sv, which is similar to the inflow modelled by Budgell (2005) of 3.6 Sv. The inflow modelled by Maslowski et al. (2004) was about twice as large as the measured flow, but the modelled flow also included inflow in the coastal current. The volume flow of the coastal current is not well known but is around 0.5-1 Sv (Ingvaldsen et al., 2004). When the fractions calculated in this work are employed to the total model volume flows the result is a net inflow of 2.35 Sv AW through the BSO (Table 8).

The main outflow from the Barents Sea occurs between Franz Josef Land and Novaya Zemlya and the net outflow based on observations was estimated to 1.9 Sv by Leikvin (2003). The modelled outflow through this passage was 2.56 Sv, again about 1.5 times larger than the measured. The larger model volume flows may depend on the absence of tides in the model (Maslowski et al., 2004) since tides can result in strong tidal currents in the Barents Sea, also opposing the main flow direction. Another reason is that the volume flows in the model can be calculated from coast to coast and are not limited by the extent of the mooring array.

The consequence of the larger model volume flows is a reduction in the residence time of the waters within the modelled Barents Sea, the combined inflows from Maslowski et al. (2004) divided by the volume of the Barents Sea results in a mean residence time of all waters of ~1.5 years. This is a shorter residence time than is achieved if the calculations are done with the smaller measured volume flows. Asplin et al. (in prep.) found that it takes 2-4 years for the water to flow through the Barents Sea. A residence time of two years is used in the budget; the residence time is needed for the calculations outlined in section 2.2 to differentiate between uptake of CO_2 driven by cooling of AW and by export production. If a longer residence time is used then more of the extra DIC found in the BSAW and BSBW origins from direct uptake of CO_2 from the atmosphere and less from remineralised export production.

The DIC concentrations used in the budget were taken from measurements and in this context the definitions of the water masses are essential for the results. The AW that flows into the Barents Sea through the BSO is the only thoroughly characterised water mass in the Barents Sea; it can always be recognised by its relatively high salinity and in winter by its high temperature. In this work a salinity of 34.95 was used as the lower limit for AW in the BSO, a somewhat lower limit than the classical 35.0 (Loeng, 1991) but this lower limit is used in order to include the entire water mass and not only the core as stricter definitions do. After the salinity range was chosen the mean salinity was taken from the measurements. For the other water masses salinity spans had to be chosen based on available data and comparisons with the literature. The water mass that is most difficult to characterise is the ArW since it is surface water mass from which few DIC measurements exist. The use of 34.4 as the mean salinity for ArW was forced by the mean salinities from the model since its mean salinity in the inflow between Franz Josef Land and Novaya Zemlya was 34.43 and some of this water is AW from the Fram Strait branch. The mean salinity of ArW may be a bit higher, 34.5-34.7, depending on what area of the northern Barents Sea is investigated (Loeng, 1991;

Pfirman et al., 1994; Steele et al., 1995; Harris et al., 1998). Using a higher mean salinity in the ArW, and thus higher mean DIC concentration, would lead to a larger outflux of DIC from the Barents Sea since more ArW is exported than imported. DIC concentration data for the outflowing water between Franz Josef Land and Novaya Zemlya were taken from a cruise in the northern St. Anna Trough (*Polarstern* ARK XII, 1996) since no DIC measurements to our knowledge exist in that passage. It has been assumed that the changes in DIC concentration in the water masses are insignificant between the Franz Josef Land-Novaya Zemlya passage and the northern St. Anna Trough. It is possible that the subsurface water may experience an increase in DIC concentration due to remineralisation of more export production as they travel along St. Anna Trough in which case the amount of exported remineralised export production from the Barents Sea have been overestimated. The ArW on the other hand may have experienced more atmospheric uptake as it flows south from the northern St. Anna Trough to the Barents Sea resulting in too low DIC concentrations.

In the context of DIC concentrations is should be noted that the salt budget showed a small net influx of salt to the Barents Sea even though the volume flow budget was balanced by adding 0.04 Sv to the fluxes from Maslowski et al. (2004). During winter DIC concentration in sea water is strongly related to salinity with increasing concentrations following increasing salinities. If the salt budget was balanced the advective outflux would be even larger compared to the advective influx as discussed in section 4.1 and a larger outflux would improve the balance of the carbon budget (see Table 9).

In addition to the references on DOC concentrations in Table 5 it may be noted that both Amon (2004) and Wheeler et al. (1997) report DOC concentrations of 58 µM in the AW layer in the Eurasian Basin. The concentrations used for BSAW and BSBW in this work (see Table 5) are higher and the transport of DOC to the AO may thus be overestimated. POC concentrations in sea water are seldom measured, it is more often the vertical flux of POC that is measured, but the uncertainty that the scarcity of data introduces into the budget is small since the POC concentrations are an order of magnitude smaller than the DOC concentrations.

6. Summary and conclusions

The carbon fluxes into, out of, and within the Barents Sea have been examined by constructing a carbon budget based on volume flows from a model, measured DIC concentrations, and a compilation of DOC and POC concentrations from the literature. The resulting budget shows a total input/output of ~$5600 \cdot 10^6$ t C yr^{-1} to/from the Barents Sea. The main part of the budget consists of advected DIC followed by advection of organic carbon, uptake of atmospheric CO_2, river runoff and land sources, and burial of organic carbon in the sediments. The Barents Sea is a net importer of water and carbon through the passage between Norway and Svalbard while it is a net exporter of both water and carbon through the other three passages. The DIC export to the AO is ~$2500 \cdot 10^6$ t C yr^{-1} of which ~$1800 \cdot 10^6$ t C yr^{-1} (72%) is in subsurface water

masses (BSAW and BSBW). The TOC part of the budget shows a net outflux from the Barents Sea. The AO is supplied with a net flux of TOC, $80 \cdot 10^6$ t C yr^{-1}, of which $20 \cdot 10^6$ t C yr^{-1} is labile.

Shelf pumping in the Barents Sea results in that the dense waters formed in the area, BSAW and BSBW, exits with higher DIC concentrations from uptake of atmospheric CO_2. The total amount of CO_2 taken up from the atmosphere and exported in these dense waters was $30 \cdot 10^6$ t C yr^{-1}, the main part of this was channelled through export production ($23 \cdot 10^6$ t C yr^{-1}). Since the dense waters originating from AW penetrates the water column in the Eurasian Basin below the halocline and the carbon content of these waters is thus sequestered from the atmosphere for decades to hundreds of years.

Acknowledgements

This study was supported by the Norwegian Research Council, NORKLIMA Programme through the CABANERA Project (project no. 155936/700) and the 6th Framework Programme (EU FP6 CARBOOCAN Integrated Project, Contract no. 511176). We are grateful to A. Olsen and A. Omar for the permission to use data from the 2000 *Håkon Mosby* and 2003 *G. O. Sars* cruises. Thanks are also due to T. Johannessen and A. Olsen who provided constructive comments to the manuscript. This is contribution number XXX of the Bjerknes Centre.

References

Aagard, K., Foldvik, A., Gammelsrød, T. and Vinje, T., 1983. One-year records of current and bottom pressure in the strait between Nordaustlandet and Kvitøya, Svalbard, 1980-81. Polar Research, I n.s.: 107-113.

ACIA, 2005. Arctic Climate Impact Assessment, ACIA Scientific report, Cambridge University Press.

Ådlandsvik, B. and Loeng, H., 1991. A study of the climate system in the Barents Sea. In: E. Sakshaug, C.C.E. Hopkins and N.A. Øritsland (Editors), Proceedings of the Pro Mare symposium on Polar Marine Ecology. Polar research, Trondheim, pp. 45-49.

Amon, R.M. and Budéus, G., 2003. Dissolved organic carbon distribution and origin in the Nordic Seas: Exchange with the Arctic Ocean and the North Atlantic. Journal of geophysical research, 108(C7): 3221.

Amon, R.M., 2004. The role of dissolved organic matter for the organic carbon cycle in the Arctic Ocean. In: R. Stein and R.W. Macdonald (Editors), The organic carbon cycle in the Arctic Ocean. Springer-Verlag, Berlin Heidelberg New York, pp. 83-99.

Anderson, L.G., Olsson, K. and Chierici, M., 1998. A carbon budget for the Arctic Ocean. Global Biogeochemical Cycles, 12(3): 455-465.

Anderson, L.G., Falck, E., Jones, E.P., Jutterström, S. and Swift, J.H., 2004. Enhanced uptake of atmospheric CO_2 during freezing of seawater: A field study in Storfjorden, Svalbard. Journal of geophysical research, 109: C06004.

Andreassen, I.J., Nöthig, E.-M. and Wassmann, P., 1996. Vertical particle flux on the shelf off northern Spitsbergen, Norway. Marine ecology progress series, 137: 215-228.

Asplin, L., Ingvaldsen, R., Sætre, R. and Loeng, H., Features of the mean Barents Sea circulation. in prep.

Bates, N.R., 2006. Air-sea CO_2 fluxes and the continental shelf pump of carbon in the Chukchi Sea adjacent to the Arctic Ocean. Journal of geophysical research, 111`: C10013.

Bussmann, I. and Kattner, G., 2000. Distribution of dissolved organic carbon in the central Arctic Ocean: the influence of physical and biological properties. Journal of marine systems, 27: 209-219.

Böniisch, G. and Schlosser, P., 1995. Deep water formation and exchange rates in the Greenland/Norwegian Seas and the Eurasian Basin of the Arctic Ocean derived from tracer balances. Progress in oceanography, 35: 29-52.

Borges, A.V., Delille, B. and Frankignolle, M., 2005. Budgeting sinks and sources of CO_2 in the coastal ocean: Diversity of ecosystems counts. Geophysical Research Letters, 32: L14601.

Budgell, W.P., 2005. Numerical simulation of ice-ocean variability in the Barents Sea region Towards dynamical downscaling. Ocean Dynamics, 55: 370-387.

Carrol, J.L., A. Zaborska, C. Papucci, A. Schirone, M. L. Carrol, J. Pempkowiak. Accumulation of organic carbon in western Barents Sea sediments. This issue.

Dickson, A.G. and Millero, F.J., 1987. A comparison of the equilibrium constants for the dissociation of carbonic acid in seawater media. Deep Sea Research, 34: 1733-1743.

Eide, L.I., Reigstad, M. and Guddal, J., 1985. Database av beregnede vind og bølgeparametere for Nordsjøen, Norskehavet, og Barentshavet, hver 6. time for årene 1955-1988 (in Norwegian), Norwegian Meteorlogical Institute, Oslo.

Fransson, A., M. Chierici, L. G. Anderson, I. Bussmann, G. Kattner, E. P. Jones, J. H. Swift, 2001. The importance of shelf processes for the modification of chemical consistuents in the waters of the Eurasian Arctic Ocean: impliactions for carbon fluxes. Continental shelf research, 21: 225-242.

Friis, K., Körtzinger, A. and Wallace, D.W.R., 2003. The salinity normalization of marine inorganic carbon chemistry data. Geophysical Research Letters, 30(2): 1085.

Gascard, J.-C., Raisbeck, G., Sequeira, S., Yiou, F. and Mork, K.A., 2004. The Norwegian Atlantic Current in the Lofoten basin inferred from hydrological and tracer data (^{129}I) and its interaction with the Norwegian Coastal Current. Geophysical Research Letters, 31: L01308.

Gasparovic, B., Plavsic, M., Boskovic, N., Cosovic, B. and Reigstad, M., 2007. Organic matter characterization in Barents Sea and eastern Arctic Ocean during summer. Marine Chemistry, 105:151-165

Gordeev, V.V., Martin, J.M., Sidarov, I.S. and Sidarova, M.V., 1996. A reassessment of the Euroasian river input of water, sediment, major elements, and nutrients to the Arctic Ocean. American journal of science, 296(6): 664-691.

Harris, C.L., Plueddemann, A.J. and Gawarkiewicz, G.G., 1998. Warer mass distribution and polar front structure in the western Barents Sea. Journal of geophysical research, 103(C2): 2905-2917.

Hopkins, T.S., 1991. The GIN Sea - A synthesis of its physical oceanography and literature review 1972-1985. Earth-Science Reviews, 30: 175-318.

Ingvaldsen, R.B., Asplin, L. and Loeng, H., 2004. The seasonal cycle in the Atlantic transport to the Barents Sea during the years 1997-2001. Continental shelf research, 24: 1015-1032.

Jakobsson, M., 2002. Hypsometry and volume of the Arctic Ocean and its constituent seas. Geochemistry, Geophysics, Geosystems, 3(5).

Jutterström, S., 2006. Dissolved inorganic carbon in the Arctic Ocean and the Nordic Seas. PhD Thesis, Göteborg University, Göteborg.

Kaltin, S., Anderson, L.G., Olsson, K., Fransson, A. and Chierici, M., 2002. Uptake of atmospheric cabon dioxide in the Barents Sea. Journal of marine systems, 38: 31-45.

Kivimäe, C., Bellerby, R.G.J., Sundfjord, A. and Omar, A.M., Variability of new production and CO_2 air-sea exchange in the north-western Barents Sea in relation to sea ice cover. In review, Journal of Marine Research.

Leikvin, Ø. 2003. Currents and water mass fluxes between Franz Josef Land and Novaya Zemlya 1991-1993. Cand. Scient. thesis in physical oceanography Thesis, University of Bergen, Bergen, 86 pp.

Lewis, E. and Wallace, D.W.R., 1998. Program Developed for CO2 System Calculations. ORNL/CDIAC-105. Carbon Dioxide Information Analysis Center, Oak Ridge National Laboratory, U.S. Department of Energy, Oak Ridge, Tennessee.

Loeng, H., 1991. Features of the physical oceanographic conditions of the Barents Sea. In: E. Sakshaug, C.C.E. Hopkins and N.A. Øritsland (Editors), Proceedings of the Pro Mare symposium on polar marine ecology, Trondheim, pp. 5-18.

Lundberg, L. and Haugan, P.M., 1996. A Nordic Seas- Arctic Ocean carbon budget from volme flows and inorganic carbon data. Global Biogeochemical Cycles, 10(3): 493-510.

Martin, S. and Cavalieri, D.J., 1989. Contributions of the Siberian shelf polynyas to the Arctic Ocean intermediate and deep water. Journal of geophysical research, 94(C9): 12725-12738.

Martin, T. and Augstein, E., 2000. Large-scale drift of Arctic Sea ice retrieved from passive microwave satellite data. Journal of geophysical research, 105(C4): 8775-8788.

Maslowski, W., D. Marble, W. Walczowski, U. Schauer, J. L. Clement, A. J. Semtner, 2004. On climatological mass, heat, and salt transports through the Barents Sea and Fram Strait from a pan-Arctic coupled ice-ocean medel simulation. Journal of geophysical research, 109: C03032.

Maus, S., 2003. Interannual variability of dense shelf water salinities in the north-western Barents Sea. Polar Research, 22(1): 59-66.
Mehrbach, C., Culberson, C.H., Hawley, E.J. and Pytkowicz, R.M., 1973. Measurements of the apparent dissociation constants of carbonic acid in seawater at atmospheric pressure. Limnology and Oceanography, 18: 897-907.
Midttun, L., 1985. Formation of dense bottem water in the Barents Sea. Deep-Sea Research, 32(10): 1233-1241.
Novitsky, V.P., 1961. Permanent currents of the northern Barents Sea. Trudy gosudarstvennogo okeanografigreskogo instituta, 64: 1-32.
Olli, K., P. Wassmann, M. Reigstad, T. N. Ratkova, E. Arashkevich, A. Pasternak, P. A. Matrai, J. Knulst, L. Tranvik, R. Klais, A. Jacobsen, 2007. The fate of production in the central Arctic Ocean - top-down regulation by zooplankton expatriates? Progress In Oceanography, 72(1): 84-113.
Olsen, A., A. M. Omar, R. G. J. Bellerby, T. Johannessen, U. Ninnermann, K. R. Brown, K. A. Olsson, J. Olafsson, G. Nondal, C. Kivimäe, S. Kringstad, C. Neill, S. Olafsdottir, 2006. Magnitude and origin of the anthropogenic CO_2 increase and ^{13}C Suess effect in the Nordic Seas since 1981. Global Biogeochemical Cycles, 20: GB3027.
Omar, A.M., T. Johannessen, R. G. J. Bellerby, A. Olsen, L. G. Anderson, C. Kivimäe, 2005. Sea-ice and brine formation in Storfjorden: Implications for the Arctic wintertime air-sea CO_2 flux. In: H. Drange, T. Dokken, T. Furevik, R. Gerdes and W. Berger (Editors), The Nordic Seas: An integrated perspective. Geophysical Monograph. American Geophysical Union, Washington DC, pp. 177-187.
Omar, A.M., Johannessen, T., Olsen, A., Kaltin, S. and Rey, F., 2007 Seasonal and interannual variability of the air-sea CO_2 flux in the Atlantic sector of the Barents Sea. Marine chemistry, 104: 203-213.
Panteleev, G., Ikeda, M., Grotov, A., Nechaev, D. and Yaremchuk, M., 2004. Mass, heat and salt balances in the eastern Barents Sea obtained by inversion of hydrographic section data. Journal of oceanography, 60: 613-623.
Pfirman, S.L., Bauch, D. and Gammelsrød, T., 1994. The Northern Barents Sea: Water mass distribution and modification, The polar oceans and their role in shaping the global environment. American Geophysical Union, pp. 77-94.
Reigstad, M., Wexels Riser, C., Wassmann, P. and Ratkova, T., Vertical export of carbon: Attenuation, composition and loss rates in the northern Barents Sea. Deep-Sea Research II, This issue.
Rysgaard, S., Glud, R.N., Sejr, M.K., Bendtsen, J. and Christensen, P.B., 2007. Inorganic carbon transport during sea ice growth and decay: A carbon pump in the polar seas. Journal of geophysical research, 112: C03016.
Sakshaug, E., 2004. Primary and secondary production in the Arctic Seas. In: R. Stein and R.W. Macdonald (Editors), The organic carbon cycle in the Arctic Ocean. Springer-Verlag, Berlin Heidelberg New York, pp. 57-81.
Sakshaug, E. and Slagstad, D., 1992. Sea ice and wind: Effects on primary productivity in the Barents Sea. Atmosphere-Ocean, 30(4): 579-591.

Schauer, U., Muench, R.D., Rudels, B. and Timokhov, L., 1997. Impact of eastern Arctic shelf waters on the Nansen Basin intermediate layers. Journal of geophysical research, 102(C2): 3371-3382.

Schauer, U., Loeng, H., Rudels, B., Ozhigin, V.K. and Dieck, W., 2002a. Atlantic Water flow through the Barents and Kara Seas. Deep-Sea Research I, 49(12): 2281-2298.

Schauer, U., B. Rudels, E. P. Jones, L. G. Anderson, R. D. Muench, G. Björk, J. H. Swift, V. V. Ivanov, A.-M. Larsson, 2002b. Confluence and redistribution of Atlantic Water in the Nansen, Amundsen and Makarow basins. Annales Geophysicae, 20: 257-273.

Skogseth, R., Haugan, P.M. and Haarpaintner, J., 2004. Ice and brine production in Storfjorden from four winters of satellite and in situ observations and modeling. Journal of geophysical research, 109: C10008.

Skogseth, R., Haugan, P.M. and Jakobsson, M., 2005. Watermass transformations in Storfjorden. Continental shelf research, 25: 667-695.

Smolyar, I. and Adrov, N., 2003. The quantitative definition of the Barents Sea Atlantic Water: mapping of the annual climatic cycle and interannual variability. ICES Journal of Marine Sciences, 60: 836-845.

Steele, M., Morison, J.H. and Curtin, T.B., 1995. Halocline water formation in the Barents Sea. Journal of geophysical research, 100(C1): 881-894.

Thomas, H., Bozec, Y., Elkalay, K. and de Baar, H.J.W., 2004. Enhanced open ocean storage of CO_2 from shelf sea pumping. Science, 304: 1005-1008.

Tsunogai, S., Watanabe, S. and Sato, T., 1999. Is there a "continental shelf pump" for the absorption of atmospheric CO_2? Tellus, 51 B(3): 701-712.

Vetrov, A. and Romankevich, E., 2004. The Barents Sea: Distribution, sources, variability and burial of organic carbon. In: R. Stein and R.W. Macdonald (Editors), The organic carbon cycle in the Arctic Ocean. Springer-Verlag, Berlin Heidelberg New York, pp. 266-278.

Wanninkhof, R., 1992. Relationship between wind speed and gas exchange over the ocean. Journal of geophysical research, 97(C5): 7373-7382.

Wassmann, P., Andreassen, I.J. and Rey, F., 1999. Seasonal variation of nutrients and suspended biomass on a transect across Nordvestbanken, north Norwegian shelf, in 1994. Sarsia, 84: 199-212.

Wassmann, P., E. Bauerfeind, M. Fortier, M. Fukuchi, B. Hargrave, B. Moran, T. Noji, E.-M. Nöthig, K. Olli, R. Peinert, H. Sasaki, V. Shevchenko, 2004. Particulate organic carbon flux to the Arctic Ocean sea floor. In: R. Stein and R.W. Macdonald (Editors), The organic carbon cycle in the Arctic Ocean. Springer-Verlag, Berlin Heidelberg New York, pp. 101-138.

Wassmann, P., Slagstad, D., Wexels Riser, C. and Reigstad, M., 2006. Modelling the ecosystem dynamics of the Barents Sea including the marginal ice zone II. Carbon flux and interannual variability. Journal of marine systems, 59: 1-24.

Wheeler, P.A., Watkins, J.M. and Hansing, R.L., 1997. Nutrients, organic carbon and organic nitrogen in the upper water column of the Arctic Ocean: implications for the sources of dissolved organic carbon. Deep Sea Research II, 44(8): 1571-1592.

Yool, A. and Fasham, M.J.R., 2001. An examination of the "continental shelf pump" in an open ocean general circulation model. Global Biogeochemical Cycles, 15(4): 831-844.

Paper II

Variability of new production and CO_2 air-sea exchange in the north-western Barents Sea in relation to sea ice cover

Kivimäe, C., R. G. J. Bellerby, A. Sundfjord, A. Omar and T. Johannessen

In review, Journal of Marine Research

Variability of new production and CO_2 air-sea exchange in the north-western Barents Sea in relation to sea ice cover

Caroline Kivimäe[a], Richard G. J. Bellerby[b,a], Arild Sundfjord[c,a], Abdirahman M. Omar[b,a] and Truls Johannessen[a,b]

[a] Geophysical institute, University of Bergen, Bergen, Norway.
[b] Bjerknes Centre for Climate Research, University of Bergen, Bergen, Norway
[c] Norwegian Polar Institute, Polar Environmental Centre, Tromsø, Norway.

E-mail adresses:
caroline.kivimae@gfi.uib.no
richard.bellerby@bjerknes.uib.no
arild.sundfjord@npolar.no
abdirahman.omar@gfi.uib.no

Abstract

The spatial variability of seasonal new production and CO_2 air-sea exchange in the north-western Barents Sea and its dependence on the sea ice cover is investigated based on data collected during a field study in July 2003. New production and uptake of CO_2 were calculated from deficits of nitrate and total inorganic carbon after the different characteristics of the contributing water masses were taken into consideration. The resulting seasonal new production is twice as high in the Atlantic Water (AW), 52 g C m^{-2} compared to 20-27 g C m^{-2} in the Arctic Water (ArW). The uptake of CO_2 was also at least twice as high in the AW, 29 g C m^{-2}, as in the ArW, 6-14 g C m^{-2}. Comparison with a study conducted in the same area confirms the pattern of higher new production and uptake of CO_2 in the AW but also shows large interannual variations. An 'Atlantification' of the northern Barents Sea in connection with the decreasing sea ice extent in the Arctic Ocean suggests that the productivity and uptake of CO_2 in that area will increase due to the larger new production and CO_2 uptake in the AW compared to the ArW.

1. Introduction

The Arctic sea ice concentration has decreased during the last 25 years (Parkinson *et al.* 1999; Johannessen *et al.* 2004) due to increasing global mean temperatures. Climate models predict that the temperatures will continue to rise during the coming century with up to 4º C (IPCC, 2007). Similarly models predict that the shrinking of the sea ice cover will continue in the future (Vinnikov *et al.* 1999; Johannessen *et al*. 2004; Arzel *et al.* 2006). If, in addition to this, the multi-year ice extent decreases more than the winter sea ice extent, large areas of the Arctic Ocean will be transformed into a seasonal marginal ice zone. Such a change in ice conditions will have large effects on the ecosystems and biogeochemical cycles in the Arctic.

Air-sea exchange and primary production are two important processes controlling the distribution of total inorganic carbon in the ocean. Both processes are dependent on variables such as temperature, wind speed, and ice cover. The interannual variations of these parameters can be large in the Barents Sea (Ådlandsvik and Loeng, 1991; Loeng, 1991) and to be able to discern any long term changes in the future air-sea exchange and primary production need to be quantified under different conditions. The knowledge of the size and variability of both primary production and air-sea exchange of CO_2 is limited in the Barents Sea, especially in the seasonally ice covered area north of the Polar Front. The model by Sakshaug and Slagstad (1992) indicates that primary production is larger in the Atlantic then the Arctic domain of the Barents Sea. Kaltin *et al.* (2002) showed through measurements, while focusing on uptake of CO_2, that this was the case for new production and possibly also for uptake of CO_2 in 1999.

A change in the inorganic carbon content of the surface ocean is conveyed into the ocean interior through the formation of intermediate and deep waters. This primarily takes place at high latitudes and hence the carbon cycling at high latitudes has implications for the global oceans ability to sequester atmospheric carbon dioxide. The carbon cycling in the Barents Sea is important in this context since both intermediate and deep waters are formed in this region (Swift *et al.*, 1983; Midttun, 1985; Schauer *et al.*, 2002). Of special interest is the Atlantic Water (AW) that enters the Barents Sea from the south because it is cooled during its passage through the Barents Sea and transformed into an intermediate water mass (Schauer *et al.*, 2002). All these modified waters exiting the Barents Sea contribute to the intermediate layers in the Arctic Ocean (Schauer *et al.*, 1997), the Nordic Seas, and eventually to the deeper layers of the North Atlantic Ocean (Mauritzen, 1996; Rudels *et al*, 2002).

The marginal ice zone of the western Barents Sea was visited the 8-22 July 2003 as part of the CABANERA (Carbon flux and ecosystem feedback in the northern Barents Sea in an era of climate change) project. The aim of this paper is to describe the hydrography related to the encountered biogeochemical features and calculate seasonal new production and air-sea exchange of CO_2 in the marginal ice zone.

2. Data and methods

Four stations were occupied during the field study, named I-IV in the order they were visited (Figure 1). Multiple CTD casts were made at each station, which were occupied between 32 and 38 hours. A Sea Bird SBE 9 CTD and rosette with 12 6-l Niskin bottles were used for hydrography and water samples respectively. Total dissolved inorganic carbon (C_T) was analyzed by acidification of the sample followed by coulometric titration (Johnson *et al.* 1993). The accuracy was determined by running certified reference material from Scripps Institute of Oceanography. The precision determined by running duplicates was ± 2.5 μmol kg^{-1}. Total alkalinity (A_T) was analyzed with a VINDTA 3S (Versatile Instrument for the Determination of Titration Alkalinity) system, by potentiometric titration with 0.1 M HCl (Mintrop *et al.* 2000). The same reference material was used as for C_T and the duplicate precision was

± 1.5 μmol kg^{-1}. Nutrient samples were frozen and stored for later analysis on land by National Environmental Research Institute in Roskilde, Denmark. The ice coverage and percent first-year/multi-year ice was visually estimated from the bridge.

3. Study area

The Barents Sea is the largest and deepest of the Arctic Ocean shelf seas and is heavily influenced by the Atlantic Water which crosses the sea from west to east on its way to the deep Arctic Ocean (Figure 1). The Polar Front separates the Barents Sea into two regions:

1. The Atlantic domain is the area dominated by warm AW south of the Polar Front.
2. The Arctic domain lies north of the Polar Front where the upper part of the water column is dominated by cold Arctic Water (ArW).

The Arctic domain is ice covered during winter, the ice normally starts to melt in May and the whole area is generally ice free in September. No ice is formed in the Atlantic domain but ice can drift across the Polar Front and be melted by the warm AW. The position of the marginal ice zone in the Barents Sea varies considerably both on intra- and interannual time scales due to wind and freezing/melting. The ice in the Barents Sea is either produced locally or imported. The two import routes are from the Kara Sea through the strait between Novaya Zemlya and Franz Josef Land and from the Arctic Ocean through the straits between Nordaustlandet (Svalbard) and Franz Josef Land. The importance of the two routes varies between years with the dominant wind field, as does the amount of imported ice (e.g. Martin *et al.*, 2000; Korsnes *et al.*, 2002; Pavlov *et al.*, 2004). This variability along with the permanently ice free Atlantic domain means that the Barents Sea is a good area to study how the processes of the inorganic carbon cycle are affected by different sea ice conditions.

The warm and saline AW in the Barents Sea originates in the Norwegian Atlantic Current (NwAC) of the Norwegian Sea. When the NwAC reaches the Barents Sea Opening it splits into two branches (Figure 1), the North Cape Current (NCC) and the West Spitsbergen Current (WSC). The NCC enters the Barents Sea south of Bear Island and flows east and north-east, AW from this current will in this work be referred to as Southern Barents-Atlantic derived Water (SBAW) following Pfirman *et al.* (1994). The WSC flows north on the western side of Svalbard until it splits into several branches north of Svalbard, one of the branches flows east along the northern shelf edge of the Barents Sea. Parts of this branch are diverted into the northern Barents Sea. AW with this origin will be referred to as Northern Atlantic derived Water (NBAW) in order to distinguish it from SBAW.

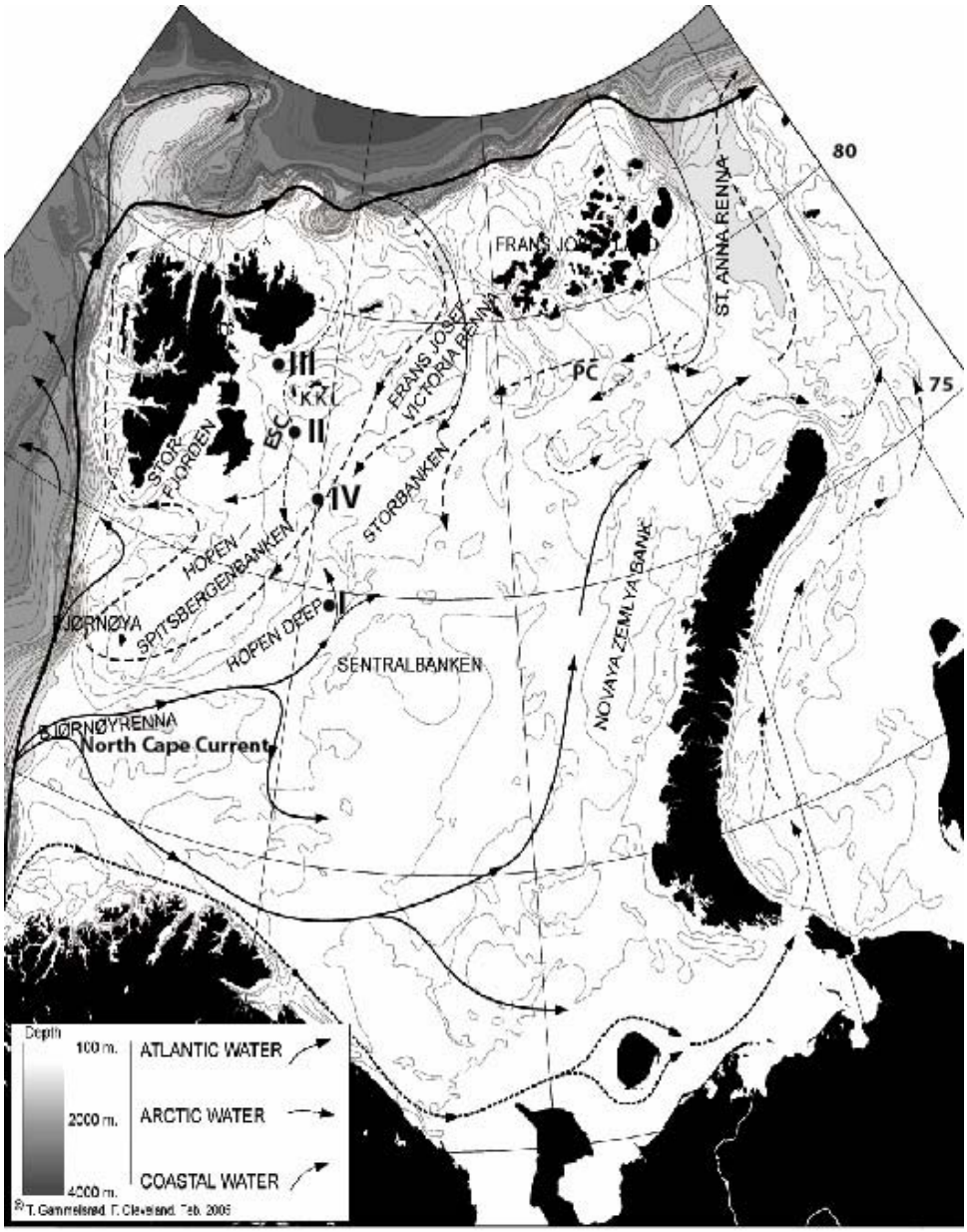

Figure 1: Map of the Barents Sea with surface currents and some topographical features. Solid arrows represent Atlantic Water, dashed arrows Arctic Water and dotted arrows coastal water. K.K.L. is Kong Karls Land. Figure by courtesy of T. Gammelsrød and F. Cleveland, Geophysical institute, University of Bergen.

The Arctic Water (ArW) found in the Barents Sea is formed either domestically or is imported, mainly via the Persey Current (PC) and the East Spitsbergen Current (ESC) (Novitsky, 1961; Loeng, 1991). The PC flows from the Kara Sea westwards into the Barents Sea between Franz Josef Land and Novaya Zemlya and crosses the whole northern Barents Sea. In the area of the Svalbard Bank the PC encounters the ESC which flows southwards east of Svalbard (Figure 1).

Table 1: The four water masses encountered during the study and their mean thermohaline and chemical properties.

	Southern Barents Atlantic-derived Water (SBAW)	Northern Barents Atlantic-derived Water (NBAW)	Arctic Water (ArW)	Sea ice melt water	River runoff
Temperature (˚C)	>1.0	>1.0	<-1.0	any	any
Salinity	>34.95	34.7<S<34.95	34.0<S<34.7	6	0
A_T (µmol kg^{-1})				395	1400
C_T (µmol kg^{-1})				395	1400
Nitrate (µmol kg^{-1})				2.1	4

a, Water masses

The temperature and salinity measurements achieved during the field study showed distributions of these two variables that do not entirely fit within previous water mass definitions in this area. In order to achieve the best possible estimate of production and air-sea exchange water mass definitions were slightly modified to fit the encountered temperature and salinity distributions (Figure 2 and Table 1). The modified water mass definitions do not deviate dramatically from earlier definitions in this area (Hopkins, 1991; Loeng, 1991; Pfirman *et al.*, 1994; Steele *et al.*, 1995: Harris *et al.*, 1998; Rudels *et al.*, 1999). The need to modify the water mass definitions is due to the mixing and transformation the water masses experience to in this area. The new definitions are applied in the calculations of the physical and chemical properties of the studied station.

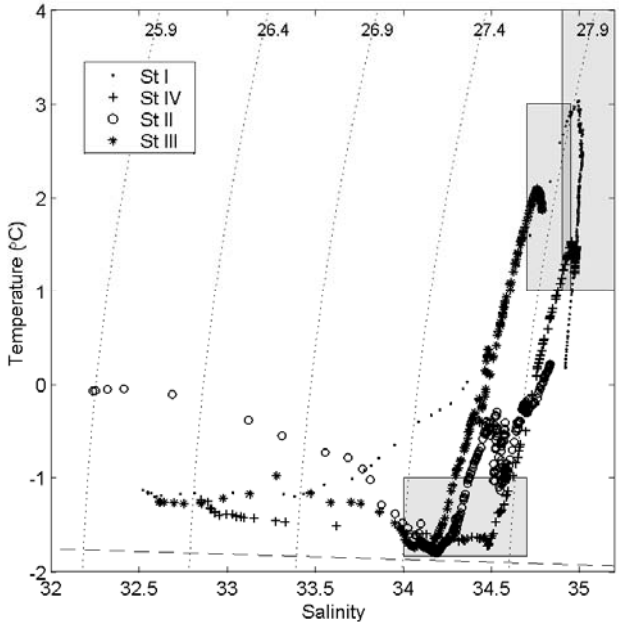

Figure 2: T-S diagram of the one CTD cast from each station. Boxes represent the water mass definitions used in this work with T>1.0° and S>34.9 for SBAW, T>1.0° and 34.7<S<34.95 for NBAW and T<-1.0° and 34.0<S<34.7 for ArW.

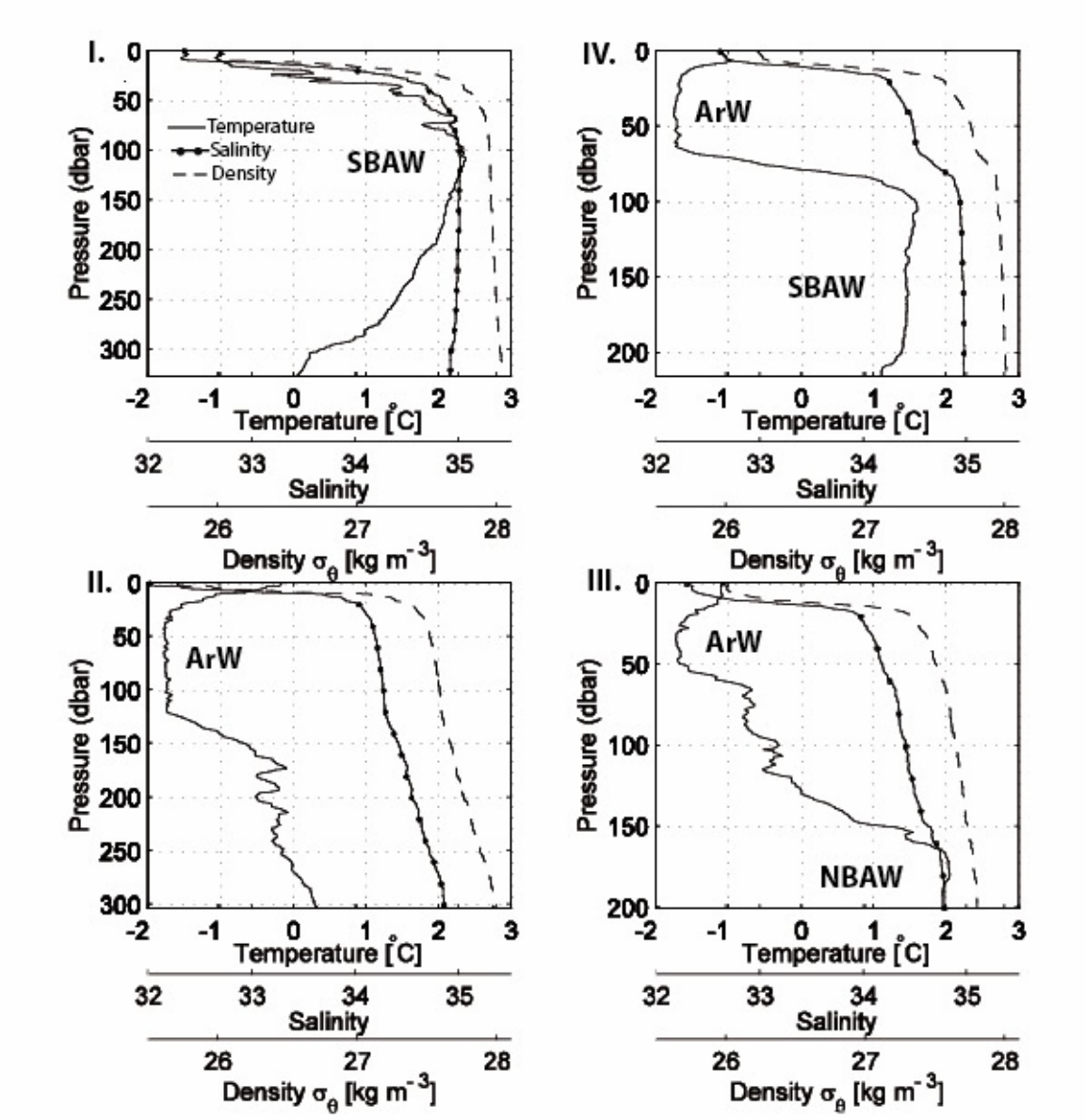

Figure 3: Profiles of temperature, salinity, and density versus pressure for Station I-IV. Dominating water masses are marked by their abbreviation. Note that the scale of the y-axis changes between the panels, reflecting the bottom depth at each station.

b. Hydrographic setting at stations

The four stations differs in degree of ice cover, stratification, water mass composition, and ocean currents. The stations I, IV, II and III presents the geographical order from south to north (Figure 1). The ice coverage was extensive in the northwestern Barents Sea in 2003 and the ice encountered during the present study was mainly first-year ice (80-90 %, visual estimate). The physical properties at all stations are plotted in figure 3.

Station I, at 75.6°N and 30.2°E, in the northern part of the Hopen Deep lies south of the mean position of the Polar Front (Loeng, 1991), but ice can drift into and cover this area in years with extensive ice cover. At the time of investigation the ice coverage was about 40-70%. The water column was mainly occupied by SBAW while cold freshwater from melting ice was mixed into the surface layer. The upper 8-10 meters of the water column were well mixed with a salinity of 32.5 and a temperature of -1°C. Below a marked pycnocline the core of the SBAW was found between 50-150 m and had salinity close to 35 and temperatures of 2-3°C. Below 150 m both salinity and temperature decreased and approached 34.9 and 0 °C close to the bottom.

Station IV (77.0°N, 29.1°E), situated in the very northern end of the Hopen Deep had slightly denser ice condition then station I. The water column here had three distinct layers. First a cold, fresh surface layer similar to that found further south, 8-10 m thick with salinity 32.5 and a temperature of -1°C. Secondly, below a 10-15 m thick pycnocline, a layer of ArW, about 40 m thick, was seen with a temperature of -1.7 °C, and salinity of 34.2-34.5. Last, below another pycnocline, an SBAW layer was seen below about 90 m. This layer had a maximum temperature of 1.5°C and salinities between 34.9 and 35.0. Near the very bottom the temperature decreased, typically to about 1.2°C.

Station II (78.1°N, 27.2°E), situated in the deep basin between Kong Karls Land, Storbanken and Edgeøya, had an ice-cover of 40-70 %. The water column had three distinct layers; a melt water layer, an ArW layer and a deep layer. The surface melt layer was only 5 m deep compared to ~10 m at station I and IV, the temperature in this layer varied between -0.5 and 0°C and the salinity between 32.0-32.3. Below a pycnocline the ArW layer was found between 30 and 120 m and it had a temperature of -1.7°C and the salinity varied from 34.1-34.3. In the deep layer below 120 m both temperature and salinity increased, reaching values of about 0.3°C and 34.8 at 300 m. Large variations in both temperature and salinity were seen below the ArW layer both at this station and at station III.

Station III (79.0°N, 25.4°E) in Erik Eriksen strait between Kong Karls Land and Nordaustlandet the ice coverage was 50-70%. At this station four layers could be identified in the water column. The surface water was cold and fresh, followed by a sharp pycnocline. An intermediate layer of ArW near freezing temperatures and with moderate but increasing salinities (34.0-34.2) was found between 20-50 m. Below 50 m a thick transition layer was seen with increasing temperatures and salinities. Close to the bottom a layer of NBAW was found with a temperature of about 2°C and salinity of almost 34.8.

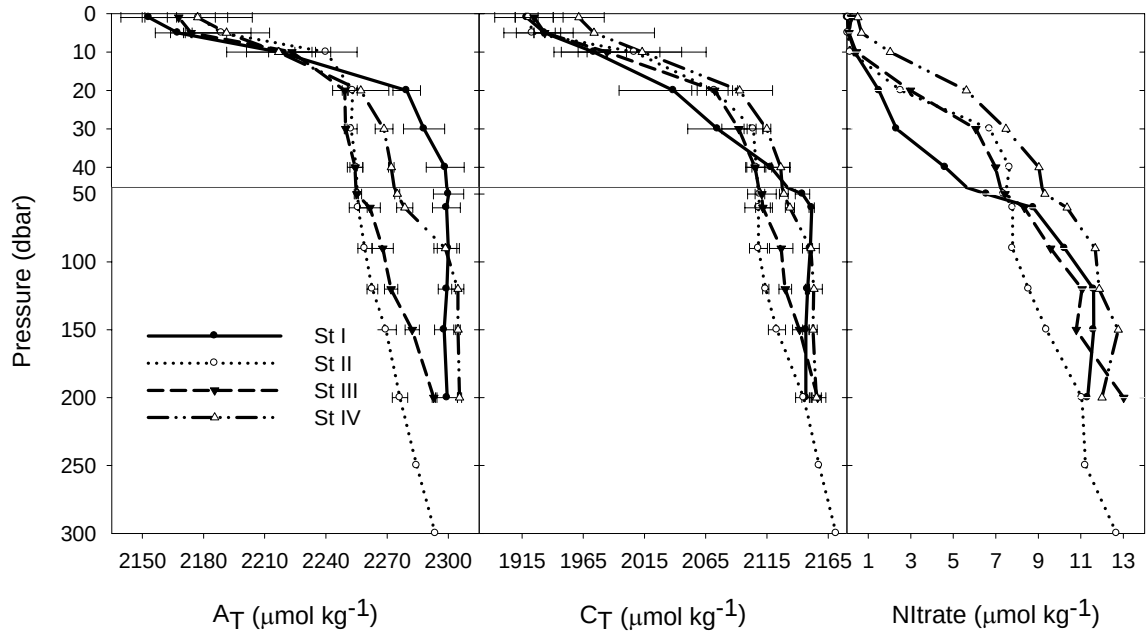

Figure 4: Mean profiles of alkalinity (A_T), total dissolved inorganic carbon (C_T), and nitrate (NO_3) for Station I-IV, note the different scale for the top 50 m. Error bars represent ± one standard deviation of all samples in a depth interval.

4. Data analysis

The variability of total alkalinity (A_T), total dissolved inorganic carbon (C_T) and nitrate (NO_3) at the studied stations depend on the physical conditions as well as primary production and CO_2 exchange with the atmosphere. Figure 4 shows the mean profiles of A_T, C_T, and NO_3 at the four stations and the variability between casts in each depth interval for A_T and C_T. In order to estimate the change in C_T, A_T, and NO_3 caused by primary production and air-sea exchange the preformed concentrations must be known, i.e. the concentrations representing the conditions in the mixed layer at the end of winter. Before this calculation could be made the following steps where taken:

a. The winter mixed layer depth was calculated.
b. The main sea water source in the winter mixed layer and the mean value of its chemical constituents were identified.
c. The sources for freshwater in the area were identified.

a. Calculation of Winter Mixed Layer Depth (WMLD)

The CTD profiles at Stations II, III, and IV (Figure 3) all had temperature minima below the seasonally heated surface layer. WMLD were found by locating the deepest of these sub-surface temperature minima of each cast, and by then applying a $\Delta\rho$ criterion as if no summer heating had occurred.

Table 2: Water mass in the mixed layer, winter mixed layer depth and properties observed at the bottom of the mixed layer.

	I	II	III	IV
Water mass	SBAW	ArW	ArW	ArW
WMLD	200	120	60	60
Salinity	34.99	34.32	34.24	34.58
A_T (μmol kg^{-1})	2299	2264	2262	2279
C_T (μmol kg^{-1})	2147	2115	2112	2134
Nitrate (μmol kg^{-1})	11.3	8.7	8.3	10.4

Following Kara *et al.* (2003) the depth of the winter mixed layer (WML) was calculated with a $\Delta\rho$ criterion corresponding to a ΔT of -0.8°C. At Station I there was no temperature minimum indicative of winter mixing and a gradient criterion (Brainerd and Gregg 1995) was used below the seasonal pycnocline ($\Delta\rho$ >0.001/m). The WMLD for the different stations are shown in Table 2.

b. Main sea water source in the winter mixed layer and the concentrations of its chemical constituents

To calculate the preformed concentrations it was assumed that each sample consists of a mixture of one seawater source and freshwater. The seawater source was ArW for all stations except Station I where it was SBAW. For each of the seawater source a mean value was calculated for salinity, A_T, C_T, and nitrate at the bottom of the WML at each station, and then assumed representing the winter conditions (Table 2).

c. Freshwater sources

The freshwater encountered in the study area is mainly derived from the melting of sea ice (Östlund and Hut, 1984). However, in view of the pathways via which Arctic Water is imported into the Barents Sea the presence of some river runoff cannot be excluded. There are two possible sources for river runoff in this area, one is surface water imported from the Kara Sea and the other is the rivers that enter the southeastern Barents Sea.

Figure 3 and 4 suggest that A_T is closely related to water mass distribution and this is confirmed by the close relation between A_T and salinity that becomes visible when alkalinity is plotted versus salinity (Figure 5). Most of the points fall around a straight line ($y = 57.6x + 288$, R^2=0.98) that is very similar to the trend Millero et al. (1998) reported for the North Atlantic. There are however a few points that deviate from the "Atlantic line" (shown by triangles in Figure 5) and these points exclusively lie above the straight line. The samples represented by triangles origin in the upper 20 m of the water column and their elevated A_T values in relation to salinity is interpreted as presence of river runoff. Waters influenced by river runoff can also be distinguished by their elevated C_T values in a C_T – salinity relation.

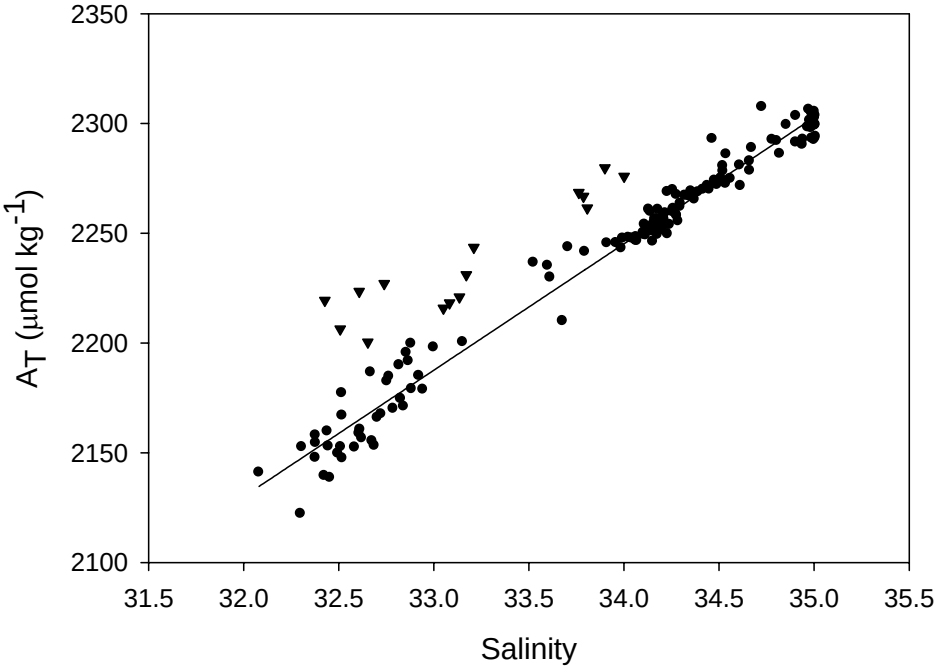

Figure 5: Nitrate corrected alkalinity versus salinity for all samples. Triangles represent the samples influenced by river runoff (RRO). The line represents the linear regression for all samples except those judged to be affected by river runoff and is equal to $y = 57.6x + 288$ ($R^2 = 0.98$).

The reason for this is that inorganic carbon in river runoff mainly occurs as HCO_3^- which give an equal contribution to A_T and C_T. Therefore a plot of A_T versus C_T of samples from river runoff influenced waters will produce a 1:1 relation even though the A_T and C_T values of these samples deviate from the Atlantic relation with salinity. This was the case for the samples shown as triangles in Figure 5.

Due to the presence of river runoff as well as sea ice melt water in the study area the water in the WML is a mixture of three source waters; seawater (SW) represented by either SBAW or ArW, sea ice melting (SIM), and river runoff (RRO). Thus a three component mixing model was used to calculate the fractions of different water masses on which the calculations of preformed concentrations of NO_3 and C_T are based. The fraction (f) of the source waters in each sample was calculated according to

$$f^{SW} + f^{SIM} + f^{RRO} = 1 \quad (1)$$

$$f^{SW} \cdot S^{SW} + f^{SIM} \cdot S^{SIM} + f^{RRO} \cdot S^{RRO} = S^{MEAS} \quad (2)$$

$$f^{SW} \cdot A_T{}^{SW} + f^{SIM} \cdot A_T{}^{SIM} + f^{RRO} \cdot A_T{}^{RRO} = A_T{}^{MEAS} \quad (3)$$

where S is the salinity. The A_T values used in the calculations were corrected for the effect of nitrate uptake during production.

The salinity for the SIM was set to 6 (Table 1) since the ice in the area mainly was first-year ice (e.g. Eicken 2003, Wadhams 2000). The A_T of the SIM was calculated by assuming no fractionation of the A_T when sea ice freezes. If the ice is frozen from seawater with a salinity of 34.5 and an A_T of 2274 this will give a concentration of 395 μmol kg^{-1} Figure 5. For river runoff an A_T of 1400 μmol kg^{-1} was used (Anderson and Dyrssen, 1981; Anderson *et al.*, 2004). The resulting fractions are shown in Figure 6.

The fractions were then used to calculate the preformed concentration of C_T (C_T^0) and nitrate (NO_3^0) according to

$$C_T^0 = f^{SW} \cdot C_T^{SW} + f^{SIM} \cdot C_T^{SIM} + f^{RRO} \cdot C_T^{RRO} \quad (4a)$$

$$NO_3^0 = f^{SW} \cdot NO_3^{SW} + f^{SIM} \cdot NO_3^{SIM} + f^{RRO} \cdot NO_3^{RRO} \quad (4b)$$

The A_T in river runoff consists mainly of hydrogen carbonate ions (HCO_3^-) and the concentration of C_T is thus the same as for A_T (1400 μmol kg^{-1}). The nitrate value in the river runoff is set to 4 μmol kg^{-1} following Gordeev *et al.* (1996). For the C_T of the SIM the same value is used as for A_T (395 μmol kg^{-1}), similar to the case with river runoff. To our knowledge few measurements have been performed on nitrate in ice. Since no appropriate values can be found a non fractionation with salinity during freezing assumption is used here as for A_T. It was assumed that the melted ice was frozen from seawater with a salinity of 34.5 and a nitrate concentration of 11.8 μmol kg^{-1}, giving a nitrate concentration of the SIM of 2.1 μmol kg^{-1}.

From the preformed concentrations and the measured values the deficit of C_T (ΔC_T) and nitrate (ΔNO_3^-) were calculated

$$\Delta C_T = C_T^0 - C_T^{MEAS} \quad (5a)$$

$$\Delta NO_3 = NO_3^0 - NO_3^{MEAS} \quad (5b)$$

ΔNO_3 is attributed solely to primary production since vertical transport and advection are set to zero (see below). ΔC_T summarizes the uptake of inorganic carbon by biological activity (ΔC_T^{bio}), the uptake by air-sea exchange ($\Delta C_T^{air\text{-}sea}$), the vertical transport ($\Delta C_T^{vertical}$) and the advection ($\Delta C_T^{advection}$)

$$\Delta C_T = \Delta C_T^{bio} + \Delta C_T^{air\text{-}sea} + \Delta C_T^{vertical} + \Delta C_T^{advection} \quad (6)$$

In this equation the latter two terms are set to zero. The water advected into the area of each station is assumed to be the same water mass with the same seasonal development. The vertical transport is set to zero primarily to use the same computation scheme as Kaltin *et al.* (2002), to make the results comparable, and secondly because typical mixing rates in this part of the Barents Sea are not well

known. The effect of this simplification on the results will be discussed in section 5*b i*. The biological contribution to the change in C_T can be calculated from the change in nitrate according to

$$\Delta C_T^{bio} = C/N \cdot \Delta NO_3^- \quad (7)$$

where C/N is the carbon to nitrate uptake ratio. Since there is an ongoing debate concerning the best C/N ratio two were used in this study, the classical ratio described by Redfield *et al.* (1963) of 6.6 and the ratio calculated by Takahashi *et al.* (1985) of 8.75. Equation 7 does not include the effect of production of hard parts since it was assumed to be so small that it had an insignificant effect on the A_T. The air-sea exchange ($\Delta C_T^{air\text{-}sea}$) is then calculated as the difference between the primary production and the total deficit in C_T

$$\Delta C_T^{air\text{-}sea} = \Delta C_T - \Delta C_T^{bio} \quad (8)$$

where negative values represent uptake of CO_2 from the atmosphere.

5. Results

Station I had the largest contribution of freshwater in the water column (Figure 6), the SBAW was diluted with freshwater down to about 50 m. The SIM contribution at Station I was maximum 8 % in the surface while the RRO contribution was a maximum of about 4.5 % at 10 m. At Station IV the influence of freshwater on the ArW went down to about 30 m, with a surface max of 5.5 % SIM and with a max RRO contribution of 2 % at 10 m. The ArW at Stations II and III was only influenced by freshwater down to 20 m, both with a SIM content of 5 % at the surface. The RRO contribution was at a maximum 2% at 5 m at Station II and 3 % at 10 m at Station III.

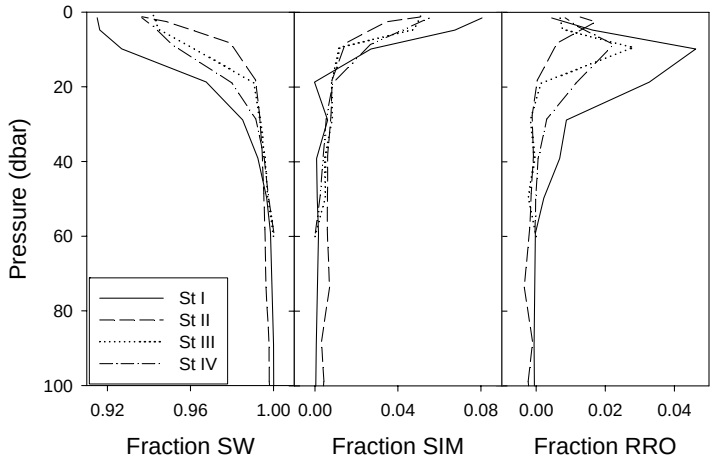

Figure 6: The fractional contributions of each source water to the water column at station I-IV. Left Seawater (SW) source, middle sea ice melt water (SIM) and right river runoff (RRO).

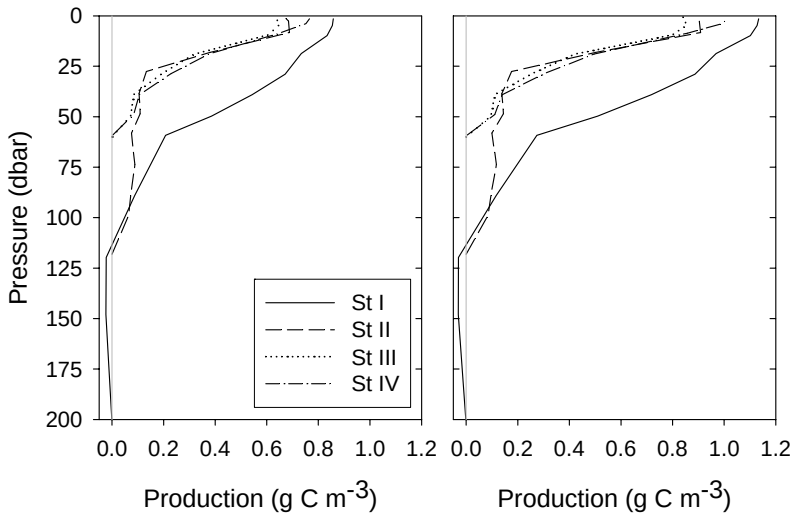

Figure 7: New production, ΔC_T^{bio}, versus pressure as calculated with the Redfield ratio (left) and the Takahashi ratio (right).

The new production (ΔC_T^{bio}) was largest at the surface and gradually decreased with depth (Figure 7). Production had taken place in the entire WML at all stations except for Station I where signs of production can be seen down to about 110 m.

The distribution of CO_2 taken up from the atmosphere ($\Delta C_T^{air\text{-}sea}$) throughout the WML (Figure 8) show a different distribution than the new production. The profiles of CO_2 uptake show a subsurface maximum, the three northerly stations have a peak at about 20 m while the peak was at 50 m at the southernmost station, this feature will be discussed in section 5*d iii*.

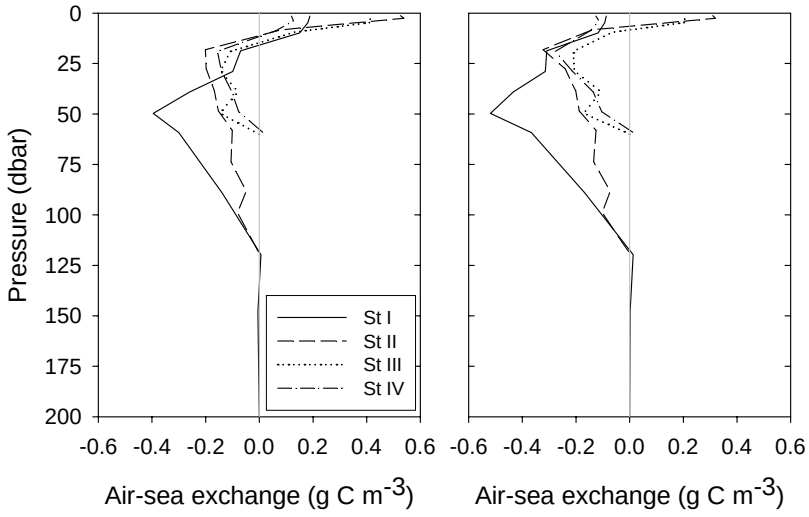

Figure 8: Air-sea CO_2 exchange, $\Delta C_T^{air\text{-}sea}$, versus pressure as calculated with the Redfield ratio (left) and the Takahashi ratio (right). Uptake of CO_2 from the atmosphere is negative in this figure following equation 8.

Table 3: Production and air-sea CO_2 exchange (in g C m^{-2}) calculated with the Redfield *et al.* (1963) ratio, 6.6, and the Takahashi *et al.* (1985), 8.75, ratio. Uncertainties due to measurement precision are included as super- and subscripts.

Station	Production Redfield (g C m^{-2})	Produktion Takahashi (g C m^{-2})	Air-sea exchange Redfield (g C m^{-2})	Air-sea exchange Takahashi (g C m^{-2})
I	$39.5^{+0,1}_{-0,1}$	$52.2^{+0,0}_{-0,1}$	$16.3^{+3,5}_{-3,6}$	$29.0^{+3,5}_{-3,5}$
II	$20.4^{0,0}_{-0,1}$	$26.9^{+0,1}_{-0,0}$	$8.1^{+2,2}_{-2,1}$	$14.7^{+2,1}_{-2,1}$
III	$15.2^{+0,1}_{-0,0}$	$20.1^{+0,1}_{-0,0}$	$1.2^{+1,1}_{-1,1}$	$6.1^{+1,1}_{-1,1}$
IV	$17.2^{+0,1}_{-0,0}$	$22.7^{+0,0}_{-0,0}$	$3.4^{+1,1}_{-1,0}$	$8.9^{+1,1}_{-1,0}$

The air-sea CO_2 flux profiles also show outgassing at the surface for some profiles; this is unrealistic since the surface water fCO_2 values were below atmospheric levels. The reason for this error is probably the C/N ratio used to convert nitrate deficit to carbon deficit (see section 5*b ii*). The profiles show smaller outgassing when a higher C/N ratio is used. The profiles of new production and uptake of CO_2 were integrated down to the depth of the station-mean WMLD with the exception of Station I since water samples only were taken down to 200 m. The results are listed in Table 3.

a. Uncertainties

Both the measurement errors and the errors due to the choice of a three fraction model have been assessed. In the first case the new production and air-sea exchange were calculated with C_T +2.5 µmol kg^{-1} and then with C_T -2.5 µmol kg^{-1} to see the implications of the ± 2.5 µmol kg^{-1} precision of the C_T measurement. The same was done for the measurement uncertainty for A_T (± 1.5 µmol kg^{-1}). The largest deviations from the mean values are displayed in Table 3, showing the largest effects on the air-sea exchange, about 1-3.5 g C m^{-2}

Table 4: Production and air-sea CO_2 exchange (in g C m^{-2}) calculation from two fractions (seawater and sea ice melt water). Change from three-fraction-scenario in parenthesis.

Station	Production Redfield (g C m^{-2})	Production Takahashi (g C m^{-2})	Air-sea exchange Redfield (g C m^{-2})	Air-sea exchange Takahashi (g C/m^{-2})
I	39.6 (+0.1)	52.3 (+0.2)	18.6 (+2.3)	31.3 (+2.4)
II	20.5 (+0.2)	27.1 (+0.2)	2.4 (-5.7)	9.0 (-5.8)
III	15.3 (+0.1)	20.2 (+0.1)	-0.7 (-1.9)	4.2 (-1.9)
IV	17.3 (+0.1)	22.9 (+0.2)	2.5 (-0.9)	8.1 (-0.8)

In the second case the effect of the RRO fraction is evaluated and the calculations are done with only two fractions, sea water and sea ice melt water. The properties of these two fractions are kept the same as before (Table 1). The results, shown in Table 4 indicate a change larger than the measurement error primarily in the air-sea exchange calculations at stations II and III. It is especially noteworthy that the air-sea exchange changes sign at station III when the Redfield ratio is used.

i. Vertical transport

The vertical transport over the base of the WML was set to zero in this study. To evaluate the influence that this assumption has on the results the vertical transport of C_T and nitrate was calculated following Law *et al.* (2003) according to

$$\text{Vertical flux} = K_z \cdot (\Delta X/\Delta z)$$

where ΔX is the concentration difference of C_T or NO_3 over the pycnocline (Δz) and K_z is the vertical diffusivity. Vertical diffusivity varies greatly depending on physical forcing and water column stability at a particular site. To our knowledge, no measurements of turbulent vertical diffusivity in a marginal ice zone in a shelf area have been published. Crawford et al. (1999) found values around 10^{-5} m^2 s^{-1} in the pycnocline under land fast ice in the Canadian Archipelago. Somewhat higher values, $\sim 10^{-4}$ m^2 s^{-1}, have been measured under drift ice along the outer shelf north of Svalbard and in the deep Polar Ocean (Padman and Dillon 1991). We use the mean of these two estimates, K_z of $5 \cdot 10^{-5}$ m^2 s^{-1}, for our approximation. If the stratification began 60 days previous to the investigation and the gradient $\Delta X/\Delta z$ is kept constant at the value found during the study, the results give a maximum upward transport of C_T of 1.8 g C m^{-2} and nitrate corresponding to 1.2 g C m^{-2}. The gradient is not constant but develops during the period of production. Since the exact development of the gradients is not known we used a constant value to set an upper limit to the error caused by the assumption of no vertical mixing. The calculation thus indicates that the new production is underestimated by a maximum of 10 %.

ii. C/N ratio

The C/N ratio used to convert the nitrate deficit to carbon deficit is essential when calculating production from nitrate. In this study the conversion was done with a constant ratio, 6.6 or 8.75. It has however been indicated (Sambrotto *et al.* 1993, Broström, 1998) that carbon over consumption is not unusual, which would give a higher ratio. The results from the air-sea calculations (Figure 8) give outgassing in the surface of all the profiles when the usual C/N ratio of 6.6 (Redfield *et al.* 1963) is used and for two profiles when 8.75 (Takahashi *et al.* 1985) is used. These two profiles are Station II and III, i.e. the stations with the strongest blooms. This indicates that the used C/N ratios are too small, at least in the surface layer during the bloom. In order to eliminate the outgassing of CO_2 different ratios were tested and all points became zero or had an uptake of CO_2 with a ratio of 13.5. If the production is calculated with 13.5 as C/N ratio it will increase by ~50% compared to the Takahashi *et al.* (1985) ratio.

Thus the production converted to carbon units at these stations is probably underestimated, which also will give an underestimation of the atmospheric CO_2 uptake.

iii. CO_2 uptake profiles

The CO_2 uptake profiles show a curious feature, a subsurface uptake "peak" and then decreasing uptake towards the surface. This feature can not be explained with the present data. Here we can only point out two processes that potentially could produce this feature. Firstly, studies done on sea ice indicate elevated C/N ratios in ice algae growing inside sea ice (Smith *et al.,* 1990; McMinn *et al,.* 1999). This will change the relation between nitrate and total inorganic carbon in the SIM. Secondly, there are laboratory studies that show that calcium carbonate can precipitate during freezing of sea ice from sea water (Papadimitriou *et al.,* 2003) although studies done on natural sea ice were not conclusive (Olsson, 1997 and references therein). If calcium carbonate is precipitated in sea ice it may dissolve again when the ice melts. The result is an increase of the alkalinity which is twice as high as that of the total inorganic carbon. Both processes result in a composition of the SIM which is different from what we have assumed. Since we cannot say which process is responsible for the peak in CO_2 uptake we conclude that this feature needs to be investigated further in the future.

The main conclusions from the analysis of uncertainties are that the production estimates are conservative and that even though the preformed concentrations can be calculated by a two component mixing model the three component mixing model is the most correct way to represent the preformed concentrations. The discussion will be based on the results found with the C/N ratio of 8.75 since these have the least outgassing at the surface. The relation between the stations is independent of what C/N ratio is used even though the absolute numbers change.

6. Discussion

The southern part of Hopen Deep (St I) is clearly a part of the Atlantic domain of the Barents Sea. In 2003 the ice extent was large and ice had drifted across the Polar Front and was melting on top of the Atlantic Water in this area. Nevertheless, this was the area with the smallest amount of ice during the study. Ice advection and melting had created a cold and fresh surface layer of about 10 m with a SIM component of maximum 8 %. The core of the Atlantic Water at this station (50-150 m) is a part of the North Cape Current branch that recirculates in Hopen Deep. The origin of the transition layer (10-40 m) is less clear than the AW layer; it could either be a local mixing product of SBAW and ice melt water or may have been advected into the area. In this layer a clear river runoff signal was seen (Figure 6). The seasonal new production in the southern part of Hopen Deep was 52 g C m^{-2} and the uptake of CO_2 was 29 g C m^{-2} (Table 3). The production was lower than what was found by Kaltin *et al.* (2002) in the same area, 68 g C m^{-2}, even though they integrated over a shallower

depth. The reason for this discrepancy is probably that the area was covered by ice in 2003 but not in 1999, which was a year with little ice (Reigstad *et al.* 2002) in the area of investigation. This explanation is strengthened by the fact that Kaltin *et al.* (2002) found production in the same range, 49 g C m^{-2}, at the location of the ice edge (76-77.1°N). The air-sea CO_2 uptake was almost the same as Kaltin *et al.* (2002) found, ~29 g C m^{-2}. The bloom in this area (St I) was the most developed (Sturluson 2005) of the visited stations, which was indicated by the highest deficit of nitrate in the seasonal mixed layer.

The upper part of the vertically sloping Polar Front was at the time of investigation situated between Stations I and IV while the deeper part of the front was situated north of Station IV. North of the surface front ArW is encountered as the main water mass in the WML, diluted with fresh water in the top meters and is in some areas underlain by an Atlantic layer. At Station IV the ArW may be a part of the Persey Current coming from the east or northeast. The Atlantic layer has characteristics similar to the SBAW found further south (St I), only slightly colder, and the source for this layer is also the North Cape Current. The seasonal new production at this station (77.0°N) was 23 g C m^{-2}. This was lower than what was found by Kaltin *et al.* (2002) between 76-77.1°N, 49 g C m^{-2}, but larger than what they found between 77.1-78.2°N, 15 g C m^{-2}. The CO_2 uptake was 9 g C m^{-2}, the same as Kaltin *et al.* (2002) found for the transect between 77.1-78.2°N, 8 g C m^{-2}. Since the ice situation was less severe in 1999 than in 2003 it is not surprising that the results of this study are lower than those found by Kaltin *et al.* (2002) at the same positions. The ice cover had been dense recently in this area (St IV) and the bloom was the youngest encountered (Sturluson 2005). This was reflected in the fact that nitrate was not totally depleted (~0.5 μmol kg^{-1}) in the surface at this station as was found at Station I and II along with the relatively high C_T concentrations compared to the other stations (Figure 4).

The water column in the basin south of Kong Karls Land (St II) was the most heavily influenced by Arctic Water. Only below 250 m was water with temperatures above 0°C encountered and this indicates little intrusion of ArW north of the ridge between Storbanken and Spitsbergenbanken. The water below 250 m is a mixing product of AW and ArW, but whether the AW source is SBAW or NBAW (or possibly both) is not possible to deduce from our data. Judged by topography it may well be NBAW advected from the east as indicated by Novitsky (1961). The seasonal new production of 27 g C m^{-2} and the CO_2 uptake of
15 g C m^{-2} are higher than the northernmost values of Kaltin *et al.* (2002) which probably reflect different ice extent and melting pattern of the ice in 1999 and 2003. In 2003 the ice did not melt from south to north but was densest in the area around Station IV while the ice in 1999 seemed to become denser from south to north. Both the production and the air-sea exchange were larger south of Kong Karls Land than in the northernmost part of Hopen Deep, probably due to the denser ice cover in that part of Hopen Deep. The bloom was also more developed south of Kong Karls Land than in the northernmost part of Hopen Deep, as it was in midstage (Sturluson 2005).

The ArW layer in Erik Eriksen Strait (St III) was thinner than the layers of ArW found further south, being only 30 m thick, and also had a lower salinity (Figure 2). This suggests that there are several sources for the ArW spreading over the northern part of the Barents Sea. As can be seen from Table 2 the chemical properties of the ArW also vary with location. The lowest seasonal new production, 20 g C m^{-2}, and CO_2 uptake, 6 g C m^{-2}, during the study was found at this station. The light conditions at these latitudes along with the ice cover may be the reason for the low production. The bloom was similar to that at Station II, but higher nutrient concentrations showed that it was younger (Sturluson 2005). Even though this is further north than the investigation by Kaltin *et al.* (2002) the results can be compared to the northernmost part of their transect. Thus the production in Erik Eriksen Strait was larger than what Kaltin *et al.* (2002) found in the northernmost part of their transect (77.1-78.2°N), while the air-sea exchange was about the same.

When comparing the results of new production and uptake of CO_2 to other studies it is important to remember that this study was performed in July. Thus the results represent new production and uptake of CO_2 from the cessation of deep mixing until the time of investigation. In the comparison between the domains it should also be pointed out that the bloom was more developed in the Atlantic Water than further north.

If the sea ice continues to retreat in the future it is probable that the Atlantic domain will be extended into the northern Barents Sea ('Atlantification') and that the southern boundary of the Arctic domain will move north into the Arctic Ocean. The production and uptake of CO_2 associated with the different domains will thus shift to the north. The northern Barents Sea will be more affected by such a change than the southern part even though the production in the AW further south, in the Norwegian Sea, seem to be lower than that computed for the AW in the Barents Sea. Skjelvan *et al.* (2001) found production of 32 and 24 g C m^{-2} yr^{-1} at Bjørnøya-W and Gimsøy-NW sections respectively. These were calculated from oxygen budgets using a C/O_2 ratio of 106: -138. Falck and Gade (1999) also calculated production from oxygen and arrived at a net community production of 39 g C m^{-2} yr^{-1} at Ocean Weather Station Mike (66°N, 2°E).

The production in the Arctic Ocean is less then that in the Atlantic domain of the Barents Sea or in the Norwegian Sea. Zheng *et al.* (1997) calculated production from oxygen utilization rates in the Nansen Basin of the Arctic Ocean and found a new production of 19 ±5 g C m^{-2} yr^{-1} in the southern part. This is in the same range as the productions found in the Arctic domain in this study. The central Arctic Ocean has lower production, for the northern Nansen Basin Zheng *et al.* (1997) found a new production of 3 ±2 g C m^{-2} yr^{-1} and Anderson *et al.* (2003) found the export production in the central Arctic Ocean to be only 0.5 g C m^{-2} yr^{-1}.

Less is known about the air-sea exchange of CO_2 in this area. Uptake has been calculated to be between 20 and 36 g C m^{-2} yr^{-1} (Skjelvan *et al.* 2005) in the AW of the Norwegian Sea. In the ice covered waters of the Arctic Ocean CO_2 exchange with the

atmosphere is not well known but it is probably much smaller than in the AW of the Barents Sea. The result of an 'Atlantification' of the northern Barents Sea will thus increase the production as well as the uptake of CO_2 there. The northward extension of the seasonal marginal ice zone to the area north of the northern Barents Sea continental slope will probably increase the production and uptake of CO_2 since this area today generally is ice covered throughout the year.

7. Summary and conclusions

This study shows that both seasonal new production and uptake of CO_2 are larger in the Atlantic domain than in the Arctic domain of the Barents Sea. The integrated production was 52 g C m^{-2} in the Atlantic Water while the production in the Arctic Water was 20 to 27 g C m^{-2}. The CO_2 uptake was 29 g C m^{-2} in the Atlantic Water and 6-14 g C m^{-2} in the Arctic Water.

Both the intra- and interannual variability of both new production and uptake of CO_2 are controlled by the extent and concentration of the ice cover. The difference between the years is considerable, especially in the south where the new production was 16 g C m^{-2} lower in 2003 when the Atlantic Water was covered by ice. The difference is accentuated by the fact that the study was performed two weeks later in 2003.

The results suggest that a decrease of the sea ice cover and an 'Atlantification' of the northern Barents Sea will increase the production and uptake of CO_2. The differences between 2003 and 1999 show that more information about the interannual variations in this area is essential to assess potential future changes due to climate change.

Acknowledgements

This study was supported by the Norwegian Research Council, NORDKLIMA Programme (CABANERA Project 155936/700). This work has been supported by the EU FP6 CARBOOCEAN Integrated Project, Contract no. 511176. We gratefully acknowledge the captain and crew of R/V *Jan Mayen* (University of Tromsø) for assistance during the field campaign.

References

Anderson, L. and D. Dyrssen. 1981. Chemical constituents of the Arctic Ocean in the Svalbard area. Oceanologica Acta, *4* (3), 305-311.

Anderson, L. G., E. P. Jones and J. H. Swift. 2003. Export production in the central Arctic Ocean evaluated from phosphate deficits. Journal of geophysical research, *108* (C6), 3199, doi:10.1029/2001JC001057.

Anderson, L. G., S. Jutterström, S. Kaltin, E. P. Jones and G. Björk. 2004. Variability in river runoff distribution in the Eurasian Basin of the Arctic Ocean. Journal of geophysical research, *109,* C01016, doi:10.1029/2003JC001773.

Arzel, O., T. Fichefet and H. Goosse. 2006. Sea ice evolution over the 20th and 21st centuries as simulated by current AOGCMs. Ocean modeling, 12 (3-4), 401-415.

Brainerd, K. E. and M. C. Gregg. 1995. Surface mixed and mixing layer depths. Deep Sea Research Part I, *42* (9), 1521-1543.

Broström, G. 1998. A note on the C/N and C/P ratio of the biological production in the Nordic seas. Tellus, *50B,* 93-109

Crawford, G., L. Padman and M. McPhee. 1999. Turbulent mixing in Barrow Strait. Continental shelf research, *19,* 205-245.

Eicken, H. 2003. From the microscopic to the macroscopic to the regional scale: Growth, microstructure and properties of sea ice, *in* Sea Ice: An introduction to its physics, chemistry, biology and geology, D. N. Thomas and G. S. Dieckmann, eds., Blackwell science, 22-81.

Falck, E. and H. G. Gade. 1999. Net community production and oxygen fluxes in the Nordic Seas based on O_2 budget calculations. Global biogeochemical cycles, *13* (4), 1117-1126.

Gordeev, V. V., J. M. Martin, I. S. Sidorov and M. V. Sidorova. 1996. A reassessment of the euroasian river input of water, sediment, major elements and nutrients to the Arctic Ocean. American journal of science, *296,* 664-691.

Harris, C. L., A. J. Plueddemann and G. G. Gawarkiewicz. 1998. Water mass distribution and polar front structure in the western Barents Sea. Journal of geophysical research, *103* (C2), 2905-2917.

Hopkins, T. S. 1991. The GIN Sea – A synthesis of its physical oceanography and literature review 1972-1985. Earth-science reviews, *30,* 175-318.

IPCC, 2007. Summary for policymakers. In: Climate change 2007: The physical science basis. Cambridge University Press.

Johannessen, O. M., L. Bengtsson, M. W. Miles, S. I. Kuzima, V. A. Semenov, G. V. Alekseev, A. P. Nagurnyi, V. F. Zakharov, L. P. Bobylev, L. H. Pettersson. K. Hasselmann and H. P. Cattle. 2004. Arctic climate change: observed and modelled temperature and sea-ice variability. Tellus, *56A,* 328-341.

Johnson, K. M., K. D. Wills, D. B. Butler, W. K. Johnson and C. S. Wong. 1993. Coulometric total carbon dioxide analysis for marine studies: maximizing the performance of an automated gas extraction system and coulometric detector. Marine chemistry, *44,* 167-187.

Kaltin, S., L. G. Anderson, K. Olsson, A. Fransson and M. Chierici. 2002. Uptake of atmospheric carbon dioxide in the Barents Sea. Journal of marine systems, *38,* 31-45.

Kara, A. B., P. A. Rochford and H. E. Hurlburt. 2003. Mixed layer depth variability over the global ocean. Journal of geophysical research, *108* (C3), 3079, doi:10.1029/2000JC000736.

Korsnes, R., O. Pavlova and F. Godtliebsen. 2002. Assessment of potential transport of pollutants into the Barents Sea via sea ice – an observational approach. Marine pollution bulletin, *44,* 861-869.

Law, C. S., E. R. Abraham, A. J. Watson and M. I. Liddicoat. 2003. Vertical eddy diffusion and nutrient supply to the surface mixed layer of the Antarctic Circumpolar Current. Journal of geophysical research, *108* (C8), 3272, doi:10.1029/2002JC001604.

Loeng, H. 1991. Features of the physical oceanographic conditions of the Barents Sea, *in* E. Sakshaug, C. C. E. Hopkins and N. A. Øritsland, eds., Proceedings of the Pro Mare symposion on polar marine ecology, Trondheim, 12-16 May 1990.

Martin, T. and E. Augstein. 2000. Large-scale drift of Arctic Sea ice retrieved from passive microwave satellite data. Journal of geophysical research, *105* (C4), 8775-8788.

Mauritzen, C. 1996. Production of dense overflow waters feeding the North Atlantic across the Greenland-Scotland Ridge. Part 1: Evidence for a revised circulation scheme. Deep-sea research I, *43* (6), 769-806.

McMinn, A., J. Skerratt, T. Trull, C. Ashworth and M. Lizotte. 1999. Nutrient stress gradient in the bottom 5 cm of fast ice, McMurdo Sound, Antarctica. Polar biology, *21,* 220-227.

Midttun, L. 1985. Formation of dense bottom water in the Barents Sea. Deep-sea research, *32* (10), 1233-1241.

Millero, F. J., K. Lee and M. Roche. 1998. Distribution of alkalinity in the surface waters of the major oceans. Marine chemistry, *60,* 111-130.

Mintrop, L., F. F. Pérez, M. González-Dávila, J.M. Santana-Casiano and A. Körtzinger. 2000. Alkalinity determination by potentiometry: Intercalibration using three different methods. Ciencias Marinas, *26,* 23-37.

Novitsky, V. P. 1961. Permanent currents of the northern Barents Sea. Trudy Gosudarstvennogo okeanografigreskogo instituta, *64,* 1-32. Translated to English at U.S. Naval oceanographic office, Washington DC, trans. 349, 1-39, 1967.

Olsson, K. 1997. Dissolved carbon in the Arctic Ocean. PhD thesis, Göteborg University.

Padman L. and T. M. Dillon. 1991. Turbulent mixing near the Yermak Plateau during the Coordinated Eastern Arctic Experiment. Journal of geophysical research, *96* (C3), 4769-4782.

Papadimitriou, S., H. Kennedy, G. Kattner, G.S. Dieckmann and D. N. Thomas. 2003. Experimental evidence for carbonate precipitation and CO_2 degassing during sea ice formation. Geochimica et Cosmochimica Acta, *68* (8), 1749-1761, doi: 10.1016/j.gca.2003.07.004

Parkinson, C. L., D. J. Cavalieri, P. Gloersen, H. J. Zwally and J. C. Comiso. 1999. Arctic sea ice extents, areas, and trends, 1978-1996. Journal of geophysical research, *104* (C9), 20837-20856

Pavlov, V., O. Pavlova and R. Korsnes. 2004. Sea ice fluxes and drift trajectories from potential pollution sources, compted with a statistical sea ice model of the Arctic Ocean. Journal of marine systems, *48,* 133-157.

Pfirman, S. L., D. Bauch and T. Gammelsrød. 1994. The northern Barents Sea: Water mass distribution and modification, *in* The polar oceans and their role in shaping the global environment, American Geophysical Union, Geophysical Monograph 85, 77-93.

Redfield, A. C., B. H. Ketchum and F. A. Richards. 1963. The influence of organisms on the composiion of seawater. *in* M. N. Hill, ed., The sea, vol. 2, Wiley interscience, 36-77.

Reigstad, M., P. Wassmann, C. Wexels Riser, S. Øygarden and F. Rey. 2002. Variations in hydrography, nutrients and chlorophyll *a* in the marginal ice-zone and the central Barents Sea. Journal of marine systems, *38,* 9-29.

Rudels, B., H. J. Friedrich and D. Quadfasel. 1999. The Arctic circumpolar boundary current. Deep-Sea Research II, *46,* 1023-1062.

Rudels, B., E. Fahrbach, J. Meincke, G. Budéus and P. Eriksson. 2002. The East Greenland Current and its contribution to the Denmark Strait overflow. ICES journal of marine research, *59,* 1133-1154, doi: 10.1006/jmsc.2002.1284.

Sakshaug, E., D. Slagstad. 1992. Sea ice and wind: Effects on the primary productivity in the Barents Sea. Atmosphere-Ocean, *30* (4), 579-591.

Sambrotto, R. N., G. Savidge, C. Robinson, P. Boyd, T. Takahashi, D. M. Karl, C. Langdon, D. Chipman, J. Marra and L. Codispoti. 1993. Elevated consumption of carbon relative to nitrogen in the surface ocean. Nature, *363,* 248-250.

Schauer, U., R. D. Muench, B. Rudels and L. Timokhov. 1997. Impact of eastern Arctic shelf waters on the Nansen Basin intermediate layers. Journal of geophysical research, *102* (C2), 3371-3382.

Schauer, U., H. Loeng, B. Rudels, V. K. Ozhigin and W. Dieck. 2002. Atlantic Water flow through the Barents and Kara Seas. Deep-sea research I, *49*, 2281-2298.

Skjelvan, I., E. Falck, L. G. Anderson and F. Rey. 2001. Oxygen fluxes in the Norwegian Atlantic Current. Marine chemistry, *73,* 291-303.

Skjelvan, I., A. Olsen, L.G. Anderson, R.G.J. Bellerby, E. Falck, Y. Kasajima, C. Kivimäe, A. Omar, F. Rey, K.A. Olsson, T. Johannessen, and C. Heinze. 2005. A review of the inorganic carbon cycle of the Nordic Seas and Barents Sea, *in* The Nordic Seas: an integrated perspective, H. Drange, T. Dokken, T. Furevik, R. Gerdes, and W. Berger, eds., American Geophysical Union, Geophysical Monograph 158, 157-176.

Smith, R. E. H., W. G. Harrison, L. R. Harris and A. W. Herman. 1990. Vertical fine structure of particulate matter and nutrients in sea ice of the high Arctic. Canadian journal of fisheries and aquatic sciences, *47,* 1348-1355.

Steele, M., J. H. Morison and T. B. Curtin. 1995. Halocline water formation in the Barents Sea. Journal of geophysical research, *100* (C1), 881-894.

Sturluson, M. 2005. Implementing the microbial food web in the Barents Sea pelagic ecosystem. Master of Science thesis, Marine biological laboratory, University of Copenhagen.

Swift, J. H., T. Takahashi and H. D. Livingstone. 1983. The contribution of the Greenland and Barents Seas to the deep water of the Arctic Ocean. Journal of geophysical research, *88* (C10), 5981-5986.

Takahashi, T., Broecker, W. S. and S. Langer. 1985. Redfield ratio based on chemical data from isopycnal surfaces. Journal of geophysical research, *90,* 6907-6924.

Vinnikov, K. Y., A. Robock, R. J. Stouffer, J. E. Walsh, C. L. Parkinson, D. J. Cavalieri, J. F. B. Mitchell, D. Garrett and V. F. Zakharov. 1999. Global warming and Northern Hemisphere sea ice extent. Science, *286,* 1934-1937.

Wadhams, P. 2000. Ice in the ocean. Gordon and Breach Science Publishers, 351 pp.

Zheng, Y., P. Schlosser, J. H. Swift and E. P. Jones. 1997. Oxygen utilization rates in the Nansen Basin, Arctic Ocean: implications for new production. Deep-sea research I, *44* (12), 1923-1943.

Ådlandsvik, B. and H. Loeng. 1991. A study of the climatic system in the Barents Sea, *in* Proceedings of the Pro Mare symposium on polar marine ecology, E. Sakshaug, C. C. E. Hopkins and N. A. Øritsland, eds., Polar research, *10* (1), 45-49.

Östlund, H. G. and G. Hut. 1984. Arctic Ocean water mass balance from isotope data. Journal of geophysical research, *89* (C4), 6373-6381.

Paper III

Sea-Ice and Brine Formation in Storfjorden: Implications for the Arctic Wintertime Air-Sea CO_2 flux

Omar, A., T. Johannessen, R. G. J. Bellerby, A. Olsen, L. G. Anderson and C. Kivimäe

In: The Nordic Seas: an integrated perspective, H. Drange, T. Dokken, T. Furevik, R. Gerdes and W. Breger (eds), American Geophysical Union, Geophysical Monograph 158, 177-187, 2005

Sea-Ice and Brine Formation in Storfjorden: Implications for the Arctic Wintertime Air–Sea CO_2 Flux

Abdirahman Omar[1,2], Truls Johannessen[1,2], Richard G.J. Bellerby[1], Are Olsen[1,2], Leif G. Anderson[3], and Caroline Kivimäe[2]

We investigated the air–sea CO_2 flux associated with the formation of brine-enriched shelf water (BSW) in Storfjorden: a water mass formed by sea-ice formation and brine rejection during winter. We used inorganic carbon and auxiliary hydrographic data collected in August 2001 and April 2002. After accounting for the effects of biological and other processes, we found that the formation of BSW is accompanied by an uptake of atmospheric CO_2. This uptake accounted for a carbon enrichment of 17 ± 4 μmol kg^{-1} in the BSW. About 2/3 of the uptake occurred during winter in a coastal polynya for which a wintertime CO_2 flux (calculated as C) was 65 ± 40 g m^{-2}. The flux was about 13 times lower (≈5 g m^{-2}) for the nonpolynya regions of Storfjorden. The computed areal fluxes were extrapolated to polynyas (and leads) and seasonally ice–covered regions in the Arctic. Based on this extrapolation, Arctic coastal polynyas were found to account for a winter time CO_2 uptake of 2.3 (±1.4) × 10^{12} g yr^{-1}. The carbon taken up in coastal polynyas is most likely transported into the deep ocean through brine-driven deep water formation. For polynyas in the central Arctic and for seasonally ice-covered regions, a seaward wintertime air–sea CO_2 flux of 43 (±22) × 10^{12} g yr^{-1} was computed. Further, it was found that this flux can increase to 124 (±55) × 10^{12} g yr^{-1} by about year 2100, if the extent of seasonal ice increases by 43% (as modeled in *Johannessen et al.,* 2002) and central Arctic polynyas become 10 times larger than present. However, the importance of the computed flux with respect to sequestration of atmospheric CO_2 is not clear, due to limited knowledge on the depth penetration of the brine water associated with the formation of new ice in central Arctic polynyas and seasonally ice-covered regions.

1. INTRODUCTION

The Arctic Ocean (AO) could become nearly ice-free during summer by the end of this century. Simulation results from coupled atmosphere-ice-ocean models have indicated a moderate reduction in winter sea ice extent and a drastic decrease for the summer, implying a greater seasonal variability of the Arctic ice cover [*Johannessen et al.,* 2002].

A disappearance of the permanent ice cover is expected to enhance carbon fluxes into the AO. Enhanced carbon fluxes are thought to result from greater CO_2 solubility, due to freshening of the surface water, and through greater primary production, due to better light conditions [*Anderson and Kaltin,* 2001]. However, the effect of changes in the extent of

[1]Bjerknes Centre for Climate Research, University of Bergen, Bergen, Norway.
[2]Geophysical Institute, University of Bergen, Bergen, Norway.
[3]Department of Analytical and Marine Chemistry, Göteborg University, Göteborg, Sweden.

The Nordic Seas: An Integrated Perspective
Geophysical Monograph Series 158

10.1029/158GM12

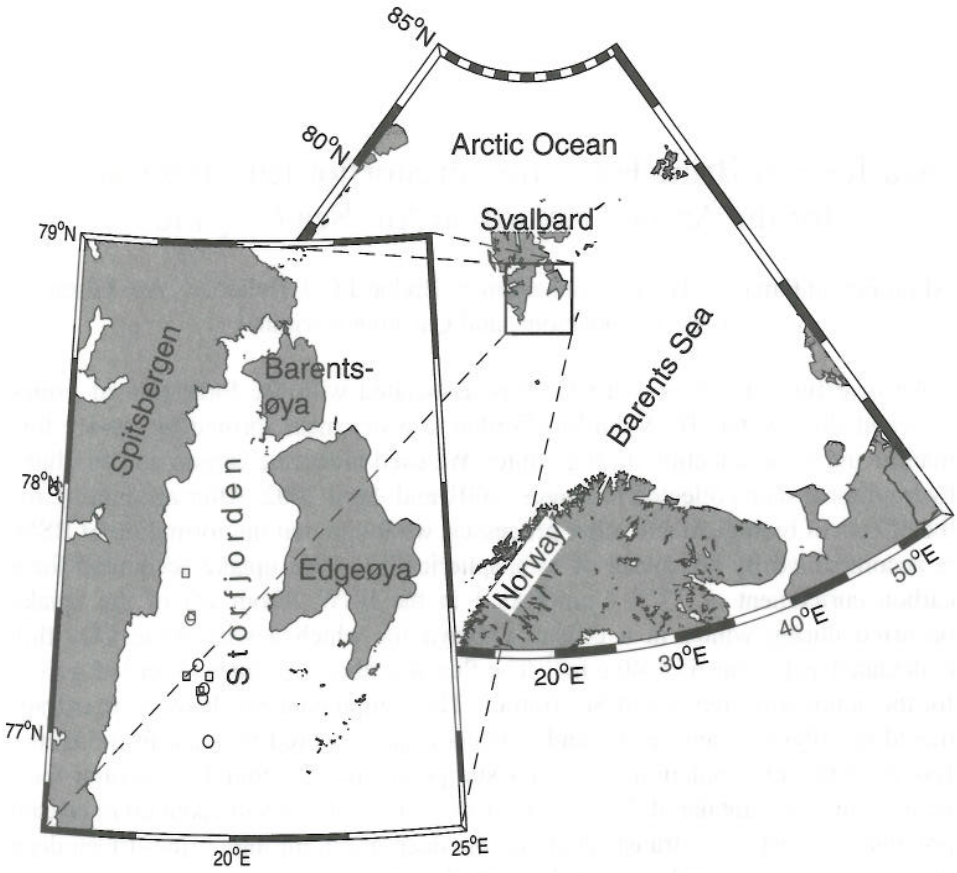

Figure 1. Map of Storfjorden, showing the stations visited during *Håkon Mosby* 2001 (squares) and *Oden* 2002 (diamonds) cruises.

seasonal ice on the carbon fluxes into the Arctic has not been studied. CO_2 flux and seasonal ice formation are related through the high-density water that forms through sea-ice formation and subsequent brine rejection. Such high-density waters supply the AO's deep and intermediate waters [e.g. *Jones et al.,* 2001]. Further, there is an important conduit of CO_2 to the AO through biological and transport processes [*Anderson and Jones,* 1991].

At present, the areal extent of seasonal ice in the Arctic is about 7×10^{12} m^2. Polynyas and leads (henceforth referred to as polynyas) are the major sites where extensive new ice formation and brine rejection occur. In the central Arctic, polynyas occupy about 1% of the winter ice extent, but they produce similar amounts of ice as that produced below multiyear ice [e.g. *Skogseth & Haugan,* 2003; *Gow and Tucker,* 1990]. Along the coastal margin, Arctic coastal polynyas produce large quantities of ice and high-density brine-enriched water [e.g. *Cavalieri and Martin* 1994]. The area of polynyas will probably increase in the future following the aforementioned greater seasonal variation of the arctic ice cover.

The present study investigates air–sea CO_2 flux during sea-ice formation and brine rejection, by using data collected from Storfjorden (Figure 1). This is a fjord situated in the western Barents Sea, between the islands of Spitsbergen, Barentsøya, and Edgeøya in the Svalbard Archipelago. Ice formation and subsequent brine rejection during winter produce brine-enriched shelf water (BSW), which is defined by $S \geq 35$ and $T < -1.5$°C [*Loeng,* 1991; referred to there as bottom water (BW)]. Further, most of the BSW production occurs in a coastal polynya situated at the lee-side of Edgeøya and Barentsøya [*Skogseth and Haugan,* 2003; *Haarpaintner et al.,* 2001], where offshore winds enhance ice production. Data on total dissolved inorganic carbon (C_T), total alkalinity (A_T), dissolved oxygen (O_2), temperature (T), and salinity (S) were collected from Storfjorden in August 2001 and April 2002. By evaluating the processes governing C_T concentration in BSW, the air–sea CO_2 flux associated with sea-ice formation and brine release over winter is determined. In particular, the flux is determined separately for the polynya and nonpolynya regions of the fjord. The computed carbon fluxes are then extrapolated to polynyas and seasonally ice-covered regions of the entire Arctic. Finally, the effect of changes in seasonal ice coverage and polynya extent on wintertime air–sea CO_2 flux in the Arctic is estimated.

2. DATA AND METHODS

2.1. Data and Analytical Methods

Data used in this work originate from two surveys (from the *Håkon Mosby* in 2001 and from the *Oden* in 2002) conducted in Storfjorden. Figure 1 shows the stations occupied during these surveys. Table 1 shows which parameters were measured during each cruise. Water samples were drawn from Niskin bottles mounted on a rosette with a CTD and analyzed onboard within 24 hours.

C_T was determined by gas extraction of acidified water samples followed by coulometric titration with a SOMMA system [*Johnson et al.*, 1985; 1987]. The precision was ±4 and ±1 μmol kg^{-1} during *Håkon Mosby* 2001 and *Oden* 2002, respectively. The accuracy in C_T measurements was set by running Certified Reference Material (CRM) supplied by Andrew Dickson at the Scripps Institute of Oceanography (San Diego, California).

A_T was determined by titrating samples with 0.1 M HCl as described by *Haraldson et al.* [1997]. The precision was determined to be ±5 and ±1 μmol kg^{-1} during *Håkon Mosby* 2001 and *Oden* 2002, respectively. The accuracy was set in the same way as for C_T.

O_2 was determined by using the Winkler method with visual detection of the titration end point during *Håkon Mosby* 2001 and with automated detection during *Oden* 2002.

2.2. Calculation Methods

Depth variations in the concentration of C_T are due to (i) biological activity, i.e., the formation/decay of organic matter and formation/dissolution of calcium carbonate, (ii) mixing of water masses, (iii) dilution/evaporation, (iv) brine rejection, and (v) air–sea CO_2 exchange. We corrected the measured C_T data for the effects of (i)–(iv) so we could evaluate the contribution from the air–sea flux of CO_2. The corrected C_T (nC_T) can be written as:

$$nC_T = (C_T - R_{C:O} \times AOU - 0.5 \times (nA_T - k) - b) \times \frac{34.17}{s} + b \quad (1)$$

where $R_{C:O}$ is the Redfield ratio of remineralization for carbon to oxygen, AOU is the apparent oxygen utilization, nA_T is the alkalinity corrected for the formation/decay of organic matter and then adjusted to a constant salinity of 34.17, and k and b are constants. The term $-R_{C:O} \times AOU$ accounts for C_T changes attributable to organic matter, while the term $-0.5 \times (nA_T - k)$ accounts for the changes due to the presence of calcium carbonate.

AOU was calculated after *Najjar and Keeling* [1997] according to:

$$AOU = (O_{2meas} - O_{2sat}) + \left(1 - \frac{p}{1013.25}\right) O_{2sat} \quad (2)$$

where O_2 is the oxygen concentration and the subscripts "sat" and "meas" refer to saturation and measured, respectively. The saturation concentration of O_2 is a function of atmospheric pressure (p). Hence, the second term of the right-hand side of Eq 2 is used to normalize our AOU values to 1 atm. For p, we used NCEP/NCAR reanalysis data of mean annual atmospheric pressure [*Kalnay et al.*, 1996] obtained from the NOAA CIRES Climate Diagnostics Center at http://www.cdc.noaa.gov. We assumed that AOU values calculated from Eq 2 quantified the amount of O_2 produced (AOU > 0) or consumed (AOU < 0) during the formation or decay of organic matter. Then we computed the corresponding changes in C_T from the product of AOU × $R_{C:O}$. We subtracted these results from the measured C_T to account for C_T changes that are due to formation/decay of organic matter (Eq 1).

Alkalinity is influenced by the same processes as for C_T except air–sea CO_2 exchange. The formation/decay of organic matter increases/decreases A_T slightly. For our area of investigation, adding the concurrent changes in nitrate to A_T will account for the above alkalinity changes [e.g. *Brewer et al.*, 1975]. We calculated the nitrate change from the product AOU × $R_{N:O}$, where $R_{N:O}$ (= −16/138) is the Redfield ratio of remineralization for nitrogen to oxygen. The results were added to the measured alkalinity. The resulting corrected alkalinity is henceforth referred to as $corrA_T$. We adjusted $corrA_T$ to a constant salinity of 34.17 to account for the changes due to mixing, dilution/evaporation, and brine rejection. For this purpose, we followed the procedure outlined by *Friis et al.* [2003], which better accounts for the effect of runoff, upwelling, and lateral mixing than does the traditional procedure. We first determined the intercept (b) of the linear relationship between $corrA_T$ and salinity and then adjusted

Table 1. Cruise Dates and Chemical Sampling From Storfjorden.

Cruise	Date (season)	S	T	C_T	A_T	O_2
Håkon Mosby 2001	Aug 23-25 (summer)	✓	✓	✓	✓	✓
Oden 2002	Apr 26-29 (winter)	✓	✓	✓	✓	✓

S = salinity, T = temperature, C_T = total dissolved inorganic carbon, A_T = total alkalinity, O_2 = dissolved oxygen.

all data of $corrA_T$ to 34.17 salinity to determine nA_T, according to:

$$nA_T = \frac{(corrA_T - b) \times 34.17}{S} + b \quad (3)$$

The intercept b was determined separately for samples influenced by brine rejection (identified by $T \leq 0°C$) and for the rest of the dataset (with $T > 0°C$). For the latter samples, mixing between modified Atlantic water (with $S \approx 34.85$ and $corrA_T \approx 2300$ μmol/kg) and fresher surface water (with $S < 33.5$ and $corrA_T < 2230$ μmol/kg) produced a linear relationship between $corrA_T$ and salinity with a slope and intercept of a_1 and b_1. A different linear relationship was found for samples influenced by brine rejection, and its coefficients were such that $a_2 > a_1$ and $b_2 \ll b_1$. Further, the two relationships intersected at $S = 34.17$. At this salinity, the value of $corrA_T$ was equal to k (see Eq 1), which is why we chose to adjust our data to $S = 34.17$. The above implies that, for each sample, any nonzero residual obtained from $(nA_T - k)$ results from the formation/dissolution of $CaCO_3$. Further, the corresponding change in C_T is one-half of this residual. Thus, we included the term $-0.5 \times (nA_T - k)$ in Eq 1 to account for this change.

Once C_T values were corrected for the effect of biological processes, i.e., once $C_T - R_{C:O} \times AOU - 0.5 \times (nA_T - k)$ was determined, the results were then adjusted to 34.17 salinity, to correct for changes due to (ii)–(iv) above. Specifically, we assumed that the freshwater alkalinity end-member (i.e., b) was entirely due to bicarbonate ions. Therefore, the same values of b could be used for C_T. Hence, by replacing $corrA_T$ in the right hand side of Eq 3 with $C_T - R_{C:O} \times AOU - 0.5 \times (nA_T - k)$, we obtained the right hand side of Eq 1.

For each cruise, we constructed a composite profile for each of the variables T, S, AOU, nA_T, and nC_T by taking the 10-m depth-averages of data acquired from different stations. These profiles reveal depth variations during each cruise; comparison between two profiles for the same parameter but from different cruises reveals the seasonal (summer–winter) variation of that particular parameter.

2.3. Uncertainties

As depicted in Eqs 1 and 3, nC_T and nA_T are functions of measured and calculated quantities. The uncertainties of the former type of quantities are given by their analytical imprecision while the uncertainties of the latter are given by their standard deviations. We calculated the total uncertainties in nC_T and nA_T that are due to the above individual uncertainties. For this purpose, we neglected the individual uncertainties in S and AOU because they were negligible compared to the individual uncertainties associated with the other parameters used for the calculation. Hence, for each pair of values of S and AOU, nC_T would be described by a linear function of C_T, $R_{C:O}$, nA_T, k, and b, with proportionality constants of (34.17/S), (34.17/S) × AOU, (34.17/2S), (34.17/2S), and (1 – 34.17/S), respectively (see Eq 1). Further, we denoted the uncertainties associated with C_T, $R_{C:O}$, nA_T, k, and b as σ_{C_T}, $\sigma_{R_{C:O}}$, σ_{nA_T}, σ_k, and σ_b, respectively. The total uncertainty in nCT was then computed according to (e.g.) *Bentley* [1988]:

$$\sigma_{nC_T} = \left(\begin{array}{l} \left(\frac{34.17}{S} \times \sigma_{C_T}\right)^2 + \left(\frac{34.17}{S} \times AOU \times \sigma_{R_{C:O}}\right)^2 \\ + \left(\frac{34.17}{2S}\sigma_{nA_T}\right)^2 + \left(\frac{34.17}{2S} \times \sigma_k\right)^2 \\ + \left(1 - \frac{34.17}{S}\right)^2 \times \sigma_b^2 \end{array} \right)^{1/2} \quad (4)$$

where by using similar arguments, σ_{nA_T} was calculated according to:

$$\sigma_{nA_T} = \left(\begin{array}{l} \left(\frac{34.17}{S} \times \sigma_{A_T}\right)^2 + \left(\frac{34.17}{S} \times AOU \times \sigma_{R_{N:O}}\right)^2 \\ + \left(1 - \frac{34.17}{S}\right)^2 \times \sigma_b^2 \end{array} \right)^{1/2} \quad (5)$$

Table 2 lists the values of the individual uncertainties (i.e. values of σ_{C_T}, $\sigma_{R_{C:O}}$, σ_{nA_T}, σ_k, σ_b and $\sigma_{R_{N:O}}$ Values of $\pm 0.15 \times R_{C:O}$ and $\pm 0.15 \times R_{N:O}$ were choosen for $\sigma_{R_{C:O}}$ and $\sigma_{R_{N:O}}$.These particular values were chosen in order to account for the wide range of values that are often reported in the literature for $R_{C:O}$ and $R_{N:O}$, which typically differ up to 15% [e.g. *Redfield et al.* [1963]; *Anderson et al.* [1988,

Table 2. Values of Individual Uncertainties Used for Computation of Eqs 4 and 5.

Parameter	Value [μmol kg^{-1}]
σ_{C_T}	±4 for *Håkon Mosby* 2001 ±1 for *Oden* 2002
σ_{A_T}	±5 for *Håkon Mosby* 2001 ±1 for *Oden* 2002
$\sigma_{R_{C:O}}$	$\pm 0.15 \times R_{C:O}$
$\sigma_{R_{N:O}}$	$\pm 0.15 \times R_{N:O}$
σ_k (see Table 3)	±4 for samples with $T \leq 0°C$ ±3 for samples with $T > 0°C$
σ_b (see b in Table 3)	±42 for samples with $T \leq 0°C$ ±46 for samples with $T > 0°C$

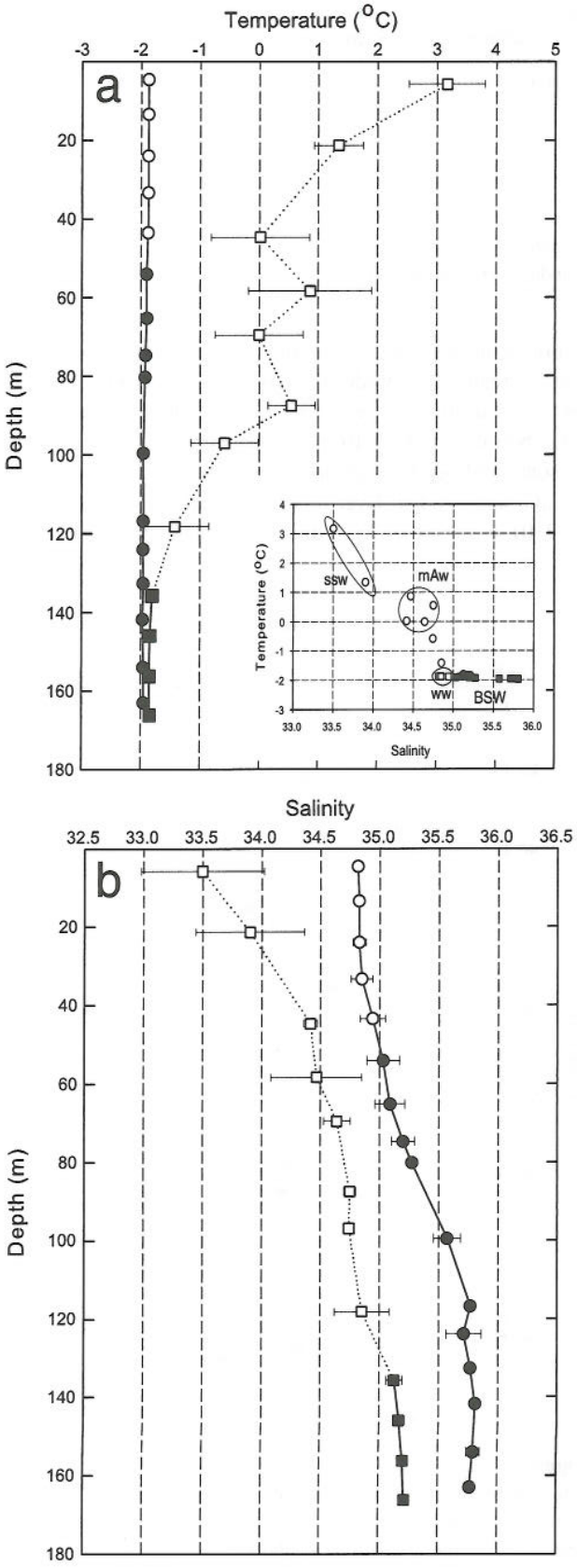

and references therein]; *Anderson and Sarmiento* [1994]; *Körtzinger et al.* [2001]].

The total uncertainty associated with each depth-averaged data point of nC_T and nA_T was calculated according to:

$$\sigma_{nC_T}(\text{mean}) = \frac{\sigma_{nC_T}}{\sqrt{n}} \text{ and } \sigma_{nA_T}(\text{mean}) = \frac{\sigma_{nA_T}}{\sqrt{n}} \qquad (6)$$

where n is the number of data points on which the averages were based. Note that according to Eqs 4, 5, and 6 greater magnitudes of measurement imprecision and/or of AOU results in higher values of σ_{nC_T} (mean) and σ_{nA_T} (mean). For the averages of T, S, and AOU we chose to present the associated standard deviations, rather than the much smaller total uncertainties which result from measurement imprecision. These standard deviations are measures of the spatial variability. The corresponding spatial variability in nC_T and nA_T were generally less than σ_{nC_T} (mean) and σ_{nA_T} (mean).The latter can, therefore, be viewed both as measures of the total uncertainty and as measures of the spatial variability.

3. RESULTS

Temperature and salinity profiles are shown in Figs 2a and 2b, the former with an inset that depicts the T and S definitions of the water masses of interest. A fresher ($S < 34$) and warmer ($T > 1°C$) water resides at the surface during summer. This water mass, which has been diluted by meltwater and runoff from Svalbard and heated by solar radiation, will henceforth be referred as to summer surface water (ssw). Temperature decreases while salinity increases with depth at the base of ssw, a consequence of mixing with the underlying modified Atlantic water (mAw) that occupies depths between 45 and 90 m. Beneath the mAw, temperature decreases to near freezing while salinity increases to over 35. This is a result of mixing with BSW, which resides at depths below 135 m. During winter, the whole water column is at or near freezing (Figure 2a). A fresher layer with $S \approx 34.83$ occupies the upper 35 m of the fjord (Fig 2b), henceforth referred to as winter water (ww). Below the ww layer, salinity increases almost linearly with depth to ≈ 35.8 at around 115 m. A nearly constant salinity of ≈ 35.8 is observed below the 115-m depth.

Figure 2. Depth profiles of (a) temperature and (b) salinity. Squares denote the summer data acquired during *Hkon Mosby* 2001.Circles denote the winter data acquired during *Oden* 2002. Inset in (a): T and S definitions of the water masses of interest, i.e., brine-enriched shelf water (BSW), modified Atlantic water (mAw), summer surface water (ssw), and winter water (ww). Note that filled symbols indicate data of BSW. Error bars depict the spatial variability (see section 2.3 of the main text).

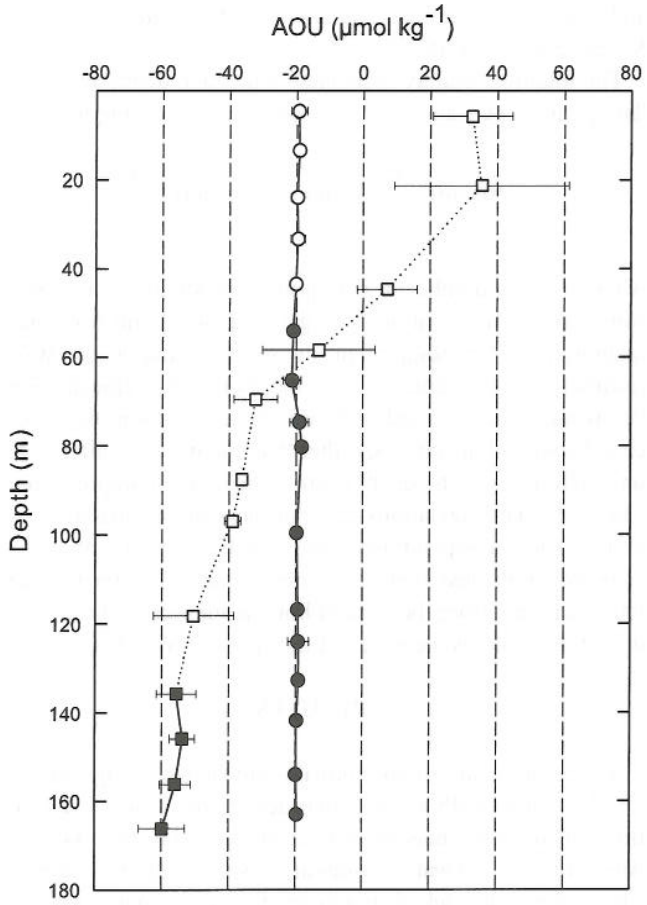

Figure 3. Depth profiles of AOU (apparent oxygen utilization). Symbols and error bars as in Figure 2.

Note that the BSW had about 0.6 higher salinity in 2002 compared to 2001 (Figure 2b). This indicates that the BSW observed in summer 2001 was effectively flushed during winter 2001/2002.

AOU values were >0 in the upper 50 m and <0 for the rest of the water column during summer (Figure 3). This means that O_2 was produced in the upper 50 m as a result of primary production, but was consumed due to decay of organic matter in the rest of the water column. During winter, on the other hand, a signature of decay of organic matter (AOU < 0) was observed throughout the water column.

Values of the coefficients and associated statistics for the two relationships between $corrA_T$ and S (section 2.2) are given in Table 3.

nA_T is constant at 2264 ± 4 µmolkg^{-1} (Figure 4), irrespective of season or depth. This means that dissolution/formation of calcium carbonate is a less significant process in Storfjorden. We also note the total uncertainties (±5.1 µmol kg^{-1}) of the summer data are higher those in winter (±1.7 µmol kg^{-1}). This is partly due to better measurement

Table 3. Values of Coefficients and Statistical Parameters for the Two Relationships Between $corrA_T$ and Salinity.

Parameter	For samples with	
	T > 0°C	T ≤ 0°C
a	55.38 ± 1.30	65.74 ± 1.20
b	372 ± 46	18 ± 42
R^2	0.99	0.96
Number of samples	15	97
Standard error of the fit (σ_k)	±3	±4

imprecision (summer: ±4; winter: ±1 µmol kg^{-1}) and partly due to greater magnitudes of AOU (summer: 30 to –60; winter: ≈ –20 µmol kg^{-1}) (see also section 2.3 and Figure 3).

Carbon contribution from air–sea exchange produces both seasonal and depth variations of nC_T (Figure 5). During winter, nC_T shows a two-layer structure; relatively constant values of 2101 ± 1.6 µmol kg^{-1} are observed in the upper 45 m,

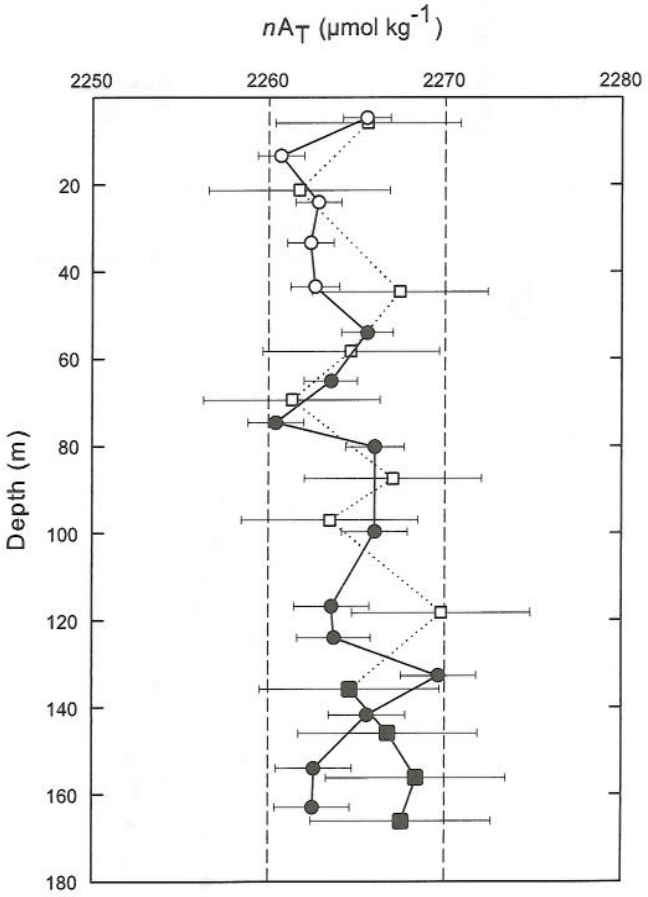

Figure 4. Depth profiles of nA_T (total alkalinity, corrected for the effect of formation/decay of organic matter, and adjusted to a constant salinity of 34.17). Error bars depict the total uncertainty (see section 2.3 of the main text). Symbols as in Figure 2.

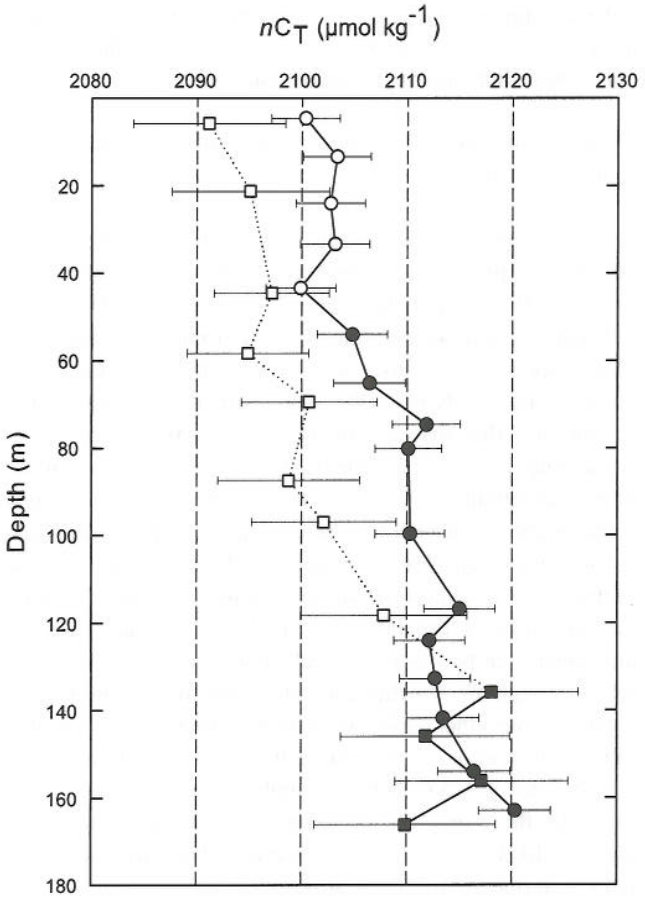

Figure 5. Depth profiles of nC_T (total dissolved inorganic carbon, corrected for the effects of processes other than air–sea CO_2 exchange, adjusted to a constant salinity of 34.17). Error bars depict the total uncertainty (see section 2.3 of the main text). Symbols and lines as in Figure 2.

2113 ± 3.2 μmol kg^{-1} in BSW. These two layers are divided by a gradient of values between 2105 and 2106 μmol kg^{-1}. The water forming this gradient is also BSW, but its nC_T values have been reduced because of mixing with the overlying water. A similar two-layer structure is evident in the summer nC_T profile: values of 2096 ± 3.3 μmol kg^{-1} observed in the upper 90 m and 2114 ± 4 μmol kg^{-1} in BSW. A strong gradient, with values between around 2100 and 2110 μmol kg^{-1}, divides these two layers. The total uncertainties for the summer data are higher (~±7.3 μmol kg^{-1}) than in winter (±3.3 μmol kg^{-1}), for the same reasons as given earlier for nA_T.

From the above, it is clear that essentially the same nC_T values were observed for BSW in the summer of 2001 and the winter of 2002. This is as anticipated, because BSW forms during winter only and no seasonal variability is expected. However, this observation also means that there were no significant year-to-year variations of BSW nC_T between 2001 and 2002. Conversely, a seasonal variability is evident for the water that occupied the upper parts of the fjord. nC_T values observed in the upper 90 m during summer were on average 5 ± 3.7 μmol kg^{-1} lower than those observed in the upper 45 m during winter.

4. DISCUSSION

4.1. Degree of Oxygen Saturation

Different magnitudes of AOU could be calculated from the O_2 data, depending on the degree of O_2-saturation assumed. The profiles shown on Figure 3 were computed by assuming 100% saturation (section 2.2). Any O_2-saturation lower than 100% would result in higher AOU values (Eq 2). For instance, if we used a 94.5% saturation, which was observed in the upper 45 m during winter, then we would obtain winter AOU values of ≈ 0 μmol kg^{-1}; for the summer profile, the transition from AOU < 0 to AOU > 0 would deepen from 50 m to 60 m (Figure 3). Also, both summer and winter nC_T profiles (Figure 5) would be shifted towards higher (15–16 μmol kg^{-1}) values. However, the magnitudes of neither depth gradients nor seasonal variations in nC_T would change. That is, the absolute values of the computed nC_T are sensitive to the choice of degree of O_2-saturation, but the relative seasonal and depth variations of nC_T are not. Therefore, nC_T changes due to air–sea CO_2 flux are correctly quantified irrespective of the degree of O_2-saturation chosen.

4.2. Uptake of Atmospheric CO_2 During the Formation of Sea-Ice and BSW

The quantification of atmospheric CO_2 uptake concurrent with the production of BSW is easier to demonstrate after the following conceptual description of the formation of this water mass. We conceptualize that heat loss to the atmosphere during fall, and brine rejection during early winter, transform ssw and mAw into ww. The ww is under-saturated with CO_2 (verified from the data used in this study, not shown). Thus, a flux of CO_2 moves into the water column in the absence of ice cover. As the winter progresses, sea-ice formation and subsequent brine rejection takes place primarily in the polynya but also under the pack ice. While air–sea CO_2 exchange is hampered in the ice-covered areas of the fjord, it continues to take place in the polynya, and the brines formed there can approach CO_2 saturation. On sinking, however, the rejected brines entrain ambient waters of intermediate depth with lower carbon concentration. The admixture forms BSW, which is not fully saturated with CO_2. "New" ww, which was ice-covered and has a lower concentration of carbon, advects or upwells into the polynya and replaces the brines that sank. As this continues throughout the winter,

the deeper part of the fjord is gradually filled with high-CO_2 BSW, while the surface of the fjord contains low-CO_2 ww (Figure 5). When a sufficient volume of BSW has been produced, it drains over the sill and flows to the open ocean as a bottom current, carrying the excess carbon with it.

Simultaneously with the transformation of ssw and mAw into ww, uptake of atmospheric CO_2 increases the nC_T of ssw by 5 ± 3.7 μmol kg^{-1} (from 2096 ± 3.3 to 2101 ± 1.6) (Figure 5). Further CO_2 uptake increases nC_T of ww by 12 ± 3.6 μmol kg^{-1} (from 2101 ± 1.6 to 2113 ± 3) (Figure 5), as this water is transformed into BSW. The latter carbon enrichment is henceforth denoted as $\Delta C_{T\text{-win}}$. We believe this enrichment takes place mainly in the polynya (see below). However, other parts of the fjord may also contribute through a one-time uptake, before the ice-cover becomes an effective barrier for air–sea gas exchange. In total, the ssw and mAw take up 17 ± 4 μmol kg^{-1} [= 5 (±3.7) + 12 (±3.6)] during their transformation into BSW. This carbon enrichment is henceforth denoted as $\Delta C_{T\text{-tot}}$.

There is a theoretical foundation for a total uptake of 17 ± 4 μmol kg^{-1}. For each sample, the increase in C_T (ΔC_T) that is expected from a temperature decrease (ΔT) can be determined according to *Watson et al.* [1995]:

$$\Delta C_T = \frac{0.0423}{RF} \times C_T \times \Delta T \quad (7)$$

where RF is the Revelle Factor. We determined this factor according to the procedure given in *Takahashi et al.* [1993] and obtained a value of 16.5. ΔT was determined by assuming that all waters were cooled from their initial temperatures to –1.9°C (the mean temperature observed in BSW). Then, using Eq 7, we obtained a mean ΔC_T of 15 ± 2 μmol kg^{-1} for ssw and mAw, which is in agreement with the observed value.

The cooling-induced uptake is not, however, instantaneous. The nC_T in ww is around 5 μmol kg^{-1} higher than that in ssw and mAw (Figure 5), only one-third of the 15 μmol kg^{-1} that would be obtained by using Eq 7. We believe the rest of the uptake happens during a prolonged residence time in the polynya. This would be especially true if sea-ice formation enhances air–sea exchange, as was suggested in a recent study by *Anderson et al.* [2004]. Hence, nonpolynya parts of the fjord may also contribute to $\Delta C_{T\text{-win}}$ under the process of formation of the ice cover. In any case, our nC_T data (Figure 5) and the above calculation show that the excess carbon observed in BSW ($\Delta C_{T\text{-tot}}$) is the same amount that would be expected from the observed temperature decrease.

We combined $\Delta C_{T\text{-tot}}$ with typical annual mean volume of BSW (V_{BSW}) to compute the corresponding total carbon uptake from the atmosphere (CU_{tot}), in grams of C per year, according to:

$$CU_{tot} = \Delta C_{T\text{-tot}} \times V_{BSW} \quad (8)$$

We determined CU_{tot} to be 0.21 (±0.06) × 10^{12} g yr^{-1}, assuming V_{BSW} = 9.9 (±1.7) × 10^{11} m^3, as modeled for the winters 1997/1998–2000/2001 by *Skogseth and Haugan* [2003].

4.3. Extrapolation of Storfjorden Wintertime Carbon Fluxes to the Entire Arctic

Sea-ice formation and production of brine-enriched water are common processes on the Arctic shelves [e.g. *Martin and Cavalieri,* 1989] and in the Arctic Ocean in general. Therefore, in this subsection, we estimate the wintertime CO_2 uptake that takes place simultaneously with ice and brine production in Arctic coastal polynyas. We also estimate the wintertime air–sea CO_2 flux that accompanies ice formation in central Arctic polynyas and in seasonally ice-covered regions. For the latter calculations, we use both present and future projections of the extent of seasonal ice and central Arctic polynyas. Note that wintertime air–sea CO_2 flux in Arctic coastal polynyas is referred to as "wintertime carbon uptake" because the word "uptake" reflects the fact that, in Arctic coastal polynyas, atmospheric carbon is most likely transported into the deep ocean through air–sea flux and subsequent formation of deep water. On the other hand, wintertime carbon flux associated with ice formation in the rest of the Arctic is referred to as "wintertime air–sea CO_2 flux", emphasizing that this is a seaward CO_2 flux across the air–sea interface and that knowledge about the likely fate of the atmospheric carbon involved is limited (i.e. it may return to the atmosphere in summer).

Table 4 shows values and sources of the different parameters used in the following calculations.

We combined $\Delta C_{T\text{-win}}$ and V_{BSW} to compute the winter carbon uptake (CU_{win}) for Storfjorden by using Eq 9.

$$CU_{win} = \Delta C_{T\text{-win}} \times V_{BSW} \quad (9)$$

During the winters of 1997/1998–2000/2001 the polynya occupied 10% of Storfjorden area but accounted for 58% of the total ice production [*Skogseth and Haugan*, 2003]. We assume that a similar partitioning also prevailed during the winter 2001/2002 and that a certain fraction (f) of V_{BSW} was produced in the polynya. Then, the winter uptake attributable to the polynya (CU^{p}_{win}) is given by:

$$CU^{p}_{win} = f \times \Delta C_{T\text{-win}} \times V_{BSW} \quad (10)$$

whereas the part of CU_{win} attributable to the nonpolynya regions of the fjord (CU^{np}_{win}) is given by:

$$CU^{np}_{win} = (1 - f) \times \Delta C_{T\text{-win}} \times V_{BSW} \quad (11)$$

The average winter CO_2 fluxes for polynya and nonpolynya regions of Storfjorden (F^{P} and F^{nP}) [C, g m^{-2}] were then

Table 4. Values and Sources of Different Parameters Used for Calculation of the Entries in Table 5.

Parameter	Value	Reference
Excess C_T ($\Delta C_{T\text{-win}}$) in BSW, due to uptake in winter	0.15 ± 0.044 g m^{-3}	This study
Area of Storfjorden	13×10^9 m^2	*Skogseth and Haugan*, 2003
Area of polynya in Storfjorden	1.3×10^9 m^2	*Skogseth and Haugan*, 2003
Volume of BSW (V_{BSW}) formed in Storfjorden in 1998-2001	$(9.8 \pm 1.8) \times 10^{11}$ m^{-3}	*Skogseth and Haugan*, 2003
Fraction (f) of V_{BSW} that form in Storfjorden polynya	0.58 ± 0.29	Assumption
Winter ice extent in the Arctic	14×10^{12} m^2	*Johannessen et al.*, 2002
Area of Arctic coastal polynyas	3.5×10^{10} m^2	*Winsor and Björk*, 2000
Area of central Arctic polynyas	11×10^{10} m^2	*Gow and Tucker*, 1990
Extent of seasonal ice in the Arctic	7×10^{12} m^2	*Johannessen et al.*, 2002
Winter ice extent in future* Arctic	12×10^{12} m^2	*Johannessen et al.*, 2002
Area of central Arctic polynyas in the future [in % of the above]	1, 10, or 20	Assumption
Extent of seasonal ice in future Arctic	10×10^{12} m^2	*Johannessen et al.*, 2002

*Around year 2100.

computed by dividing the outputs of Eqs 10 & 11 by the corresponding areas (Table 4). The first two entries of Table 5 show the results of these calculations when the value of f chosen was 0.58 ± 0.29. No information on f was available to us, but we assumed a one-to-one correspondence in the amount of ice and brine formed per unit area. Accordingly, 58% of V_{BSW} would be formed in the polynya, since 58% of the total ice production occurred there. Further, to acknowledge that this partitioning is not well constrained, we allowed the value of f to vary as much as 50%. As is evident from Table 5, the average winter CO_2 flux computed for Storfjorden polynya is about 13 times higher than the rest of the fjord. However, polynya and nonpolynya regions of Storfjorden contributed nearly equally to the total winter uptake (U_{win}) (Table 5, third entry), the area of the nonpolynya being 10 times larger than the polynyas.

Wintertime carbon uptake for Arctic coastal polynyas was determined from the product of F^P (Table 5) and the area of the polynyas (Table 4). The latter was inferred, from Tables 2 and 3 of *Winsor and Björk* [2000]. The result is shown in the fourth entry of Table 5.

We postulate that there are, analogous to Storfjorden, wintertime air–sea CO_2 fluxes occurring in central Arctic polynyas and in seasonally ice-covered regions. That is, air–sea CO_2 flux occurs in the central Arctic polynyas throughout winter, while a one-time air–sea CO_2 flux occurs in the seasonally ice-covered region, just before the ice cover becomes an effective barrier to air–sea CO_2 exchange. However, unlike the case for Arctic coastal polynyas, the carbon taken up through this process may not be transferred into the deep ocean. The reason is that deep-water formation in the Arctic takes place primarily on the shelves [e.g. *Jones*, 2001]. Nevertheless, due to the vastness of

Table 5. Computed Wintertime Air–Sea CO_2 Fluxes for Polynya and Nonpolynya Regions of Storfjorden and for Present and Future Arctic.

Parameter	Value
For Storfjorden	
Areal winter flux for the polynya region (F^P) [in g m^{-2}]	65 ± 40
Areal winter flux for the non-polynya region (F^{np}) [in g m^{-2}]	5.2 ± 3.2
Total winter uptake (CU_{win}) [in 10^{12} g yr^{-1}]	0.15 ± 0.05
For contemporary Arctic [*in* 10^{12} g yr^{-1}]	
Winter uptake for Arctic coastal polynyas	2.3 ± 1.4
Wintertime air–sea CO_2 flux for central Arctic polynyas	6.8 ± 4.2
Wintertime air–sea CO_2 flux for seasonally ice-covered Arctic	36 ± 22
Total winter flux for the Arctic, excluding coastal polynyas	43 ± 22
For future Arctic, excluding coastal polynyas* [*in* 10^{12} g yr^{-1}]	
If polynyas occupy 1% of future Arctic winter ice extent	59 ± 32
If polynyas occupy 10% of future Arctic winter ice extent	124 ± 55
If polynyas occupy 20% of future Arctic winter ice extent	196 ± 98

*Around year 2100.

the areas involved, it is important to consider the wintertime air–sea CO_2 flux associated with ice formation in central Arctic polynyas and in seasonally ice-covered regions. For this purpose, we assumed F^P and F^{nP} (Table 5) represented polynyas and seasonally ice-covered regions, respectively. Then we multiplied F^P and F^{nP} by the corresponding areas (Table 4). The obtained values for the individual fluxes and their sum are shown in entries 5–7 of Table 5. Due to the set of assumptions made during the calculations, the computed fluxes are probably subject to errors that are even larger than the uncertainties listed on Table 5. For instance, the surface waters of the Arctic are not CO_2-undersaturated everywhere during winter [e.g. *Kelley,* 1968]. Thus, in some regions the CO_2 flux may be directed to the atmosphere rather than into the ocean. The above-determined air–sea CO_2 fluxes should, therefore, be taken as first-order estimates. Nevertheless, we expect the fluxes to be in the right order of magnitude. In that case, the computed total wintertime air–sea CO_2 flux for the Arctic is comparable to that for the northern North Atlantic [*Olsen et al.,* 2003]. Hence, we suggest that there is a regionally significant wintertime air–sea CO_2 flux associated with ice formation in the Arctic.

Model results show that the extent of seasonal ice in the Arctic will increase to about 10×10^{12} m^2 [*Johannessen et al.,* 2002; their Figure 7] around year 2100. Further, observations have shown that a thinning of the ice [*Rothrock et al.,* 1999, 2003; *Johannessen et al.,* 2002] will accompany its decrease. Because of this thinning, the extent of leads and polynyas will probably increase in the future. At present, the area occupied by leads and polynyas increases from 1% of the winter ice cover to 10–20% during summer [*Gow and Tucker,* 1990]. Quantitative information on how this may change in the future was not available to us. Therefore, we calculated the total (for central Arctic polynyas + seasonally ice covered regions) wintertime air–sea CO_2 fluxes for three different future scenarios, depending on the extent of polynyas by the end of this century; For all three cases, we used a seasonal ice extent of 10×10^{12} m^2 and assumed the polynyas would occupy 1%, 10%, and 20% of the future winter ice-cover (Table 4). The results of these computations are shown in the last three entries of Table 5. As can be inferred from Tables 4 and 5, wintertime CO_2 (C) flux into the Arctic can increase by 80 ($\pm$ 60) $\times 10^{12}$ g yr^{-1}, if seasonal ice extent increases by 43% and central Arctic polynyas become 10 times larger than present.

5. CONCLUSIONS

Cold and high-salinity BSW forms in Storfjorden during winter. This is due to extensive sea-ice production, which primarily takes place in a coastal polynya. We have investigated air–sea CO_2 flux associated with this process by analyzing inorganic carbon and auxiliary hydrographic data collected in August 2001 and April 2002. Uptake of atmospheric carbon occurs simultaneously with the transformation of the source waters into BSW. This uptake accounted for a carbon enrichment of 17 $\pm$ 4 μmol kg^{-1}. The observed enrichment could be computed theoretically by using the observed temperature decrease. However, further analysis revealed that only about one-third of the carbon enrichment occurred in parallel with the heat loss, indicating that the cooling-induced CO_2 uptake was not instantaneous. The remaining two-thirds of the uptake has been suggested to occur later in the polynya. The areal wintertime CO_2 flux of 65 $\pm$ 40 g m^{-2} we computed for the polynya was about 13 times lower ($\approx$ 5 g m^{-2}) for the nonpolynya parts of the fjord.

Extrapolating the fluxes computed for Storfjorden to the entire Arctic gave a total CO_2 uptake of Arctic coastal polynyas of 2.3 ($\pm$1.4) $\times 10^{12}$ g yr^{-1}. This carbon is most likely sequestered from the surface–ocean–atmosphere system through brine-driven deep-water formation in Arctic coastal polynyas. For central Arctic polynyas and for seasonally ice-covered regions, we estimated a wintertime air–sea CO_2 flux of 43 ($\pm$22) $\times 10^{12}$ g yr^{-1} C. This is a regionally significant flux, about half of the wintertime flux into the northern North Atlantic [*Olsen et al.,* 2003]. Further, by the end of this century, this air–sea CO_2 flux can increase to 124 ($\pm$55) $\times 10^{12}$ g yr^{-1}, if seasonal ice extent increases by 43% [*Johannessen et al.,* 2002; their Figure 7] and central Arctic polynyas become 10 times larger than present. With respect to the sequestration of atmospheric carbon, the importance of the computed wintertime air–sea CO_2 flux depends on the penetration of brine–driven convection in the involved regions.

Acknowledgments. This work has been partly supported by the Norwegian Research Council under project no. 122470/720, and partly by the European Commission through the project "Tracer and Circulation in the Nordic Seas Region" (TRACTOR) under contract no. EVK2-2000-00080. This is publication no. A50 of the Bjerknes Centre for Climate Research.

REFERENCES

Anderson, L.G, E. Falck, E.P. Jones, S. Jutterström, and J.H. Swift, Enhanced uptake of atmospheric CO_2 during freezing of seawater: A field study in Storfjorden, Svalbard. *J. Geophys. Res.*, 109, C06004, doi:10.1029/2003JC002120, 2004.

Anderson, L.G. and S. Kaltin, Carbon fluxes in the Arctic Ocean–potential impact by climate change. *Polar Res.*, 20, 225-232, 2001.

Anderson, L.A. and J.L., Sarmiento. Redfield ratios of remineralization determined by nutrient data analysis. *Global Biogeochem. Cy.*, 8, 65-80, 1994.

Anderson, L.G. and E.P. Jones, The transport of CO2 into Arctic and Antarctic Seas: similarities and differences in the driving processes. *J. Marine Syst.*, 2, 81-95, 1991.

Anderson, L.G., P.E. Jones, R. Lindegren, B. Rudels, Nutrient regeneration in cold, high salinity bottom water of Arctic shelves *Cont. Shelf Res.*, 8, 1345-1355, 1988.

Bentley, J.P. *Principles of measurement systems* (2nd ed.). Longman scientific & technical, UK. 503 pp. 1988.

Brewer, P.G., G.T.F. Wong, M.P. Bacon, and D.W. Spencer, An ocean alkalinity problem? *Earth Planet. Sc. Lett.,* 26, 81-87, 1975.

Cavalieri, D.J. and S. Martin, The contribution of Alaskan, Siberian, and Canadian coastal polynyas to the cold halocline layer of the Arctic Ocean. *J. Geophys. Res.*, 99 (C9), 18343-18362, 1994.

Friis, K., A. Kortzinger, and D.W.R, Wallace, Salinity normalization of marine inorganic carbon chemistry data. *Geophys. Res. Lett.*, 30, NO. 2, 1085, doi:10.1029/2002GL015898, 2003.

Gow, A.J. and W.B. Tucker, Sea ice in the polar regions, *in Polar Oceanography, edited by* W.O. Smith, pp 47-122, Academic Press, Inc, London, 1990.

Haarpaintner, J., J. Gascard, and P.M. Haugan, Ice production and brine formation in Storfjorden, Svalbard. *J. Geophys. Res.*, 106 (C7), 14001-14013, 2001.

Haraldson, C., L.G. Anderson, M. Hasselov, S. Hulth, and K. Olsson, Rapid, high-precision potentiometric titration of alkalinity in the ocean and sediment pore waters. *Deep-Sea Res., I,* 44, 2031-2044, 1997.

Johannessen, O.M., L. Bengtsson, M.W. Miles, S.I. Kuzmina, V.A. Semenov, G.V. Alekseev, A.P. Nagurnyi, V.F. Zakharov, L. Bobylev, L.H. Pettersson, K. Hasselmann and H.P. Cattle, Arctic climate change—observed and modeled temperature and sea-ice variability. *Tellus,* 56A, 328-341, 2004.

Johnson, K.M., A.E. King, and J.M. Sieburth, Coulometric TCO_2 analyses for marine studies; an introduction, *Mar. Chem.*, 16, 61-82, 1985.

Johnson, K.M., J.M. Sieburth, P.J. Williams, and L. Brandstrom, Coulometric total carbon dioxide analysis for marine studies: automation and calibration, *Mar. Chem.*, 21, 117-133, 1987.

Jones, E. P., Circulation in the Arctic Ocean. *Polar Res.*, 20, 139-146, 2001.

Kalnay, E., M. Kanamitsu, R. Kistler, W. Collins, D. Deaven, L. Gandin, M. Iredell, S. Saha, G. White, J. Woollen, Y. Zhu, M. Chelliah, W. Ebisuzki, W. Higgins, J. Janowiak, K.C. Mo, C. Ropelewski, A. Leetmaa, R. Reynolds, and R. Jenne, 1996. The NCEP/NCAR 40-year Reanalysis Project. Bull. Am. Met. Soc. 77, 438-471.

Kelley, J., Carbon dioxide in the seawater under the Arctic Ice. *Nature* 218, 862-865, 1968.

Körtzinger, A., J.I. Hedges, and P.D. Quay, Redfield ratios revisited: Removing the biasing effect of anthropogenic CO2. *Limnol. Oceanogr.*, 46, 964-970, 2001.

Martin, S. and D. Cavalieri, Contribution of the Siberian polynyas to the Arctic Ocean intermediate and deep water. *J. Geophys. Res.*, 94, 12725-12738, 1989.

Najjar, G. and R. Keeling, Analysis of the mean annual cycle of dissolved oxygen anomaly in the world ocean. *J. Mar. Res.*, 55, 117-151, 1997.

Olsen, A., R.G.J. Bellerby, T. Johannessen, A.M. Omar, and I. Skjelvan, Interannual variability in the wintertime air-sea flux of carbon dioxide in the northern North Atlantic. *Deep Sea Res. I,* 50, 1323–1338, 2003.

Redfield, A.C., B.H. Ketchum, and F.A. Richards, The influence of organisms on the composition of seawater, *in The Sea,* edited by M. N. Hill, pp 26-77, John Wiley, New York, 1963.

Rothrock, D.A., Y. Yu, and G.A. Maykut, Thinning of the Arctic Sea-Ice Cover. *Geophys. Res. Lett.,* 26, 3469- 3472, 1999.

Skogseth, R. and P. Haugan, Ice and brine production in Storfjorden from four winters of satellite and in situ observation, *in Dense water production processes in Storfjorden (PhD thesis) by* Skogseth R., University of Bergen, Norway, 2003.

Takahashi, T., J. Olafsson, J.G. Goddard, D.W. Chipman, and S.C. Sutherland, Seasonal variation of CO_2 and nutrients in the high-latitude surface oceans: a comparative study. *Glob. Biogeochem. Cy., 7,* 843-878, 1993.

Watson, A., P.D. Nightingale, and D.J. Cooper, Modelling atmosphere-ocean CO_2 transfer. *Phil. Trans. R. Soc. lond.* B, 125-132, 1995.

Winsor, P. and G. Björk, Polynya activity in the Arctic Ocean from 1958 to 1997. *J. Geophys. Res.*, 105 (C4), 8789-8803, 2000.

L.G. Anderson, Department of Analytical and Marine Chemistry, Göteborg University, 41296 Göteborg, Sweden.

R.G.J. Bellerby, Bjerknes Centre for Climate Research, University of Bergen, Allegaten 55, N-5007 Bergen, Norway.

T. Johannessen, A. Olsen, and A. Omar, Bjerknes Centre for Climate Research, University of Bergen, Allegaten 55, N-5007 Bergen, Norway, and Geophysical Institute, University of Bergen, Allégaten 70, 5007 Bergen, Norway. (abdirahman.omar@bjerknes.uib.no)

Caroline Kivimäe, Geophysical Institute, University of Bergen, Allégaten 70, 5007 Bergen, Norway.

Paper IV

Interannual variability of net community production at Ocean Weather Station M in the Norwegian Sea during 51 years

Kivimäe, C. and E. Falck

Submitted to Global Biogeochemical Cycles.

Interannual variability of net community production at Ocean Weather Station M in the Norwegian Sea from 1955 to 2005

C. Kivimäe* and E. Falck

Geophysical Institute, University of Bergen, Norway

*Corresponding author Tel (+47) 55582704, fax (+47) 55584330, e-mail: caroline.kivimae@gfi.uib.no

Abstract

The unique time series from Ocean Weather Station M has been used for the first time to assess the interannual variability of the net community production (NCP) in the Norwegian Sea. This paper presents a 51 year time series of calculated annual NCP based on a box model for the oxygen balance in the mixed layer taking into account air-sea exchange, vertical eddy diffusion, and change in oxygen content. The annual NCP varied between 43.0 g C m^{-2} y^{-1} (4.7 mol O_2 m^{-2} y^{-1}) in 1987 and 169.1 g C m^{-2} y^{-1} (18.3 mol O_2 m^{-2} y^{-1}) in 1995, with a mean of 102.7 g C m^{-2} y^{-1} (11.1 mol O_2 m^{-2} y^{-1}). The interannual variability of the annual NCP was large, with a regime shift to generally higher NCPs occurring in 1992. No single environmental parameter was found to explain the variability in the NCP.

Index terms: 4805 Oceanography: Biological and Chemical: Biogeochemical cycles, processes, and modeling; 4273 Physical and biogeochemical interactions; 4806 Carbon cycling

1. Introduction

In an era of climate change it is essential to determine the natural variability of the oceanic biological production as it is part of the carbon cycle. Such knowledge will not only help to establish the foundation on which observations of change can build, but it can also help us to predict the direction the changes will take. In the Arctic Climate Impact Assessment (ACIA) report [*ACIA*, 2005] the Bergen Climate Model predicted an increase in sea surface temperature in the Norwegian Sea of up to 1.5ºC by 2070 with the doubling of the atmospheric CO_2 concentrations assumed in the model. The model also showed an increase of the inflow of Atlantic Water into the Nordic Seas while the strength of the internal cyclonic gyre in the Nordic Seas decreased [*ACIA*, 2005]. An assessment of the natural biological production variability in this area may be useful for quantifying the effects of such changes on the oxygen and carbon cycles in the Nordic Seas.

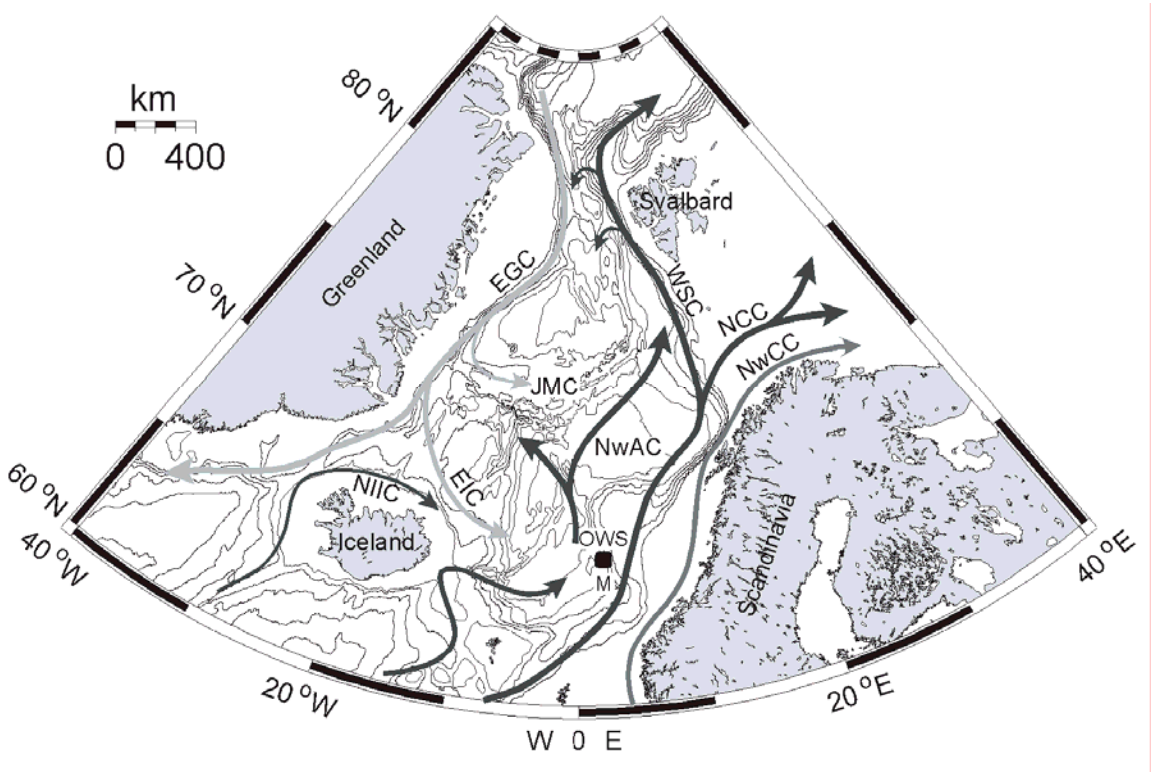

Figure 1: Map showing the position of OWS M and the main surface circulation in the Nordic Seas. Note the two cores of the Norwegian Atlantic Current (NwAC) as it enters and flows through the Norwegian Sea. Abbreviations are NwCC = Norwegian Coastal Current, NCC = North Cape Current, WSC = West Spitsbergen Current, EGC = East Greenland Current, JMC = Jan Mayen Current, EIC = East Icelandic Current and NIIC = North Icelandic Irminger Current.

The common notions of production include primary (or total) production, new production, regenerated production, net community production (NCP), and export production, which each presenting a selected view of production [e.g. *Dugdale and Goring,* 1967; *Williams,* 1993; *Falck,* 1999]. NCP represents the total biological production minus the community respiration [*Platt et al.,* 1989]. NCP can be calculated from measurements of oxygen, since either its accumulation in the euphotic zone or consumption at depth will provide estimates of net production with a characteristic timescale of months to years. After the physical processes of advection, vertical eddy diffusion, and air-sea exchange have been taken into account the resulting changes in oxygen in the water column represents the NCP.

Ocean Weather Station M (OWS M) is positioned at 66˚N and 2˚E in the Norwegian Sea (Figure 1) and is situated within the western branch of the Norwegian Atlantic Current, over the continental slope where the bottom depth is about 2000 m. The Norwegian Atlantic Current brings warm and salty water from the North Atlantic into the Norwegian Sea and towards the Arctic. It is bordered by the Arctic Front to the west and the Norwegian Coastal Current to the east. The surface influence of the Norwegian Coastal Current may reach far to the west in summer, sometimes as far

west as OWS M [*Nielsen and Falck,* 2006], as the fresh, light coastal water spreads on top of the Atlantic Water of the Norwegian Atlantic Current.

OWS M has since the start of its operation in 1948 collected a unique time series of meteorological and oceanographic data. The data set includes temperature and salinity measurements since 1948 and oxygen measurements since 1953. The OWS M time series is one of the very few oceanic data sets having sufficient resolution in time for the calculation of reliable annual production estimates as well as for the assessment of the interannual variability.

The annual production at OWS M has been studied previously with box models [*Falck and Gade,* 1999; *Falck and Anderson,* 2005] and with a coupled physical-biological-chemical model [*Broström,* 1997]. These studies aimed at finding the climatological mean production at OWS M and in the surrounding Norwegian Sea. This work presents a time series of annual NCP at OWS M from 1955 to 2005, calculated with a box model. An effort is made to understand the variability of the time series in relation to some environmental variable.

2. Data

The hydrographic measurements at OWS M have been taken with Nansen reversing bottles. Temperature and salinity are measured six days a week while samples for dissolved oxygen (hereafter only referred to as oxygen) are collected once a week. The oxygen samples were analyzed onboard using the Winkler titration method (with visual detection of the end point) since their inclusion in the time series. The oxygen measurements used in this work were quality controlled by comparing the deep water concentrations of the profiles and discarding profiles with very clear deviations from the mean. The deep water oxygen concentrations in this area are assumed to be nearly constant with time. Oxygen samples are not collected at the surface at OWS M so the oxygen concentration at 10 m are used here as the surface value. This should not have a large influence on the results since the mixed layer in this area only seldom becomes shallower then 10 m. Unfortunately the time series has some data gaps ranging from weeks to several months.

Six-hourly geostrophic wind speeds at 10 m above sea level and sea level pressure (SLP) from the Norwegian Meteorological Institute hindcast database [*Eide et al.,* 1985] were used for calculations of air-sea exchange. These parameters exist from 1955 and thus hydrographic observations on oxygen concentration, temperature, and salinity have been used for the period 1955 – 2005 to calculate the NCP.

3. Method

To estimate the yearly NCP at OWS M a box model based on changes in oxygen content in the mixed layer was employed (Figure 2). Changes in oxygen content (ΔO_2^C) in the mixed layer were calculated as:

$$\Delta O_2^C = O_2^{NCP} + O_2^{air\text{-}sea} + O_2^{vert\ diff} + O_2^{adv} \quad (1)$$

where O_2^{NCP} is the change in oxygen caused by biological production, $O_2^{air\text{-}sea}$ is the air-sea exchange of oxygen, and $O_2^{vert\ diff}$ is the eddy diffusion of oxygen across the base of the mixed layer. The horizontal advection of oxygen, O_2^{adv}, was assumed to be negligible since the water on its way northward probably experienced the same seasonal variations. The production term was thus calculated according to

$$O_2^{NCP} = \Delta O_2^C - O_2^{air\text{-}sea} - O_2^{vert\ diff} \quad (2)$$

NCP has taken place when O_2^{NCP} is positive. Calculations of all parameters were made for each day by interpolation between measurements. Air-sea exchange was calculated every six hours to avoid averaging wind-speed and SLP, even though oxygen concentrations and saturation concentrations were kept the same for a 24 hour period.

The first right-hand term in Eq. 2, the change in oxygen content in the mixed layer (ΔO_2^C), has been calculated using one of the two equations below, depending on whether the mixed layer was increasing (3a) or decreasing (3b):

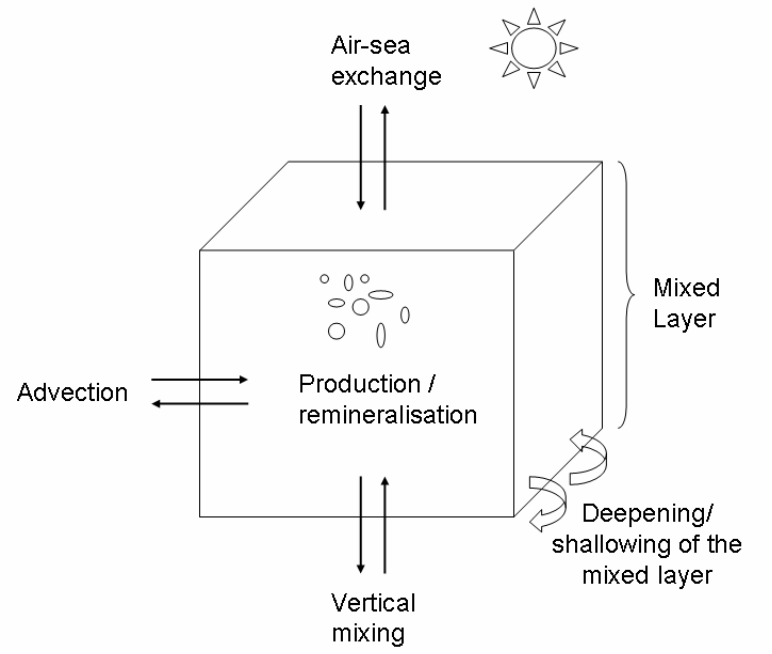

Figure 2: The conceptual box model showing the oxygen fluxes and processes that contribute to the oxygen balance of the mixed layer, production/remineralisation, air-sea exchange, vertical mixing, change in mixed layer depth, and advection.

$$\Delta O_2{}^C = \int_0^{MLD2} [O_2]_2 \, dz - \left(\int_0^{MLD1} [O_2]_1 \, dz - [O_2]_{umld1} \cdot (MLD_2 - MLD_1) \right) \quad (3a)$$

$$\Delta O_2{}^C = \int_0^{MLD2} [O_2]_2 \, dz - \left(\int_0^{MLD1} [O_2]_1 \, dz + [O_2]_{umld2} \cdot (MLD_2 - MLD_1) \right) \quad (3b)$$

where $\int_0^{MLD} [O_2] \, dz$ is the integration of the oxygen profile from the surface to the mixed layer depth (MLD), while the subscripts 1 and 2 refer to two subsequent days and $[O_2]_{umld}$ is the oxygen concentration below the mixed layer. The MLD was calculated with a density criterion ($\Delta\rho$) corresponding to a ΔT of -0.8ºC as done by *Nilsen and Falck* [2006]. The last term in 3a and 3b compensates for the day-to-day change in MLD. Without this term the change in oxygen content would express both the change within the new ML (day 2 compared to day 1) and the amount of O_2 contained in the volume by which the ML have increased/decreased (the content is calculated per m^2 of ML) from day 1 to day 2. Abrupt changes in the MLD between measurements sometimes occurred during winter, resulting in unrealistic positive peaks in NCP. Since winter is a period when little production is assumed to take place, in order to avoid these peaks the MLD was set to 100 m when it was 100 m or deeper. This resulted in the cancellation of the last term in Eq. 3a and 3b. The correct MLDs were used when the mixed layer was shallower than 100 m, this was the case during most of the productive season.

The air-sea exchange was calculated according to

$$O_2{}^{air\text{-}sea} = k \cdot \Delta[O_2] \quad (4)$$

where k is the transfer velocity and $\Delta[O_2]$ the oxygen deficit, i.e. the difference between the measured concentration ($[O2]_{meas}$) and the saturation concentration ($[O2]_S$), ($[O2]_{meas} - [O2]_S$). Following *Wanninkhof* [1992] the transfer velocity (in m d^{-1}) was calculated as

$$k = 0.0744 \cdot u_{10}{}^2 \cdot (Sc/600)^{-0.5} \quad (5)$$

where u_{10} is the wind speed at 10 m above sea level and Sc is the Schmidt number. The equation for the calculation of the Schmidt number was also taken from *Wanninkhof* [1992]:

$$Sc = 1953.4 - 128 \cdot T + 3.9918 \cdot T^2 - 0.050091 \cdot T^3 \quad (6)$$

where T is the temperature in ºC.

The oxygen saturation concentration was calculated according to *García and Gordon* [1992]. The resulting oxygen deficit (ΔO_2) was corrected for bubble-injection according to *Woolf and Thorpe* [1991] and SLP according to *Najjar and Keeling* [1997]. Air injection of bubbles is recognized as a process that enhances the flux of oxygen into the ocean. Bubble-mediated gas transfer supports a supersaturation of oxygen of about 1-2% in an equilibrium situation [*Woolf and Thorpe*, 1991]. This

implies that the net air-sea flux of oxygen will first change sign at a saturation level slightly higher than 100%. When calculating the air-sea exchange this effect is achieved by multiplying $[O_2]_S$ by the following term

$$B_{corr} = (1 + (0.01 \cdot (u_{10} / 9)^2)) \quad (7)$$

The SLP may also change the oxygen saturation state and according to *Najjar and Keeling* [1997] a correction term is added to the original oxygen deficit ($\Delta[O_2]^0$):

$$\Delta[O_2] = \Delta[O_2]^0 + (1 - SLP / 1013.25) \cdot [O_2]_S \quad (8)$$

The effect of the correction for SLP is a lower saturation concentration when the SLP is below the standard pressure (1013.25 mb) and a higher saturation concentration when the SLP is higher. Depending on the surface water concentration this may increase or decrease $\Delta[O_2]$. The final oxygen deficit was thus calculated as follows

$$\Delta[O_2] =([O_2]_{meas} - ([O_2]_S \cdot B_{corr})) + (1 - SLP / 1013.25) \cdot ([O_2]_S \cdot B_{corr}) \quad (9)$$

The eddy diffusion term of Eq. 2 can be expressed as

$$O_2^{vert\ diff} = K_z \cdot d[O_2] / dz \quad (10)$$

where K_z is the eddy diffusion coefficient, $d[O_2]$ is the change in oxygen concentration across the base of the mixed layer ($[O_2]_{umld}$ - $[O_2]_{ml}$), and dz is the distance over which the oxygen gradient exists. In this work a K_z of $1 \cdot 10^{-4}$ m^2 s^{-1} was used and dz was set to 1 m.

Annual NCP (the sum of all positive O_2^{NCP} during one year) was calculated for all years which had at least one oxygen measurement each month during all 12 months. Due to the gaps in the time series the annual NCP could not be calculated for all years. When data was missing during the winter months October-March, monthly mean values of oxygen, temperature, and salinity were inserted into the data series (these months were considered as little productive) in order to increase the number of years for which annual NCP could be calculated. Mean values for one or several months were used for 13 years (see Table 1). Annual NCP was not calculated for years with data gaps occurring in the summer months April-September, which was the case for 18 years.

4. Results

Changes in the oxygen content of the mixed layer (ΔO_2^C), air-sea exchange ($O_2^{air\text{-}sea}$), vertical eddy diffusion ($O_2^{vert\ diff}$), and O_2^{NCP} were calculated for each day from the first to the last day of the time series. To illustrate the evolution of the different parameters in the calculations

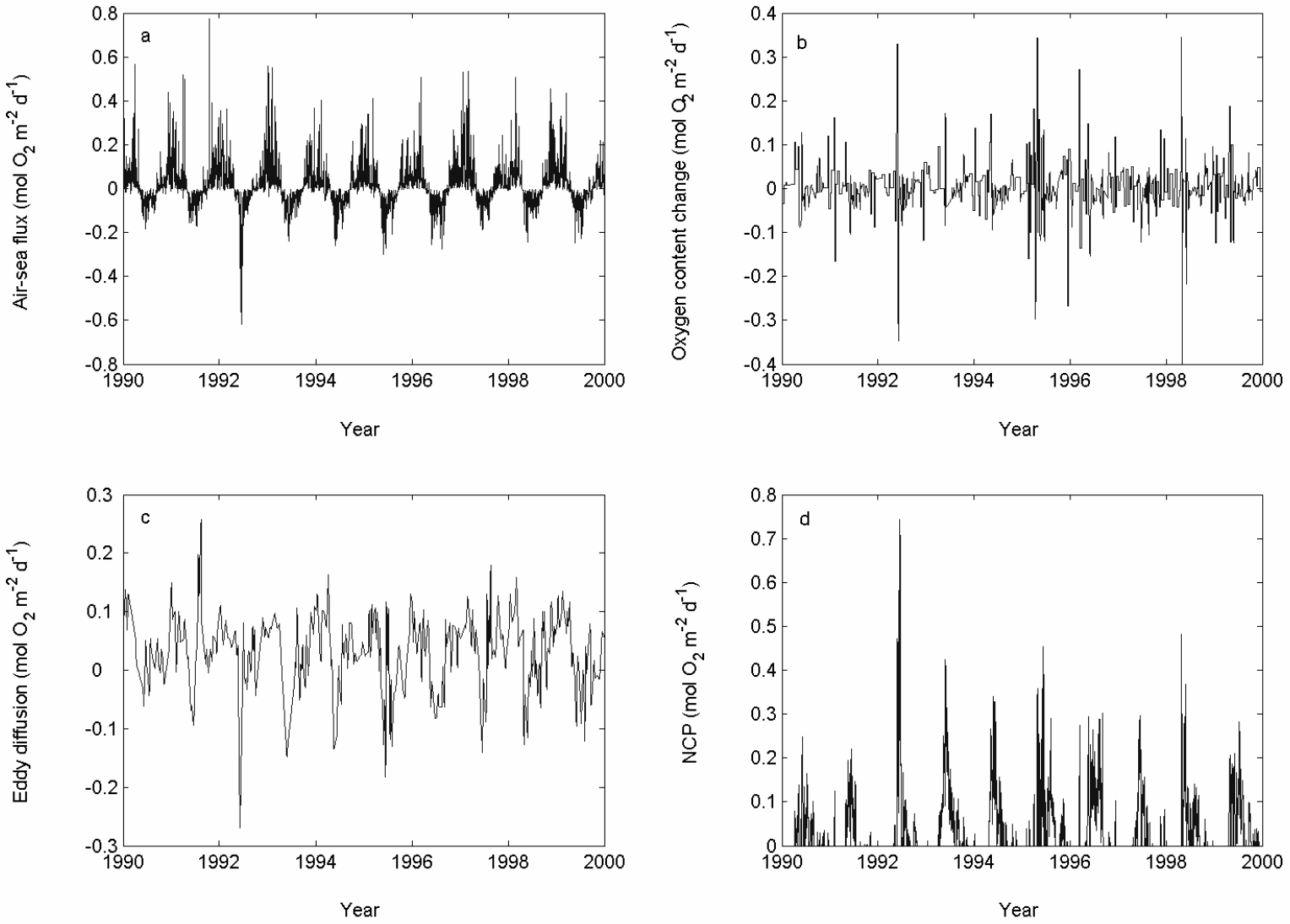

Figure 3: Evolution of the four parameters in Eq. 2, daily air-sea exchange (a), change in oxygen content of the mixed layer (b), eddy diffusion (c), and net community production (d) during the ten years (1990-1999) with the best data coverage.

Figure 3 shows the four parameters for the ten years with the best data coverage (1990-1999), although the values referred to below cover the whole time series. The seasonal evolution of air-sea exchange (Figure 3a) shows an uptake of oxygen from the atmosphere during winter (positive) and an outgassing during summer (negative), ranging between -0.62 and 0.91 mol O_2 m^{-2} d^{-1}. The change in oxygen content in the mixed layer (Figure 3b) ranges from -0.62 and 0.47 mol O_2 m^{-2} d^{-1} and has no clear seasonal cycle. The vertical eddy diffusion (Figure 3c) is smaller than the other parameters, ranging between -0.27 and 0.26 mol O_2 m^{-2} d^{-1} with a weaker seasonal cycle than the air-sea exchange. The daily NCPs (Figure 3d) show a clear seasonal cycle, with values up to 0.74 mol O_2 m^{-2} d^{-1}.

Table 1 lists the annual NCP values for all the years with enough data coverage. The period up to 1991 seems to shows a small decreasing trend in annual NCP (Figure 4), with the exception of the rather low annual NCP in 1955. In 1992 a sudden change to higher annual NCPs took place. The annual NCPs stayed high for the rest of the period, with the exception of 1997 and 2005. The mean annual NCP for the entire time series was 11.1 mol O_2 m^{-2} y^{-1}, with the annual NCP varying between 4.7 mol O_2 m^{-2} y^{-1} in 1987 and 18.3 mol O_2 m^{-2} y^{-1} in 1995. Using the conversion factor between carbon and oxygen (106/138) from *Redfield et al,* [1963] this is equivalent to a mean NCP of 102.7 g C m^{-2} y^{-1}, with a minimum and maximum of 43 and 169.1 g C m^{-2} y^{-1}, respectively.

Table 1: Annual net community production (NCP) at OWS M. N is the number of oxygen measurements available for each year. Missing months indicates which months were without data for a given year.

Year	N	NCP mol O_2 m^{-2} y^{-1}	NCP g C m^{-2} y^{-1}	Missing months	Year	N	NCP mol O_2 m^{-2} y^{-1}	NCP g C m^{-2} y^{-1}	Missing months
1955	41	5.5	50.8	10	1987	45	4.7	43.0	
1957	35	13.0	120.0		1988	32	6.7	61.5	
1959	43	11.7	107.9		1989	35	9.8	90.8	
1961	41	13.5	124.1	12	1990	29	7.5	68.8	
1962	41	12.2	112.9	11, 12	1991	34	6.6	61.3	
1963	27	11.6	107.2	1, 2, 3	1992	32	15.4	142.2	
1965	31	8.1	74.6	1, 2, 3	1993	28	16.3	150.2	3
1967	38	12.0	111.1	11	1994	31	12.9	119.2	
1969	34	12.0	110.6	11	1995	37	18.3	169.1	
1971	30	10.1	93.3	11	1996	34	16.6	153.4	
1973	33	11.9	109.4	3	1997	33	8.6	79.3	
1975	15	8.3	76.3	2, 12	1998	35	12.5	115.4	
1976	19	8.1	74.6		1999	36	13.0	120.1	12
1982	26	11.3	104.7		2002	31	15.3	141.4	
1984	28	11.6	107.1		2003	36	13.5	124.7	
1985	29	8.5	78.3		2005	26	8.5	78.1	11, 12
1986	34	11.8	108.5						

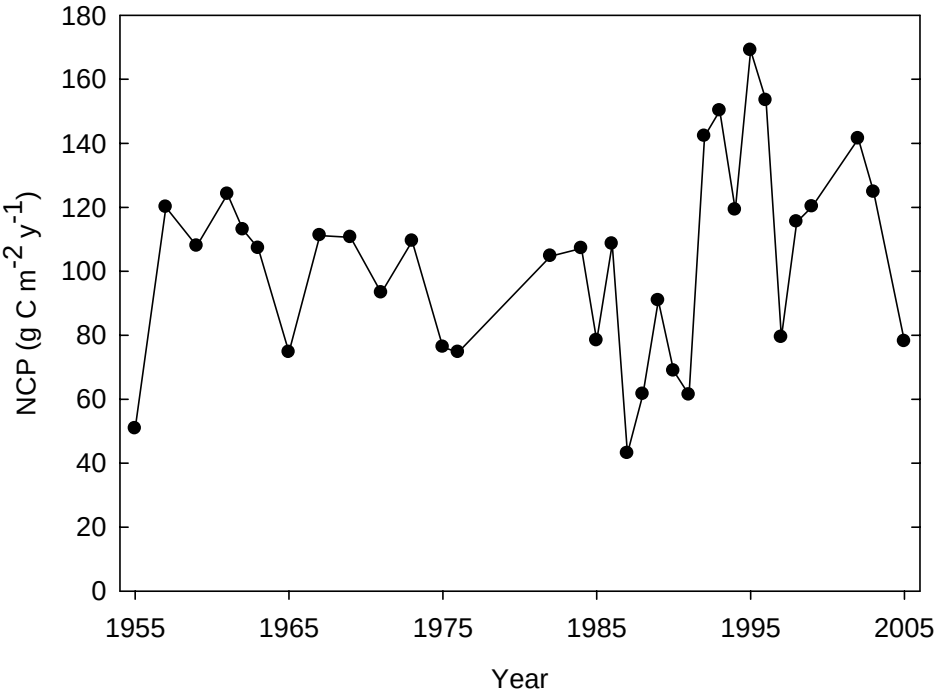

Figure 4: Time series of annual net community production at OWS M.

This gives a variability of 126.1 g C m^{-2} y^{-1}, about three times the lowest NCP. If the standard deviation (σ) of the time series, 30 g C m^{-2} y^{-1}, is considered, five years lie below -1σ (1955, 1987, 1988, 1990, 1991) and 5 years lie above +1σ (1992, 1993, 1995, 1996, 2002). The difference between the annual NCP in 1991 and in 1992, 72 g C m^{-2} y^{-1}, is the largest between any two consecutive years.

5. Discussion

The results show that the variability of the annual NCP from one year to the next can be large at OWS M (Figure 4). Examining individual years reveals that a higher peak of daily NCPs during the spring bloom generally results in a higher annual NCP, but other factors such as the length of the productive season and the duration of the spring bloom may play a part as well. What environmental parameter(s) lie behind these variations?

The spring bloom at OWS M starts when the depth of the mixed layer has decreased enough due to solar heating in spring, resulting in a shallow seasonal pycnocline, and lasts until the nutrients in the shallow mixed layer are depleted. At OWS M, May is the first month of the year when the mixed layer might get shallow enough to initiate the spring bloom, but the mean depth varies interannually between about 60 and 300 m [*Nilsen and Falck,* 2006]. In June the mean MLD is less than 100 m for all years. With a shallow mixed layer occurring already in May the bloom can start some weeks

earlier than in years with a much deeper mixed layer. Indeed 1987, which shows the lowest annual NCP for the whole time series also has the deepest May mean MLD of all the years. As an environmental parameter that could influence the timing of the spring bloom, the depth of the mixed layer in early spring is a good candidate. Mean values for MLD were calculated for each month of each year and plotted against the annual NCP. The same was also done for both mixed layer temperature and salinity to see if a relationship to the annual NCP could be found for these variables as well. A relatively good correlation was found between the annual NCPs and the depth of the mixed layer and the temperature of the mixed layer in May of the year in question, but not for any other months.

Light conditions are not a limiting factor for the initiation of the bloom in the area of OWS M but can have a great influence on the productivity once it has started. OWS M is often situated inside the track of the low pressure systems passing northward and may therefore experience many cloudy days during the productive season. In addition, the Norwegian Sea is also known for having many foggy days during summer. Meteorological conditions in this area vary considerably from year to year and a summer with good weather could result in a larger amount of NCP than a summer with bad weather.

During the spring bloom the nutrients in the mixed layer are used up, and for the rest of the biological season increased NCP will depend on entrained nutrients from below. This supply depends on the wind in the area; strong winds will induce mixing with the layer below, calm conditions will not. No relationship was found between wind speed or wind direction and the annual NCP. Other factors that might influence the annual NCP are the amount of grazing and the types of phytoplankton present at different times of the season, but this is beyond the scope of this study.

The low annual NCPs (below one standard deviation) in 1955, 1987, 1988, 1990 and 1991 seem to have different causes, which is why no single parameter stands out. In 1955 there was a rather shallow MLD in May, approximately 100 m, but the spring mixed layer temperature was one of the lowest in the time series [*Nilsen and Falck,* 2006]. In both 1987 and 1988 there was a deep MLD in May, the Atlantic Water was in addition capped with fresher surface water from the Norwegian Coastal Current during the summer of these years. 1990 and 1991 were years with relatively little wind during May-July, and this may have decreased the supply of new nutrients to the seasonal mixed layer. For the years with NCPs higher than one standard deviation no good explanation can be found. In 1992, for instance, the mixed layer in May was nearly as deep as in 1987. The conclusion is that no single environmental variable is found that explains the amount of annual NCP but it is the result of several interacting factors.

The largest uncertainties in the NCP values are assumed to lie in the calculations of the air-sea exchange ($O_2^{air\text{-}sea}$). Different parameterizations exist for the calculation of the transfer velocity [e.g. *Liss and Merlivat,* 1986; *Wanninkhof,* 1992; *Nightingale et al.* 2000] and depending on the choice of formula, the resulting NCP will change in size.

The *Wanninkhof* [1992] parameterization has been used in this work since it is the most commonly used today. Earlier studies from the Norwegian Sea show that calculated NCP from oxygen measurements with the use of the *Wanninkhof* [1992] formula are about twice as high as when the *Liss and Merlivat* [1986] formula is employed [*Falck and Gade,* 1999]. The calculated oxygen fluxes also differ considerably depending on whether the effects of bubble injection and/or changing SLP are included or not. If both bubble injection and changing SLP are excluded from the model, the mean annual NCP is about 20% higher (123 g C m^{-2} y^{-1}). If only the SLP correction is included the mean annual NCP increases by about 35 % (139 g C m^{-2} y^{-1}), in contrast to accounting for only bubble injections which results in a decrease of about 5% (98 g C m^{-2} y^{-1}). In the calculations of air-sea exchange no adjustments have been made due to the difference between the bulk and skin temperature of the water. This difference is assumed to be small but may not always be insignificant.

The uncertainty in the calculation of the change in oxygen content of the mixed layer (ΔO_2^C) lies mainly in the calculation of the MLD. Another difficulty lies in the rapid day to day changes in the MLD at OWS M that sometimes causes unrealistic estimates of oxygen content of the mixed layer. It can not be excluded that these fluctuations can influence the size of the daily NCP during winter and early spring when the mixed layer is most unstable. The oxygen change was thus calculated only for the top 100 m when the mixed layer was deeper than 100 m in order to avoid unreasonable large daily NCP during the winter when production is known to be small. If the annual NCPs are calculated only for the period between 1 April and 30 September the result is a reduction of the mean by about 6%.

For the calculations of the exchange with waters below the mixed layer ($O_2^{\text{vert diff}}$) the value of Kz is the most critical. Kz depends on the strength of the stratification and the amount of available energy. Measurements in the Nordic Seas indicate values in the order of 10^{-5} to 10^{-4} m^2 s^{-1} [*Drange et al.,* 1998; *Watson et al.,* 1999]. In this work we have used 10^{-4} m^2 s^{-1} for Kz in the $O_2^{\text{vert mix}}$ calculations. If we instead use Kz equal to 10^{-5} m^2 s^{-1} the mean annual NCP value is reduced by 9%.

Another source for uncertainties in the NCP estimates is the choice of the O_2:C ratio. The Redfield ratio [*Redfield et al.,* 1963] is used here, but the mean annual NCP would increase slightly, by about 6%, if the ratio of *Takahashi* [1985] was used instead.

Last, but not least, the data coverage in the time series of 1-5 stations per month is sometimes uneven between months and years. The frequency of measurement may be a source of error when years with different data coverage are compared. In the calculations only one profile per month has been required during all 12 months in order to calculate the annual NCP. The year 1975 is an extreme example, where January to July had only one profile each month. What data coverage can be considered sufficient to represent the annual NCP reasonably well? It takes about six weeks for the oxygen in the mixed layer to reach equilibrium with the atmosphere (Broecker, 1974). Since the oxygen concentrations are interpolated between the measurements and not kept constant for the intervening time it is assumed that one

measurement per monthe is enough even though measurements made only once a month may not resolve the peak of the bloom very well. The resulting NCPs have been compared to the density of measurements and lower data density does not consistently give high or low NCPs.

There are few estimates of biological production in the Norwegian Sea in the literature, and those that do exist generally have estimated different kinds of production, making a comparison of results difficult. For instance, *Rey* [1981] and *Broström* [1997] both estimated total production. *Rey's* [1981] estimate using the ^{14}C method was 90-120 g C m^{-2} y^{-1} for the waters in the Norwegian Coastal Current, while *Broström's* [1997] estimate with a coupled physical-chemical-biological model based on nitrogen fluxes was 180 g C m^{-2} y^{-1} at OWS M (of which new production was estimated to be 59 g C m^{-2} y^{-1}). *Falck and Anderson* [2005] calculated deficits of dissolved inorganic carbon in the Norwegian Sea and found a flux of carbon due to biological processes of 5.2 mol C m^{-2} y^{-1} (or 62.4 g C m^{-2} y^{-1}), while *Skjelvan et al.* [2001] estimated 23.6 and 31.7 g C m^{-2} y^{-1} using deficits of phosphate and oxygen for areas further north in the Norwegian Sea. *Falck and Gade* [1999] used an oxygen budget for the euphotic zone (upper 30 m) to estimate the mean NCP for the Nordic Seas but also did some separate calculations for OWS M using data from 1955-1988. Their method was similar to this work except that they neglected vertical diffusion. They used several different air-sea parameterisations and obtained 79 g C m^{-2} y^{-1} when the formulation of *Wanninkhof* [1992] corrected for bubble injection [*Woolf and Thorpe,* 1991] was used. The annual NCP values found in this work agree well with the earlier results from OWS M by *Falck and Gade* [1999], the mean annual NCP with our model for the same period gives a mean annual NCP of 93.5 g C m^{-2} y^{-1}, which is slightly higher than theirs. A somewhat higher NCP is to be expected since *Falck and Gade* [1999] did not include vertical diffusion but it also has to be remembered that *Falck and Gade* [1999] used the transfer velocity formulation for steady winds [*Wanninkhof,* 1992] and not for instantaneous winds as has been done here.

6. Summary

A time series of annual net community production at OWS M for the years 1955 to 2005 has been presented, although NCP could not be calculated for all years due to lack of data. A mean NCP of 102.7 g C m^{-2} y^{-1} was obtained, with a minimum and maximum of 43 and 169.1 g C m^{-2} y^{-1}, respectively. The uncertainties in the calculations are difficult to assess, especially since NCP is sensitive to variations in the calculated oxygen fluxes arising from the uncertainty of the parameterisation of the air-sea gas exchange. The observed rates of change in oxygen content and vertical eddy diffusion are much smaller than the air-sea oxygen exchange, such that parameterisation of the flux equation will have the most influence on the estimate of NCP.

A specific cause of the interannual variability of the net community production could not be found, due to the many different environmental variables influencing

production. The cumulative and varying effects of these variables from year to year does not show up in simple regression analyses. Presently no explanation is available for the positive regime shift seen in the annual NCP between 1991 and 1992.

Acknowledgments

We would like to thank the captains and crews of the various ships that over the years have been stationed at OWS M. Magnar Reigstad from the Norwegian Meteorological Institute kindly provided us with meteorological data.

References

ACIA (2005), Arctic Climate Impact Assessment, ACIA Scientific report, pp. 1042, Cambridge University Press.

Broecker, W.S., (1974), Chemical oceanography. Harcourt Brace Jovanovich, Inc., 214 pp.

Broström, G. (1997), Interaction between mixed layer dynamics. Gas exchange and biological production in the oceanic surface layer with application to the Northern North Atlantic, Ph.D. thesis, Göteborg University, Göteborg, Sweden.

Drange, H., G. Alendal, F. Thorkildsen, O.M. Johannessen, D. Vinkler, A. Ulvesæter, T. Johansen, and J. Giske (1998), Geophysical/economical feasibility study of ocean disposal of CO_2 at Haltenbanken, pp. 192, G. C. Rieber Climate Institute at NERSC.

Dugdale, R.C., and J.J. Goering (1967), Uptake of new and regenerated forms of nitrogen in primary production, *Limnol. Oceanogr.*, *12*, 196-206.

Eide, L.I., M. Reigstad, and J. Guddal (1985), Database av beregnede vind og bølgeparametere for Nordsjøen, Norskehavet, og Barentshavet, hver 6. time for årene 1955-1988 (in Norwegian), in *Prosjekt hindcast-database*, Norwegian Meteorlogical Institute, Oslo.

Falck, E. (1999), On the behaviour of oxygen in the euphotic zone of the Nordic Seas and on carbon and nutrients in the Northeast Water Polynya mixed layer, Ph.D. thesis, University of Bergen, Bergen, Norway.

Falck, E., and L.G. Anderson (2005), The dynamics of the cabon cycle in the surface water of the Norwegian Sea, *Mar. Chem.*, *94* (1-4), 43-53.

Falck, E., and H.G. Gade (1999), Net community production and oxygen fluxes in the Nordic Seas based on O_2 budget calculations, *Glob. Biogeochem. Cycl.*, *13* (4), 1117-1126.

García, H.E., and L.I. Gordon (1992), Oxygen solubility in seawater: Better fitting equation, *Limnol. Oceanogr.*, *37* (6), 1307-1312.

Liss, P.S., and L. Merlivat (1986), Air-sea gas echange rates: Introduction and synthesis, in *The role of air-sea echange in geochemical cycling*, edited by P. Buat-Ménard, pp. 113-129, D. Reidel Publishing Company, Hingham, Mass.

Najjar, R.G., and R.F. Keeling (1997), Analysis of the mean annual cycle of the dissolved oxygen anomaly in the World Ocean, *J. Mar. Res.*, *55* (117-151).

Nightingale, P.D., G. Malin, C.S. Law, A.J. Watson, P.S. Liss, M.I. Liddicoat, J. Boutin, and R.C. Upstill-Goddard (2000), In situ evaluation of air-sea gas exchange parameterizations using novel conservative and volatile tracers, *Glob. Biogeochem. Cycl.*, *14* (1), 373-387.

Nilsen, J.E.Ø., and E. Falck (2006), Variations of mixed layer properties in the Norwegian Sea for the period 1948-1999, *Prog. Ooceanogr.*, *70*, 58-90.

Platt, T., W.G. Harrison, M.R. Lewis, W.K.W. Li, S. Sathyendranath, R.E. Smith, and A.F. Vezina (1989), Biological production of the oceans: the case for a consensus, *Mar. Ecol. Prog. Ser.*, *52*, 77-88.

Redfield, A.C., B.H. Ketchum, and F.A. Richards (1963), The influence of organisms on the composition of sea-water, in *The Sea*, edited by M.N. Hill, pp. 26-77, Interscience, New York.

Rey, F., (1981) Primary production estimates in the Norwegian Coastal Current between 62º N and 72º N, in *The Norwegian Coastal Current, vol 2*, edited by R. Sætre, and M. Mork, pp. 640-648, Reklametrykk, Bergen, Norway.

Skjelvan, I., E. Falck, L.G. Anderson, and F. Rey (2001), Oxygen fluxes in the Norwegian Atlantic Current, *Mar. Chem.*, *73*, 291-303.

Takahashi, T., W.S. Broecker, and S. Langer (1985), Redfield ratio based on chemical data from isopycnal surfces, *J. Geophys. Res.*, *90*, 6907-6924.

Wanninkhof, R. (1992), Relationship between wind speed and gas exchange over the ocean, *J. Geophys. Res.*, *97* (C5), 7373-7382.

Watson, A.J., M.-J. Messias, E. Fogelqvist, K.A. Van Scoy, T. Johannessen, K.I.C. Oliver, D.P. Stevens, F. Rey, T. Tanhua, K.A. Olsson, F. Carse, K. Simonsen, J.R. Ledwell, E. Jansen, D.J. Cooper, J.A. Kruepke, and E. Guilyardi (1999), Mixing and convection in the Greenland Sea from a tracer-release experiment, *Nature*, *401*, 902-904.

Williams, P.J.l. (1993), On the definition of plankton production terms, *ICES Mar. Sci. Symp.*, *197*, 9-19.

Woolf, D.K., and S.A. Thorpe (1991), Bubbles and the air-sea exchange of gases in near-saturation conditions, *J. Mar. Res.*, *49*, 435-466, 1991.

Future work

Future work

With the goal to understand and quantify the carbon fluxes in the Arctic Mediterranean and their variability and fate much work still remains. Some of the needed studies in this area require collection of new data; the heavy ice cover in large parts of the Arctic Mediterranean makes data collection difficult and costly, and the consequence is a general scarcity of data in the area.

In the Barents Sea there is an urgent need to obtain better seasonal data coverage for the variables in the inorganic carbon system, DOC, and POC. The absence of winter data limits the understanding of the Barents Sea as a system e.g. as a sink for atmospheric CO_2. It also makes it difficult to predict and detect future changes. In relation to paper II the critical question in this context is how well the water in the deeper parts of the winter mixed layer represents the situation at the end of the previous winter? If winter data can be obtained this type of uncertainties will be avoided and calculations of the CO_2 uptake from the atmosphere will be more robust. Data during autumn would also make it possible to obtain more information about the amount and variability of annual new and/or net community production from observations. Observation based estimates of annual production has to date only been done along the Kola transect (Olsen et al., 2002) and the results are much smaller than those obtained from seasonal studies and models. Since the Barents Sea is such an important area for fisheries the amount of production it can sustain is of large interest. Currently the most extensive knowledge of production comes from models, but to rely on them with confidence they need to be validated with field data.

Data from the eastern parts of the Barents Sea, where no dissolved inorganic carbon measurements have been made to date, would provide much information on how the carbon content of the Atlantic Water is modified. Of particular interest is the modification caused by mixing between the Atlantic Water and brine water that origin on the Central Bank and the western Novaya Zemlya bank. Inorganic carbon measurements from currents and water masses are here essential for increased knowledge. From the Barents Sea carbon budget (paper I) it is also clear that more information on volume flows and residence times of the water masses are needed to achieve a more precise budget. A better understanding of the physical oceanography will improve the knowledge of the inorganic carbon transports in the area significantly.

Due to the large importance of the Atlantic Water inflow for the Barents Sea it is essential to know the long term mean values and variability of biogeochemical variables such as oxygen and pCO_2 in the water mass. The pilot project on pCO_2 and O_2 measurements on a mooring in the Barents Sea Opening is important for this type

of data gathering. A continuation or increase of this effort could provide the basis for a new promising time series on chemical variability in addition to the ongoing measurements of physical variables (e.g. Ingvaldsen et al., 2004).

As indicated in paper II the bulk properties of sea ice are not well known, an investigation of these would help to decrease the uncertainties when calculating air-sea exchange and biological production in ice covered waters.

In the Norwegian Sea the long time series from Ocean Weather Station M (OWS M) is of large value for the understanding of the state of the biogeochemistry and physics in the area. It can also give an insight into its seasonal, interannual, and decadal variability and change. The time series may also be used to validate models. In an era of climate and environmental change it is urgent to ascertain the future existence of OWS M so that its unique time series is continued.

A lot of new measurements of volume transports and carbon system variables have been collected in the Nordic Seas during the last decade. This gives the potential to construct a Nordic Seas carbon budget. Lundberg and Haugan (1996) published a carbon budget for the Arctic Mediterranean with the limited data then available. A budget based on the new observations could provide a better estimate of the carbon fluxes into and out of the Nordic Seas as well as identifying where future efforts should be directed to achieve increased understanding of this area.

The modification of the Barents Sea branch of Atlantic Water was investigated in paper III but less is known about the evolution of the carbon content, air-sea exchange and production in the West Spitsbergen Current. An investigation of the carbon fluxes in the West Spitsbergen Current would be valuable both to compare them to the Barents Sea branch of Atlantic Water and to get an overview of the total input of Atlantic Water, carbon and related variables into the Arctic Ocean.

The environmental factors that are important for the large variability in annual net community production at OWS M (paper IV) are not well understood. This rise two questions:

1. Is the variability as large in the entire ice free Nordic Seas as observed at OWS M?
2. Could understanding of the environmental variability on a lager scale of the whole Nordic Seas and North Atlantic facilitate the identification of the environmental forces behind the variability observed at OWS M?

Due to the lack of systematic sampling in time and space and the different variables used to calculate biological production it is at present difficult to directly compare results between different areas, e.g. the Nordic Seas and the Barents Sea, or even within the same water mass, e.g. the Atlantic Water. A more systematic approach that ensures the possibility to compare production in different areas could reveal some of the mechanisms behind the variability observed at OWS M that could not be explain in paper IV.

A time series of air-sea oxygen exchange at OWS M is calculated and used in paper IV, but is not presented in detail. A separate study examining this time series is in preparation. The time series at OWS M also holds the possibility for several other studies e.g. changes in intermediate and deep water circulation based on oxygen content.

Other interesting questions for the future are:

- What controls the branching of the Atlantic Water in the northern Norwegian Sea into the West Spitsbergen Current and North Cape Current and its variability? Will future changes of the controlling mechanism direct larger amounts of Atlantic Water either directly northwards or into the Barents Sea?
- How large is the concentration and rate of increase of anthropogenic carbon in the Coastal and Arctic Waters in the Norwegian and Barents Seas?
- How much can we learn from satellites about productivity in the cloudy high northern latitudes? Could OWS M be a good facility for groundthruthing satellite images of biological production in the Nordic Seas?
- How permeable is sea ice for gas exchange? If considerable amounts of CO_2 are exchanged through sea ice it will change the estimate of total uptake of atmospheric CO_2 in the Arctic Mediterranean.

The field of marine biogeochemistry is a rather new area of research where terms and concepts are still developing. This field is also a cross road between physical, chemical and biological oceanography and requires interdisciplinary work. Due to the cooperation between scientists from different areas it is not unusual that there arises some confusion around terms and concepts. It would therefore be helpful for many to try and collect the consensus of the community into some form of communication.

References

Ingvaldsen, R.B., L. Asplin, and H. Loeng, 2004. The seasonal cycle in the Atlantic transport to the Barents Sea during the years 1997-2001. Continental shelf research, 24: 1015-1032.

Lundberg, L. and P. M. Haugan, 1996. A Nordic Seas- Arctic Ocean carbon budget from volume flows and inorganic carbon data. Global Biogeochemical Cycles, 10(3): 493-510

Olsen, A., L. G. Anderson and T. Johannessen, 2002. The impact of climate variations on fluxes of oxygen in the Barents Sea. Continental shelf research, 22: 1117-1128.